

“Whenever I don’t know whether to fight or not, I fight” - Emily Murphy

“The choice isn’t between good and evil. That’s easy. The real choices of life are choosing between the lesser of two evils or the greater of two goods” - Fanaa movie

University of Alberta

**The association of geochemical and microbiological parameters with the deposition
of mud in marginal marine settings.**

By

Ozlem Suleyman



**A thesis submitted to the Faculty of Graduate Studies and Research in partial
fulfillment of the requirements for the degree of Master of Science**

Department of Earth and Atmospheric Sciences

Edmonton, Alberta

Spring 2008



Library and
Archives Canada

Bibliothèque et
Archives Canada

Published Heritage
Branch

Direction du
Patrimoine de l'édition

395 Wellington Street
Ottawa ON K1A 0N4
Canada

395, rue Wellington
Ottawa ON K1A 0N4
Canada

Your file Votre référence
ISBN: 978-0-494-45890-7
Our file Notre référence
ISBN: 978-0-494-45890-7

NOTICE:

The author has granted a non-exclusive license allowing Library and Archives Canada to reproduce, publish, archive, preserve, conserve, communicate to the public by telecommunication or on the Internet, loan, distribute and sell theses worldwide, for commercial or non-commercial purposes, in microform, paper, electronic and/or any other formats.

The author retains copyright ownership and moral rights in this thesis. Neither the thesis nor substantial extracts from it may be printed or otherwise reproduced without the author's permission.

AVIS:

L'auteur a accordé une licence non exclusive permettant à la Bibliothèque et Archives Canada de reproduire, publier, archiver, sauvegarder, conserver, transmettre au public par télécommunication ou par l'Internet, prêter, distribuer et vendre des thèses partout dans le monde, à des fins commerciales ou autres, sur support microforme, papier, électronique et/ou autres formats.

L'auteur conserve la propriété du droit d'auteur et des droits moraux qui protègent cette thèse. Ni la thèse ni des extraits substantiels de celle-ci ne doivent être imprimés ou autrement reproduits sans son autorisation.

In compliance with the Canadian Privacy Act some supporting forms may have been removed from this thesis.

Conformément à la loi canadienne sur la protection de la vie privée, quelques formulaires secondaires ont été enlevés de cette thèse.

While these forms may be included in the document page count, their removal does not represent any loss of content from the thesis.

Bien que ces formulaires aient inclus dans la pagination, il n'y aura aucun contenu manquant.


Canada

ABSTRACT

The salinity, particle concentration, organic matter, turbulence, turbidity, micro-organisms and isotopic compositions present in the sediments or pore waters surrounding the sediments play an important role in predicting the depositional history of mud in estuarine settings.

One method of predicting the depositional history of fresh and marine-water mixing is by establishing a recent salinity record in the estuarine deposits. Recent salinity records can be established from systematic variations of stable isotopes (δD and $\delta^{18}O$). The salinities and stable isotope values of pore water samples collected from 3 locations on the Shepody River, south east coast of New Brunswick indicate a linear relationship between stable isotope compositions and recorded (annual) precipitation records, and an inverse relationship between salinity and precipitation. Comparing the time series of local annual precipitation to the isotopic signature retained in sedimentary layers (in this case, Inclined Heterolithic Stratification) shows that the δD and $\delta^{18}O$ values are stored in the pore water after sediment accumulation and can be used to show that the primary stratification represents annual sedimentation. Thereby, the salinity record stored in these deposits can be established from the seasonal rhythmites and can contribute to assessing the depositional history of the Shepody River.

The study of flocculation can also help to better understand the depositional processes in marginal marine settings. Flocculation is the process in which smaller particles collide and stick together by the absorption of ions of opposite charge to form an aggregate. Three experiments were conducted to examine the effects of physicochemical aggregation on turbidity, microbial effects on turbidity, and hydrodynamic effects on flocculation and microbial community.

Time series turbidity profiles were produced that show in a closed, aerobic system (containing bacteria), turbidity generally decreased with time; however, turbidity sharply increased after 5 and 7 days. With sterilized samples, the turbidity decreased at a slower rate than both the non-sterile environments and those that were with cultivated bacteria. The results presented show that bacteria and other physico-chemical conditions facilitate floc settling by increasing the size of flocs. Metabolic by-products such as carbon dioxide facilitate fluctuations in turbidity. The time series bacteria and floc size profiles further

suggest that the interaction between aggregates and sediment biota are influenced by the hydrodynamics.

This thesis is dedicated to YouTube for keeping awake at nights as I watched cartoons and other TV shows that I was raised with during my childhood. I was able to connect the experiments in the Flocculation chapter to one story after watching an episode of the animated 'Adventure of Tom Sawyer' involving the fall of Tom's teacher into a hole dug by Tom and Huck.

Acknowledgements

A lot of happy moments and challenges were involved during the preparation of my thesis. The MSc program was like a roller coaster ride and I would like to thank Dr. Murray Gingras for “riding the roller coaster” with me, i.e. he was there for me in all my good and bad times.

I would like to thank Dr. Karlis Muelenbachs for helping me with the isotope laboratory work that was required for one of my chapters. He also contributed with his ideas and editing. I give many thanks to Dr. Sarah Gleeson for giving me insights and suggestions, which improved the quality of my thesis.

I am thankful to Dr. Robert Burrell for his help with the microbiology section in my thesis and for treating me as one of his own students. Because of him I was hooked into the study of bacteria. He also introduced me to other professors and research scientists such as Dr. Anthony Naylor, who I appreciate for sharing some of his knowledge pertaining to changes in turbidity. I thank Dr. Yeong Kim for acting as my laboratory mentor while I was studying the relation of bacteria with sediments. I learnt a lot from him.

I thank Igor Jakob, Michael Fisher and Christopher Lough for fixing the technical problems that I faced while preparing tables, figures and format changes in my thesis. My work was more enjoyable whenever I worked with them. I would like to acknowledge Shahin Dashtgaard and Andrew Lawfield for sampling the tidal deposits in the Shepody River Estuary, New Brunswick.

It was a pleasure to work with Tyler Hauck, Sarah Gunn, Jesse Schoengut, Curtis Lettley, Marilyn Zorn, Kevin Balshaw, Maureen Stonehouse, Lynn Dafeo and Patricia Nadworny. I could not ask for better colleagues or lab mates. I would like to thank my family for their moral support and encouragement. They had and still do have faith in my abilities. I also am thankful to all my friends in Eta Mondo dance group, the salsa dance group and the Turkish Community for being the best friends I could ever ask for.

Lastly, I would like to thank the Natural Science and Engineering Research Council (NSERC), BP Canada, ConocoPhillips Houston, Devon Energy, Nexen Energy, Petro Canada and Talisman Energy for their financial support.

TABLE OF CONTENTS

	Page
Chapter 1: Introduction	
1.1. Opening statement	1
1.2. Thesis outline	2
1.3. Geological setting	2
1.4. Inclined Heterolithic Stratification Inclined (IHS)	3
1.5. Flocculation and its significance	4
1.6. Objectives	5
1.7. References	6
Chapter 2: Establishing a recent salinity record from seasonal rhythmites of the Shepody River, New Brunswick, Canada	
2.1. Introduction	12
2.2. Methods	13
2.2.1. Field sampling	13
2.2.2. Laboratory analysis	14
2.2.2.1. Stable isotopes (δD and $\delta^{18}O$)	14
2.2.2.2. Salinity	15
2.3. Results/observations	15
2.3.1. Field observations	15
2.3.2. δD and $\delta^{18}O$	15
2.3.3. Annual precipitation	16
2.3.4. Salinity (Na and Cl)	18
2.5. Interpretation	18
2.4.1. δD and $\delta^{18}O$	19
2.4.2. Annual precipitation	19
2.4.3. Salinity (Na and Cl)	20
2.4.4. Derivatives of precipitation, salt ion concentrations (Na and Cl) and isotopic compositions (δD)	22
2.5. Discussion	27
2.6. Conclusion	23
2.7. References	29
Chapter 3: The importance of micro-organisms in promoting flocculation and their relation to sediment dynamics	
3.1. Introduction	50
3.2. Study area	51
3.3. Methods	51
3.3.1. Experiment 1: Effects of physicochemical aggregation on turbidity	53
3.3.2. Experiment 2: Bacterial effects on turbidity	53
3.3.3. Experiment 3: Hydrodynamic effects on turbidity, aggregation and bacteria	55
3.4. Results	56
3.4.1. Effects of physicochemical aggregation on turbidity	56

3.4.2. Bacterial effects on turbidity	58
3.4.3. Hydrodynamic effects on turbidity, aggregation and bacteria	59
3.5. Interpretation	59
3.5.1. Effects of physicochemical aggregation on turbidity	59
3.5.2. Bacterial effects on turbidity	60
3.5.3. Hydrodynamic effects on turbidity, aggregation and bacteria	60
3.6. Discussion	61
3.7. Conclusion	63
3.8. References	64
Chapter 4: Conclusion	
4.1. Introduction	84
4.2. Research findings in chapter 2	84
4.3. Research findings in chapter 3	84
4.4. Limitations	85
4.5. Future research	86
Appendices	87

LIST OF TABLES

Table	Page
2.1. Isotopic compositions at locations 1, 2 and 3 in the Shepody River Estuary. $\delta D_{(MWL)}$ represents the theoretical deuterium values that lie on the meteoric water line which represent the relationship $\delta D = 8 \delta^{18}O + 10$ (Craig, 1961).	31
2.2. Annual precipitation obtained from the Alma station from 1991 to 2005 and isotopic compositions in the IHS layers at locations 1, 2 and 3.	32
2.3. The derivatives and second derivatives of precipitation, salt ion concentrations (Na and Cl) and isotopic compositions (δD) in the IHS at location 2.	33
2.4. Estimated seawater and freshwater percentages in the pore waters in the sedimentary layers of the IHS at location 2.	34
3.1. Turbidity and average floc size for different particle concentrations.	67
3.2. Turbidity and average floc size under various saline conditions.	68
3.3. Turbidity and average floc size from a turbulent experiment .	69
3.4. Representation of turbidity under different environmental and bacterial conditions.	70
3.5. Representation of turbidity, average floc size and bacterial counts under various water discharges and turbulent energy levels.	71

LIST OF FIGURES

Figure	Page
1.1. Map of the study area.	9
1.2 An inclined tidal point bar deposit in the Shepody River Estuary with approximately 5 m of vertical surface and 26 m of horizontal surface. The white and yellow striped measuring tape at the far end of the sedimentary layers is 203 cm. Each step represents a single inclined seasonal unit. Migration of the channel may be confined because of the narrow channel due to the narrow meandering river. The resultant surfaces from accretion are limited in orientation such that dip obliquely down the meandering half of the river and they do not form lateral accretions (Lettley, 2004).	10
1.3. Macroflocs of approximately 5 cm in scale observed floating in muddy water (to the left). A loosely bound macrofloc mainly composed of clay and silt particles by the Scanning Electron Microscope (SEM) (to the right).	11
2.1. Location map of the Shepody River located in the northeast of Chignecto Bay.	36
2.2. Photograph of IHS deposit at location 1 showing the sampled layers correlated to their depths.	37
2.3. Photograph of IHS deposit at location 2 showing the sampled layers correlated to their depths.	38
2.4. Photograph of deposit in location 3 showing the inclined sampled layers correlated to their depths.	39
2.5. Correlation of δD and $\delta^{18}O$ in the pore waters of IHS from locations 1, 2 and 3. The shaded triangles represent the theoretical deuterium and oxygen-18 values that lie on the meteoric water line.	40
2.6. Variations of δD and $\delta^{18}O$ with depth of the IHS deposits from locations 1, 2 and 3.	41
2.7. The variations of isotopic signatures and corresponding annual precipitation record with time in locations 1, 2 and 3. The annual precipitation is obtained from the Alma weather station.	42

2.8. The variations of δD and salt ion concentrations in the IHS at location 2.	43
2.9. Time series of the annual precipitation (rainwater brought into the estuary by the fluvial system) and salt ion concentrations representing the marine water compositions.	44
2.10. The rate of change of freshwater (precipitation), salt ion concentrations and isotopic compositions (δD) through the layers of the IHS at location 2.	45
2.11. The rate of change of the derivatives of freshwater (precipitation), salt ion concentrations (Na and Cl) and isotopic compositions (δD) through the stratified layers of the IHS at location 2.	46
2.12. The annual deposition of fresh and marine-water mixing in the IHS of the Shepody River Estuary during recent years.	47
3.1. Map of Moncton and Riverside situated in the upstream of the Petitcodiac River, New Brunswick.	72
3.2. Macroflocs of approximately 5 cm in scale observed floating in muddy water (to the left). A loosely bound macrofloc mainly composed of clay and silt particles is being observed by the Scanning Electron Microscope (SEM) (to the right).	73
3.3. Time series of turbidity and average floc size with a range of particle concentrations.	74
3.4. Time series of turbidity and average floc size in different saline conditions.	75
3.5. Variations of turbidity and floc size with time from a turbulent experiment.	76
3.6. The internal structure of flocs from the basic flocculation experiment; A) a rod-shaped diatom B) a diatom C) The rod shaped in the left close to a u-shaped nematode in the right d) a zircon grain.	77
3.7. Internal constituents of flocs; A) a rod-shaped plankton; B) a phytolite present in the flocs taken from very saline waters; C) Sphaerotilus (a type of a long iron -bacteria) observed in flocs taken from dilute waters; D)Some organic scattered debris.	78
3.8. Time series of turbidity under different bacterial conditions.	79
3.9. Variation of turbidity levels by various turbulent energies.	80
3.10. Times series of bacterial counts and floc size under the influence of various	

turbulent energies.	81
3.11. Variations of log of bacterial counts and log of floc size with time under the influence of various turbulent energies.	82
3.12. Predicting the roles played by aggregation, sediment biota and their multiple interactions as well as their significant effects on sediment dynamics.	83

List of Appendices

	Page
Appendix 1. Grain size distribution in the Petitcodiac River system. The grain sizes of the sampled sediments were determined using a sedigraph.	88
Appendix 2. The annual precipitation data obtained from the Alma weather station. The amount of rain obtained from snow involved the following conversion: 1.5 cm of snow = 1mm of water.	87
Appendix 3. Age of deposition determined for the sedimentary layers of the IHS at Location 1 (top) and IHS at location 3 (bottom) by comparing the isotopic signature to the associated annual precipitation.	94

CHAPTER 1: INTRODUCTION

1.1 OPENING STATEMENT

An estuary is defined as “the seaward portion of a drowned valley system which receives sediments from both fluvial and marine sources and which contains facies influences by tide, wave and fluvial processes” (Dalrymple et al., 1992). This transition zone represents the primary sedimentary catchment in marginal marine settings (Nikol, 1991). Estuaries are complex because they act as depositional sinks and receive sediments from both fluvial and marine sources (Aston and Chester, 1976; Lettley et al., 2006). They are generally generated during sea level rise (Dyer, 1979). Thereby, they are ephemeral features (Fairbridge, 1980). Sediments are also transported seawards during flood stage to accumulate and form deposits in subtidal and intertidal settings at the head of the embayment (Dalrymple et al., 1990). They are deposited in the form of point bars (generally mud-dominated) (Knigton, 2984; Leeder, 1999; Pearson and Gingras, 2006). Three possible regions of deposition are: continental shelf, deep sea and estuary (Bogs, 2001). Continental shelves and deep seas accommodate a small percentage (an estimate of 10 %) of the sedimentary input; this leaves estuaries as the main areas of sedimentation because they offer shelters against strong waves and currents so that the fine-grained sediments settle (Postma, 1980). Also, the estuarine circulation traps sediments and reduces the transport of fine-grained sediments to the open sea (Kranck, 1981).

The accumulation processes assist in sediment supply resulting in the formation of estuarine environments and increasing the rate of estuary development (Postma, 1980). Some of the large space of accommodation of estuarine development is filled with a set of stacked sedimentary beds when sea-level increases during periods of transgression (Dalrymple, 1991). These sequences in the deposits can be rhythmic in their nature and provide good record of tidal cyclicities (Nio and Yang, 1999).

The turbidity maximum zone can play a crucial role in the enhancement and location of suspended load deposition during flood events (Thomas et al., 1987). During calm-water seasons, fine-grained suspended particles settle into the efficient sinks form mud blankets (Fan and Li, 2002). The fine grained particles may flocculate as a result of the

shear stress in flow (Dyer, 1979). Stormy seasons lead to erosion and suspension of the sediments near the bottom (Fan and Li, 2002).

1.2 THESIS OUTLINE

Chapter 1 is an introduction focusing on an opening statement, geological setting and objectives of the thesis.

Chapter 2 presents the use of stable isotopes (δD and $\delta^{18}O$) in establishing a recent salinity record from seasonal rhythmites. The isotopic signatures of the pore water in the interbeds of the IHS deposits in the Shepody River Estuary are compared to the local annual precipitation from Alma Station (about 45 km from Shepody River) to determine the age of each stratified layer. Comparing the isotope and precipitation trends to the historical salinity record can contribute to the depositional history of marine and fresh water mixing.

Chapter 3 documents the significance of micro-organisms during the formation of flocs. This chapter provides a description of three experiments that were conducted to examine the effects of physicochemical aggregation on turbidity, microbial effects on turbidity, and hydrodynamic effects on aggregation and the microbial community.

Chapter 4 is the conclusion or summary of the previous chapters discussing the significance of geochemical and microbiological parameters in the depositional systems.

1.3. GEOLOGICAL SETTING

The Petitcodiac River is located on the South East coast of New Brunswick and drains into the Bay of Fundy (Fig. 1.1). A causeway was built in 1968 approximately 22 km from the head of the tide and affected the physical and biological processes such as tidal exchange and sediment transport (AMEC Earth and Environmental, 2005). Moncton and Riverside (study areas) are located upstream of the Petitcodiac River approximately 50 km from the head of the tide. Silt is dominant in the sediments of these regions (60%). These sediments are also composed of 10 % clay and 30% sand (Appendix 1).

The Bay of Fundy is a large macrotidal estuary that supplies sediments to the Petitcodiac River at a rate of 2 Mm^3 per year (AMEC Earth and Environmental, 2005). A portion of the sediment that flows up into the river accumulates in the river banks

(AMEC Earth and Environmental, 2005). The funnel-shaped bay is 270 km in length and is divided into two smaller bays, Chignecto Bay and the Minas Basin.

The 107 km long, Chignecto Bay is a turbid estuary situated at the head of the Bay of Fundy (Amos, 1991). Chignecto Bay is surrounded by Paleozoic cliffs composed of mud stones and some sandstones. The sediments eroded from these cliffs are transported to the Chignecto Bay. Hence, the Bay is “muddy” (Amos, 1987; Pearson and Gingras, 2006).

The study area, the Shepody River Estuary is situated at the upper (North East) portion of Chignecto Bay and just below Shepody Bay (Fig. 1.1). It covers an area of about 51 km² at mean high tide and has a high sediment load of 21g/L (Pearson and Gingras, 2006). The sediments are fine-grained with mean values: 60% silt, 30 % clay and 10% sand (Appendix 1). The tidal point-bar deposits are made up of dipping, interbedded mud, silt and slightly sandy beds (Gingras and Bann, 2006). These tidal deposits are also known as Inclined Heterolithic Stratification and they range between 1 and 5 meters in height (Fig. 1.2). They are also laterally continuous (exposed over a horizontal distance of about 26 m) and their depositional surfaces are bioturbated (Choi et al., 2004; Pearson and Gingras, 2006).

1.4 INCLINED HETEROLITHIC STRATIFICATION (IHS)

Any heterogeneous siliclastic bed formed from inclined sediment layers that are deposited parallel to the strike of the layers is called an Inclined Heterolithic Stratification (IHS) (Thomas et al., 1987). Common sedimentary structures present in IHS include trough and planar cross-stratification, graded bedding, parallel laminations and ripple cross-lamination (Thomas et al., 1987; Pearson and Gingras, 2006). Trace fossils can also be seen in IHS beds deposited in estuarine settings (Gingras et al., 2002).

Inclined Heterolithic Stratification is mainly formed by lateral accretion of point bars in meandering channels (Choi et al., 2004). It is abundant in tidal settings (Thomas et al., 1987); the interbeds of the IHS in tidal settings result from tidal rhythmicity (Gingras et al., 2002). The sediment supply is altered by seasonal variations; this can be noticed from the stacked alternations of light (silt/sand-rich) and dark (mud-rich) layers.

Inclined Heterolithic Stratification has played an important role in the overall sedimentological understanding and economic significance of an outcrop (Thomas et al., 1987). The presence of IHS sets explains the local nature of sediment deposition (Gingras et al., 2002). The nature of the IHS is useful in predicting the stratigraphy and the hydrological characteristics of the estuarine deposition (Lettley et al., 2006). The occurrence of the IHS is also useful for the paleoenvironmental and paleogeographic reconstruction such as identifying river channels in coastal plain settings, predicting of their relative proximity to the shorelines and yielding approximate values for the magnitude of tidal changes experienced by the river channels (Thomas et al., 1987).

1.5 FLOCCULATION AND ITS SIGNIFICANCE

Flocculation (also known as aggregation and coagulation) is the formation of aggregates by collision and adhesion of smaller particles in suspension (Kranck, 1981). This process depends on suspended sediment concentrations, salinity, pH, temperature, organic matter and organisms (Milligan and Hill, 1998; Tisdall and Oades, 1982; Burban et al., 1989).

Two types of flocs are known to exist in estuaries: microflocs and macroflocs (Eisma, 1986). Microflocs have a maximum size of 125 μm and are composed of mineral particles and organic matter (Tisdall and Oades, 1982). These flocs are strong enough to withstand higher levels of turbulent energies (Dyer and Manning, 1999). Microflocs cluster further to form macroflocs (Fig. 3), also known as “marine snow” (Kranck and Milligan, 1980). The sizes of macroflocs range between 125 μm to about 3-4 mm. Because of their large size, they are fragile and can be broken down back into microflocs (Eisma, 1986; Dyer and Manning, 1999).

Flocculation affects the transport and deposition of suspended particles in estuaries because it modifies the texture of particles (Chen, 2005). Hence, the settling velocity of particles also varies with grain size (Fettweis et al., 2006). Generally, settling rates of particles increase due to aggregation (Kranck, 1981) resulting in the segregation of clay minerals in estuarine water (Algan et al., 1994). Thus, flocculation can play a vital role in the distribution of clay minerals (Feuillet and Fleischer, 1980). Coagulation also increases the trapping effect of estuarine circulation, which increases the accumulation

processes in the estuary (Kranck, 1981). Although the formation and break up of flocs can alter the sediment transport dynamics, sedimentation research has been restricted to characterizing suspended particles as primary for quite some time (Droppo and Ongley, 1994). However, the effect of flocculation on the sedimentology and geochemistry of estuaries received more attention over the recent years.

1.6 OBJECTIVES

The objectives of chapter 2 are to demonstrate that: (1) inclined heterolithic stratified deposits in the Shepody River Estuary exhibit a record of seasonal sedimentation, (2) the preserved mode of stratification is annual; and (3) comparing the annual isotopic signature to the salinity record preserved in the stratified estuarine sediments can better assist in the understanding of the depositional history of fresh and salt-water mixing in the estuary.

The objectives of chapter 3 are to: (1) determine the importance of bacteria in controlling the floc size and turbidity under various physicochemical parameters with time, and 2) develop a procedure for the artificial production of aggregates similar to the natural flocs under various hydrodynamics.

1.7. REFERENCES

- Algan, O., Clayton, T. Tranter, M. and Collins, M.B. (1994). Estuarine mixing of clay minerals in the Solent region, southern England. *Sedimentary Geology*, 92, 241-255.
- AMEC Earth and Environmental. (2005). *Environmental Assessment report for Modifications to the Petitcodiac River Causeway*. (Technical Report Series, YB299A, TE23520.4). A division of Amec Americas Limited. Submitted to New Brunswick Department of Supply and Services.
- Amos, C.L. (1987). Fine-grained sediment transport in Chignecto Bay, Bay of Fundy, Canada. *Continental Shelf Research*, 7, 1295-1300.
- Amos, C.L, Tee, K. T. and Zaitlin, B. (1991). The post-glacial evolution of Chignecto Bay, Bay of Fundy, and its modern environment of deposition. In: *Clastic tidal sedimentology*. (Ed. Smith, D., Reinson, G., Zaitlin, B., Rahmani, R). Canadian Society of Petroleum Geologists. Memoir 16. pp 59-90.
- Aston, S. R. and Chester, R. (1976). Estuarine sedimentary processes. In: *Estuarine chemistry*. (Ed. Burton, J.D. and Liss, P. S). Academic Press Inc, London. pp 37-52.
- Boggs, S. (2001). Principles in Environmental Interpretation and Classification. In: *Principles of Sedimentology and stratigraphy*. (Ed. Boggs, S.). Prentice Hall, New Jersey. pp 25-56.
- Burban, P., Lick, W. and Lick, J. (1989). The flocculation of fine-grained sediments in estuarine waters. *Journal of Geophysical Research*. 94, 8323-8330.
- Chen, M.S., Wartel, S. and Temmerman, S. (2005). Seasonal variation of flocc characteristics on tidal flats, the Scheldt estuary. *Hydrobiologia*, 540, 181-195.
- Choi, K.S., Dalrymple, R.W., Chun, S.S. and Kim, S. (2004). Sedimentology of modern, inclined heterolithic stratification (IHS) in the macrotidal Han River delta, Korea. *Journal of Sedimentary Research*, 74, 677-689.
- Dalrymple, R. W, Knight, R., Zaitlin, B. A, Middleton, G.V. (1990). Dynamics and facies model of a macrotidal sand-bar complex, Cobequid Bay-Salmon River Estuary (Bay of Fundy). *Sedimentology*, 3, 577-612.
- Dalrymple, R. W., Makino, Y. and Zaitlin, B. A. (1991). Temporal and spatial patterns of rhythmic deposition on mud flats in the macrotidal Cobequid Bay Salmon-River Estuary, Bay of Fundy, Canada. In : *Clastic tidal sedimentology* (Ed. Smith, D.G., Zaitlin, B. A., Reinson, G.E. and Rahmani, R.A. Canadian Society of Petroleum Geologists. Memoir 16. pp 137-160.
- Dalrymple, R.W., Zaitlin, B.A. and Boyd, R. (1992). Estuarine facies models: conceptual basis and stratigraphic implications. *Journal of Sedimentary Petrology*, 62, 1130-1146.
- Dronkers, J and van Leussen, W. (1988). Physical processes in estuaries: An introduction. In: *Physical processes in estuaries*. (Ed. Dronkers, J and van Leussen, W). pp 1-18.
- Droppo, I.G and Ongley, E.D. (1994). Flocculation of suspended sediment in rivers of Southeastern Canada. *Wat. Res.* 28 (8), 1799-1809.

- Dyer, K. R. (1979). Estuaries and estuarine sedimentation. In: *Estuarine hydrography and sedimentation*. (Ed. Dyer, K). Cambridge University Press. Great Britain. pp 1-18.
- Dyer, K.R. and Manning, A.J. (1999). Observation of the size, settling velocity and the effective density of flocs, and their fractal dimensions. *Journal of Sea Research*, 41, 87-95.
- Eisma, D. (1986). Flocculation and de-flocculation of suspended matter in estuaries. *Netherlands Journal of Sea Research*, 10 (2/3), 183-199.
- Fairbridge, R. W. (1980). The estuary: its definition and geodynamic cycle. In: *Chemistry and biogeochemistry of estuaries*.(Ed. Oalussion, E and Cato, I). John Wiley and Sons Ltd, Northern Ireland, pp 1-35.
- Fan, D. and Li, C. (2002). Rhythmic deposition on mudflats in the mesotidal ChangJiang estuary, China. *Journal of Sedimentary Research*, 72, 543- 551.
- Fettweis, M., Francken, F., Pison, V., Van den Eynde, D. (2006). Suspended particulate matter dynamics and aggregate sizes in a high turbidity area. *Marine Geology*, 235, 63-74.
- Feuillet, J. and Fleischer. (1980). Clay mineral distribution in James River Estuary, Virginia. *Journal of Sedimentary Petrology*, 50, 1, 267-279.
- Gingras, M.K., Rasanen, M. and Ranzi, A. (2002). The significance of bioturbated inclined heterolithic stratification in the Southern part of the Miocene Solimes Formation, Rio Acre, Amazonia Brazil. *Palaios*, 17, 591-601.
- Gingras, M.K. and Bann, K.L. (2006). The bend justifies the leans: Interpreting recumbent ichnofabrics. *Journal of Sedimentary Research*. 76, 483-392.
- Hoefs, J. (1997). Theoretical and experimental principles. In: *Stable isotope geochemistry*. (Ed. Hoefs, J.). Springer –Verlag, Germany, p 1-26.
- Knighton, D. (1984). Sediment deposition. In: *Fluvial forms and processes*. (Ed. Knighton, D), The Chaucer Press, Great Britian, p 81-84.
- Krank, K. (1981). Particulate matter grain-size characteristics and flocculation in a partially mixed estuary. *Sedimentology*, 28:107-114.
- Krank, K. and Milligan, T. (1980). Macroflocs: Production of marine snow in the laboratory, *Marine Ecology- Progress Series*, 3, 19-24.
- Leeder, M. (1999). Rivers. In: *Sedimentology and sedimentary basins: From turbulence to tectonics* (Ed. M. Leeder), The Blackwell Science, U.K., p 307-329.
- Lettley, C. D., Pemberton, S. G., Gingras, M. K., Ranger, M. J. and Blakney, B.J. (2006). Integrating sedimentology and ichnology to shed light on the system dynamics and paleogeography of an ancient riverine estuary. In: *Applied Ichnology, Society of Economic Paleontologists and Mineralogists short course notes*. (Ed. MacEachern, J.A., Bann,K.L., Gingras, M.K. and Pemberton, S.G.), p 142-160.
- Milligan, T.G. and Hill, P.S. (1998). A laboratory assessment of the relative importance of turbulence, particle composition, and concentration in limiting maximal floc size and settling behaviour. *Journal of Sea Research*, 39, 227-241.

- Nikol, S. (1991). Zonation and sedimentology of estuarine facies in an incised-valley, wave-dominated, microtidal setting, New South Wales, Australia. In: *Clastic tidal sedimentology*. (Ed. Smith, D., Reinson, G., Zaitlin, B. and Rahmani, R.). Canadian Society of Petroleum Geologists. Memoir 16. pp 41-57.
- Nio, S. and Yang, C. Diagnostic attributes of clastic tidal deposits: a review (1991). In: *Clastic tidal sedimentology*. (Ed. Smith, D., Reinson, G., Zaitlin, B., Rahmani, R.). Canadian Society of Petroleum Geologists. Memoir 16. pp 3-28.
- Pearson, N. and Gingras, M. (2006). An ichnological and sedimentological facies model for muddy point-bar deposits. *Journal of Sedimentary Research*, 76, 1-12.
- Postma, H. (1990). Sediment transport and sedimentation. In: *Chemistry and biogeochemistry of estuaries*. (Ed. Oalussion, E. and Cato, I.). John Wiley and Sons Ltd, Northern Ireland, p 153-186.
- Tisdall, J. M. and Oades, J.M. (1982). Organic matter and water-stable aggregates in soils. *Journal of Soil Science*, 33, 141-163.
- Thomas, R.G., Smith, D.G., Wood, J.M., Visser, J., Calverley-Range, E.A. and Koster, E.H. (1987). Inclined Heterolithic Stratification - terminology, description, interpretation and significance. *Sedimentary Geology*, 53, 123-179.

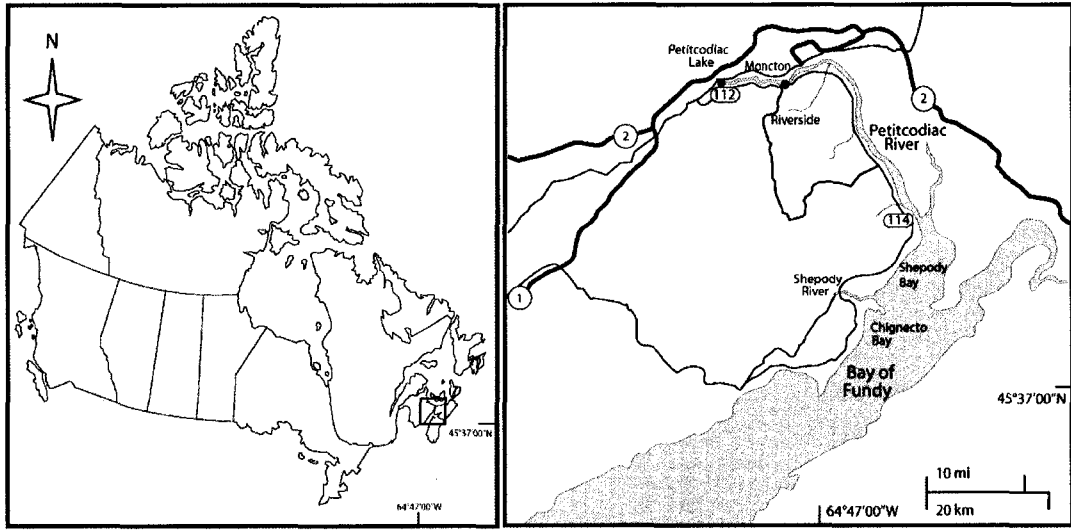


Figure 1.1. Map of the study area.



Figure 1.2. An inclined tidal point bar deposit in the Shepody River Estuary with approximately 5 m of vertical surface and 26 m of horizontal surface. The white and yellow striped measuring tape at the far end of the sedimentary layers is 203 cm. Each step represents a single inclined seasonal unit. Migration of the channel may be confined because of the narrow channel due to the narrow meandering river. The resultant surfaces from accretion are limited in orientation such that dip obliquely down the meandering half of the river and they do not form lateral accretions (Lettley, 2004).

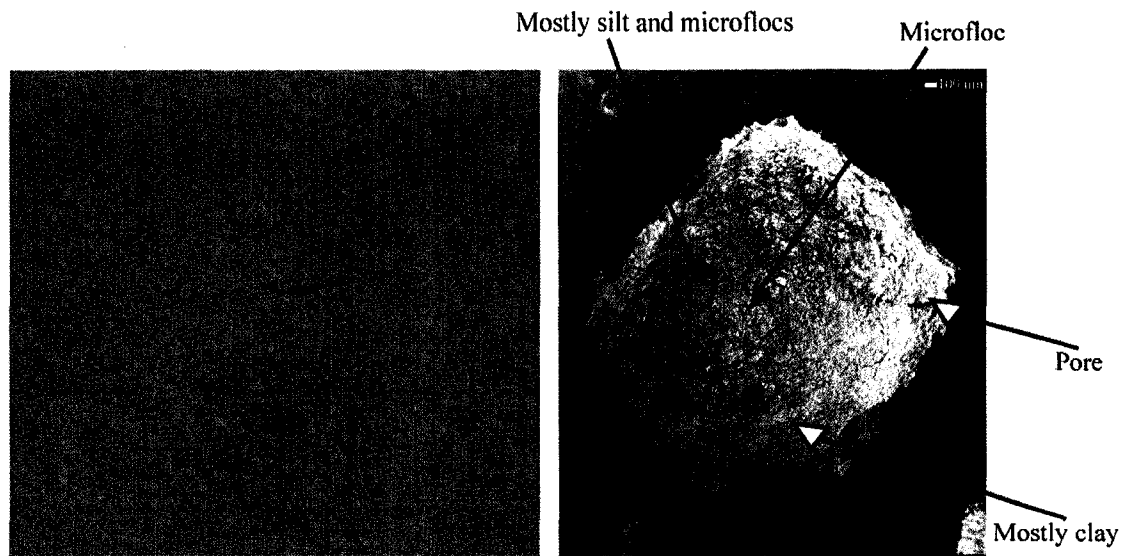


Figure 1.2. Macroflocs of approximately 5 cm in scale are observed floating in muddy water (to the left). A loosely bound macrofloc mainly composed of clay and silt particles observed by the Scanning Electron Microscope (SEM) (to the right).

CHAPTER 2. ESTABLISHING A RECENT SALINITY RECORD FROM SEASONAL RHYTHMITES OF THE SHEPODY RIVER, NEW BRUNSWICK, CANADA.

2.1. INTRODUCTION

It is difficult to assess the time represented by stratification styles and deposit types observed in the sedimentary record. In general, sediments that are transported into estuaries and deltas are deposited in the form of point-bars on the interior curve of channels (Knighton, 1984; Leeder, 1999), or in longitudinal bars that form amid channels (Boggs, 2001). These deposits are built seaward by the migration of channels (Friedman et al., 1999) and aggrade due to the accumulation of flocculated materials and “traction-borne” sediments carried onto the bar surface during the rising and falling of tides (Knighton, 1984). Some fine materials are carried in suspension by over-bank flood waters and accumulate on the adjacent tidal flat during periods of slack water either as silt and clays or fine and medium sand (Pearson and Gingras, 2006). When point-bars and longitudinal bars build up laterally, they develop inclined sedimentary surfaces. When these inclined units comprise alternations of sand and mud, they are referred to as Inclined Heterolithic Stratification (IHS) (Thomas et al., 1987). The individual inclined units of IHS are rhythmic in their nature (Pearson and Gingras, 2006), and they can represent seasonal layering (Gingras, et al., 2002).

δD , $\delta^{18}O$ and salinity are conservative tracers that can be modified rapidly by evaporation, precipitation and mixing with marine waters (Benway and Mix, 2004). Interestingly, on a global scale, a positive relation exists between δD , $\delta^{18}O$ and precipitation (Arnason and Sigurgeirsson, 1966; Dansgaard, 1975; Merlivat and Jouzel, 1979). Precipitation (rain or snow) is the result of cooling of vapour mass. Storm clouds that form at higher latitudes tend to cool and precipitate water. Isotopes are enriched due to the fractionation between vapour and condensing phases during the cooling of vapour mass (Hoeffs, 1997). Therefore, isotopically enriched rain forms and falls from a diminishing vapour mass, and the residual vapour becomes isotopically depleted. This is known as the Rayleigh distillation process (Clark and Fritz, 1997). δD and $\delta^{18}O$ are also enriched in seasons with less rain because evaporation during rainfall imparts a kinetic fractionation, a unidirectional process that separates isotopic molecules from each other

by their mass differences, on the drops (Hoefs, 1997; Clark and Fritz, 1997). During the process of evaporation, isotopically-lighter water molecules (^{16}O) evaporate more rapidly than the isotopically-heavier water molecules (^{18}O). Hence, when oxygen isotopes fractionate, the clouds and atmosphere become enriched with ^{16}O (Hoefs, 1997). Areas characterized by high rainfalls are not affected by this process, which is called “amount effect” (Clark and Fritz, 1997). A positive relationship also exists between salinity and evaporation, and in areas of fresh and salt-water mixing, reduced fresh-water input results in less freshening of the marginal-marine seawater (Schone et al., 2003).

The aim of this paper is to use the isotopic tracers and the precipitation record to show that: (1) inclined heterolithic stratified deposits in the Shepody River Estuary are records of seasonal sedimentation, (2) the preserved mode of stratification is annual; and, (3) the salinity record preserved in the stratified estuarine sediments can assist in the understanding of the depositional history of fresh and salt-water mixing in the estuary.

The Shepody River in New Brunswick (Fig. 2.1) was chosen as the study area for its well-displayed strata exposed in deeply incised tidal creek cut banks. The area is accessible and its size manageable, covering an area of approximately 51 km² at mean high tide (Pearson and Gingras, 2006), so, sampling across the estuary is possible. Strata exposed at Shepody River are of two types; (1) cm to dm- scale horizontally bedded, mud-dominated, intensely bioturbated mudflat deposits; and (2) cm to dm scale, gently inclined burrowed to laminated silts and sandy silts that represent IHS. This study focuses on the isotopic signatures and salinity record within the IHS.

2.2. METHODS

2.2.1. Field sampling

Field sampling was conducted on exposed sections of the point bar deposits at 3 locations in the Shepody River Estuary. Twenty-five cm long x 5 cm diameter cores were used for the sampling of 2 point-bar deposits in May, 2005. The cores were inserted horizontally into each bed of the deposits (Fig. 2.2; Fig. 2.3). The two ends of the cores were closed with caps and taped tightly on their open ends.

Because of the excellent exposure of freshly exposed stratification at Location 3, plastic bags were used to collect sediments from each IHS beds (Fig. 2.4). Approximately

800 g of sediments was collected from each bed. Sample bags were placed into larger plastic bags and tightly sealed. Finally, all of the plastic bag and core samples were placed in air-tight containers for shipping.

2.2.2. Laboratory analysis

The sediment from Locations 1 and 2 was removed from the middle part of the cores (~ 15-17 cm) because the parts at either ends of the cores were susceptible to oxidation and evaporation. These sediments were cohesive and yielded small quantities of water (a few ml) extracted by centrifugation. The sediments from Location 3 were soupy and upon centrifugation yielded 50 ml of water.

2.2.2.1. Stable isotopes (δD and $\delta^{18}O$)

The water samples were analyzed for their hydrogen isotopic composition using the water reduction zinc method following similar procedures as Coleman et al. (1982) as well as Horita and Kendall (2004). Approximately 0.25 g of zinc was weighed into each reaction vessel, which was then warmed to about 100°C on a vacuum line, using a hot air gun, to clean the zinc. Then, 3 μ L of water sample was introduced into the bottom of the vessel using a syringe. The vessel was reattached to the vacuum line and the water sample was frozen with liquid nitrogen to evacuate the vessel. The evacuated vessel containing zinc and the water sample was detached from the vacuum line and heated at 450° – 500 °C for about 20 minutes: this releases Hydrogen (H_2) of identical isotope concentration to that of the original water: (i.e. $H_2O_{(liquid)} + Zn_{(solid)} \rightarrow ZnO_{(solid)} + H_{2(gas)}$). The H_2 was subsequently analyzed for δD using a Finnigan Mat 252 Isotope Mass Spectrometer.

To analyze for $\delta^{18}O$, the carbon dioxide – water equilibration or “Epstein-Mayeda” procedure was used (Horita and Kendall, 2004). One ml of water sample was introduced into the bottom of a reaction vessel before attaching it to a vacuum line. Because of the limited amount of pore water extracted from the sediments, not all water samples could be analyzed for $\delta^{18}O$. Carbon dioxide (CO_2) was frozen in the vessel and separated from the water sample by freezing the vessel with liquid nitrogen to avoid contamination with atmospheric nitrogen. The water samples were then frozen in CO_2 . $^{18}O/^{16}O$ ratio of water was determined by equilibration of a small amount of CO_2 with a

surplus amount of water at 25°C. The carbon dioxide was then analyzed for $\delta^{18}\text{O}$ using the Isotope Mass Spectrometer.

ALB.003 was used as a standard for the analyses of δD and $\delta^{18}\text{O}$. The δD and $\delta^{18}\text{O}$ values presented are relative to Vienna – Standard mean Ocean Water (V-SMOW) with a standard error of +/- .15.

2.2.2.2. *Salinity*

The dissolved ion concentration of Na and Cl in the pore waters of the sediments from Location 2 were determined in the Slowpoke Nuclear Reactor Facility at the University of Alberta using Neutron Activation Analysis (NAA). Neutron Activation Analysis is a sensitive technique used for determining certain element concentrations in solid, liquid or gaseous samples. This nuclear process uses the absorption of neutrons to generate radioactivity in a sample. The gamma spectrometry measures the resulting radioactivity where elements such as Sodium (Na) and Chlorine (Cl) can be identified and quantified. Sodium (Na) and Chlorine (Cl) were measured with a standard error of +/- 1σ and a confidence limit of 68%.

2.3. RESULTS/ OBSERVATION

2.3.1 *Field observations*

In general, the IHS deposits of the Shepody River Estuary consist of laminated and bioturbated beds. The sedimentary layers comprise of silty and sandy mud and their thicknesses are between 8 and 25 cm. The IHS observed in the 3 locations are 1 to 5 m high. Visual observations show that the burrowed beds are slightly sandy when compared to the laminated beds, which are slightly silty. Planar laminations and soft sediment deformations are also encountered. The upper 0 to 23 cm is observed to be red-brown in colour. The medial parts of the sections are characterized by dark-brown laminated and burrowed sediments (Fig. 2.2). The lower parts (approximately 145 to 193 cm) are dark brown. The studied IHS sediments at location 3 are water-rich compared to the IHS at locations 1 and 2. Laminations and soft sediment deformations are not easily observed in location 3 (Fig. 2.4).

2.3.2. *δD and $\delta^{18}\text{O}$*

As shown in Table 2.1 and Figure 2.5, most deuterium and oxygen isotope values of the sediments from the IHS of the Shepody River lie below the meteoric water line. The Global Network of Isotopes in Precipitation (GNIP) is a world wide survey conducted by International Atomic Energy Agency (IAEA) and World Meteorological Organization (WMO) on the hydrogen and oxygen content in precipitation on a global scale. Deuterium and oxygen isotopes data are presented on the GNIP maps to record the distribution of water isotope ratios. The pore waters present in the IHS in locations 1 and 2 (Table 1) are isotopically richer (-5 to -34 ‰ for δD and -2.3 to -3.1 ‰ for $\delta^{18}O$) when compared to the δD and $\delta^{18}O$ values on the GNIP maps of North America, New Brunswick (-38 to -70 ‰ for deuterium and -6 to -10 ‰ for oxygen-18) (IAEA, 2001). However, the pore waters of location 3 possess δD values (-18.2 to -48.9 ‰) that are isotopically similar to those on the GNIP map. The oxygen isotopic values measured from the pore waters of location 3 (-1.4 to -6.7‰) are consistent with those on the GNIP maps (IAEA, 2001).

Table 2.2 and Figure 2.6 represent the deuterium and oxygen-18 isotope trends in the stratified layers of the estuarine deposits at locations 1, 2 and 3. The δD and $\delta^{18}O$ trends are similar to each other particularly at location 3. At location 1, δD peaks at layer 4 (-13.4 ‰) and abruptly decreases to -27 ‰ in layer 5. δD and $\delta^{18}O$ increase steadily from layers 5 to 7 (Fig. 2.6). The relation of δD and $\delta^{18}O$ is not as strong as in locations 1 and 3. δD increases dramatically within the first six layers (-5.5 ‰) and there is an abrupt decrease at layer 7 (approx. -28 ‰). It rises again in layer 8 (-5 ‰), subsequently decreases from layers 8 to 12, and climbs again to layer 13 (Fig. 2.6). $\delta^{18}O$ also increases from layer 5 to 6 (-2.3 ‰) and it gradually decreases to -2.4 ‰ at layer 8. δD and $\delta^{18}O$ appear to be decoupled at layers 7 and 8 (Fig. 2.6). At location 3, both δD and $\delta^{18}O$ increase from layer 2 to layer 3 and decrease steadily onto the preceding layers. They are fairly constant till layer 9 and drop again to layer 11. Decoupling of δD and $\delta^{18}O$ is also noticeable in layer 6 (Fig. 2.6).

2.3.3. Annual Precipitation

The annual precipitation data listed in Table 2.2 and Appendix 2 were obtained from the Alma weather station (Fig. 2.1) in the Atlantic Climate Centre, approximately 45 km from Shepody River (Environment Canada, 2004). The IHS deposits at locations

1, 2 and 3 were sampled in the summer of May 2005 and September 2006. Assuming that the top layers were formed within the year that they were sampled or prior to the field sampling, attempts were made to correlate the most recent precipitation data to the isotopic compositions in the layers. This was done by correlating the top most layers with the most recent precipitation data (year of sampling) and correlating the sedimentary layers below to the preceding precipitation data (Table 2.2). The precipitation data from the Alma station (Appendix 1) represent the fresh water input contributed to the Shepody River Estuary by the fluvial system and show some correspondence to the deuterium values present in the pore waters of the IHS layers.

At location 1, δD in layer 1 does not correspond to the annual precipitation in 2005. However, change in the δD trend between layers 3 and 7 correspond to the change in the annual precipitation between 2003 and 1996. δD increases within the first four layers (approx. -13 ‰), drops at layer 5 (approx. -27 ‰), and gradually increases at layer 7 (Fig. 2.7). The annual precipitation increases from 2003 to 2002 which correspond to layers 3 and 4. A decrease in precipitation is seen in the year 2001 (corresponding to layer 5) and an increase for the remaining years that correspond to layers 5 to 7 (Fig. 2.7). At Location 2, both δD and correlative precipitation are high (approx. -24 ‰, 1631.6 mm) at layer 2 (corresponds to year 2002) and drop abruptly at layer 3 (-30 ‰, 977.2 mm). Subsequently, δD and the conterminous precipitation data from the Alma weather station increase to layer 6 (corresponds to year 1997) and fall again to layer 7 (-28 ‰, 1146.8 mm). They are high at layer 8 (approx. -5 ‰, 1513 mm), descend progressively through layers 9 to 12 (1995 to 1992), and increase again at the oldest layer (Fig. 2.7).. At location 3, δD is highest at layer 3 (-18.2 ‰); it falls steadily to layer 6 (-49 ‰), increases again at layer 8 (-30.6 ‰), and unlike observed with precipitation, it falls slightly to layer 10 (- 35.4 ‰). The annual precipitation data between 2005 and 1997 corresponds to the δD values between layers 1 and 9 and show an increase in trend at layer 4 (approx. 1600 mm) and a decrease (1146 mm) at layer 5. They also show a peak at layer 8 (1557.5 mm), a slight drop at layer 9 (1486.9 mm) and a final increase at layer 10 (Fig. 2.7).

Table 2.1 and Figure 2.7 also show that the pore waters in layers 3 and 12 of the IHS sets at Location 2 have the lowest δD values for the lowest precipitation amounts in

2001 and 1991. At Location 3, the lowest precipitation in 2004 and 2001 contained the lowest δD values (Fig. 2.7).

2.3.4. Salinity (*Na and Cl*)

The Na concentrations retained in the pore water of the sedimentary layers from the IHS deposits of Location 2 vary between 8000 and 9700 ug/mL (Table 2.3) and is somewhat lower than the Na concentration in seawater (~10,760 ug/mL). The Cl concentration in pore waters (16,000- 17,800 ug/mL) (Table 2.2) are also similar to that of marine water (~19,350 ug/mL) (Drever, 1997; Burton, 1976; McSween et al., 2003a). Table 2.3 shows estimates of concentrations and percentages of salt ions incurred in the pore waters relative to sea water salt ion concentrations (~10,760 ug/mL of Na and (~19,350 ug/mL of Cl). Figure 2.8 and Fig. 2.7 demonstrate a strong inverse relationship between the salt ions and the isotopic ratios at location 2. The Na and Cl concentrations of the pore water samples are highest in the first layer and descend steeply to reach their lowest values in the second layer. They then increase to layer 4 and fall slightly to layer 5. Na and Cl ions are fairly constant between layers 5 and 7. They ascend to layer 12 and drop to layer 13 (Fig. 2.8). δD peaks slightly at layer 2 (-24 ‰); it falls to layer 3 (approx. -30‰) and increases steadily to layer 6. It drops abruptly at layer 7 and ascends to layer 8 (approx. -5 ‰). It then falls to layer 12 (approx. -25 ‰) and increases to layer 13 (Fig. 2.8).

2.4. INTERPRETATION

2.4.1. δD and $\delta^{18}O$

The isotopic ratios of the pore waters extracted from the sedimentary layers of the IHS from the three locations are isotopically lower and most of them lie below the meteoric water line (Fig. 2.5). δD and $\delta^{18}O$ are sensitive to the contribution of fresh-water mixing, diffusion, evaporation and local runoff (Ingram et al., 1996). In this case, marine and fresh-water mixing in the pore waters plays a dominant role in the negative shifting of deuterium and oxygen-18 values below the meteoric water line. The pore waters which are the seawater-freshwater mixing zones are controlled by the amount of freshwater delivered into them (Schone et al., 2003). The heavy rainfalls brought into the pore

waters tend to be more negative in isotopic compositions shifting the deuterium and oxygen-18 values below the meteoric water line.

2.4.2. Annual precipitation

The annual precipitation data show a strong correspondence to the isotopic compositions present in the sedimentary layers of the IHS (Fig. 2.6; Fig. 2.7). The strong, positive relation of the isotopic compositions and the corresponding annual precipitation (Table 2; Fig. 2.6; Fig. 2.7) suggests that the δD and $\delta^{18}O$ values reflect a mixing relationship between the marine waters and local runoff. The heavy rainfalls mixed in the pore waters of these estuarine sediments tend to be more negative in isotopic compositions. Thus, intense rains tend to deliver more runoff that has more negative isotope values (Schone et al., 2003). The fresh water fluctuates seasonally in the Shepody River Estuary and the Bay of Fundy, with maximum amounts of rainfalls flowing during winter to late spring due to precipitation and melt water runoff (Ingram et al., 1996). Thus, the isotopic ratios in Figure 2.7 also vary in response to the corresponding annual precipitation that is brought into the pore waters by the fluvial systems. Figures 2.6 and 2.7 also support the hypothesis that the individual inclined units of IHS are can represent seasonal layering and the age of these annual stratified units can be determined by comparing the isotopic composition trends to the annual precipitation records. The more negative isotopic compositions present in the least precipitation amounts in layers 3 and 13 may be a result of mixing of diffused ground water or surface water with the pore waters.

2.4.3. Salinity (Na and Cl)

A poor correlation between salt concentrations and isotopic compositions is evident in Figure 2.8. However, the relation between the salt ion concentrations and the annual precipitation is somewhat stronger (Fig. 2.9). The salt ion concentrations in the pore waters somewhat correspond inversely to the associated annual precipitation (Fig. 2.9). The Na and Cl concentrations of the pore water samples are highest in the first layer and descend steeply to reach their lowest values in the second layer. They then increase to layer 4 and fall slightly to layer 5. Na and Cl ions are fairly constant between layers 5 and 7. They ascend to layer 12 and drop to layer 13 (Fig. 2.9). The concurrent precipitation comparatively shows a peak at layer 2 and a steep fall at layer 2. It also

shows an increase at layer 6 and a drop at layer 7; another increase at layer 10, a decrease at layer 12 and a final rise at layer 13 are also observed (Fig. 2.9).

Like isotopic compositions, salinity is very sensitive to the changes in fresh water influx in to the Shepody River Estuary. The high amounts of rainfalls from early spring to late winter result in decreasing the salinity in the Shepody system (Ingram et al., 1996). Fine-grained particles (silt and clay) are brought into the upper estuary by the fresh water system during suspension (Knighton, 1984). These suspended particles trapped by the estuarine circulation at the head of the estuary (Kranck, 1981) stick together to form aggregates and settle as the current decreases. The settling of flocs out weighs clastic deposition (Lettley, 2004). The rapid sedimentation by the settling of flocs during slack tide periods has the ability to trap pore water in the large spaces between the settling flocs (Pearson and Gingras, 2006). Thus, settled muds accumulate with “ambient” water that will likely accumulate in the deposited mud due to the low permeability of the aggregates (Lettley, 2004). During late summer, the estuarine system is more saline; salinity shifts landward resulting in maximum salinity conditions in the estuary (Ingram et al, 1996). The clastic suspended particles are more susceptible to flushing that settling as flocs.

Variations of salt ion concentrations in pore water as well as the annual precipitation record studied here clearly indicate annual fluctuations and the age of the sedimentary layers can be discerned by inferring the precipitation to the sedimentary units. Thus, comparing the salinity record and isotope signatures to the correlative annual local precipitation can contribute to the depositional history of the IHS.

2.4.4. Derivatives of precipitation, salt ion concentrations (Na and Cl) and isotopic compositions (δD)

Further evidence is shown in Figure 2.10 and Table 2.3 for the earlier noted relation between the salt concentrations and associated annual precipitation records as well as isotopic compositions and annual precipitation data. Figure 2.10 compares the rate of change of fresh water input to the rate of change of salt concentrations and deuterium values through the inclined, stratified layers. The rate of change of the concentrations of salt ions, δD and the conterminous precipitation data is derived by taking the difference of the salt ion concentrations, deuterium compositions or the precipitation values in the top layers from the bottom layers. The rate of change of

rainfall waters brought in by the fluvial system is high at the first layer; it abruptly decreases at layer 2 (est. year 2002) and suddenly jumps to layer 3 (Fig. 2.10). The derivative values of the rainfalls stored in the IHS layers gradually decrease to layer 5 (inferred as year 1999); a sharp fall is noticed in layer 6 followed by a precipitous jump at layer 7. They steadily decrease in layer 10 (speculated as year 1994) and ascend to layer 12 (Fig. 2.10). The concentration gradients (rate of change) of Na and Cl salt ions fluctuate annually through layers due to the contribution of annual rainfalls into the Shepody River Estuary. The rainfall waters are delivered by the fluvial system when the IHS deposits are exposed during low tides and they dilute the pore water in the IHS layers. Thus, the rate of change of the amount of rainfall contributed to the estuarine waters is inversely proportional to the concentration gradients of the salt ions (Na and Cl). In contrast to the trends of the derivatives of annual precipitation data, the concentration gradients of Na and Cl abruptly increase at layer 2 and gradually fall to layer 4. They decrease very slowly to layer 7 (deduced as year 1997), gradually increase at layer 10 and falls to layer 12 (Fig. 2.10).

The rate of change of δD is linearly related to that of the concomitant precipitation. A decrease in δD and associated annual precipitation data is noticed in layer 2. A sudden increase in layer 3 followed by a slight decrease in layer 4 (inferred as year 2000) is seen in the δD and precipitation trend (Fig. 2.10). The derivatives of δD and corresponding precipitation data jump slightly in layer 5, decrease rapidly in layer 6, increase rapidly in layer 7 and fall steeply in layer 8 (inferred as 1997). A gradual increase in both δD and conterminous annual precipitation trends is seen from layer 8 to layer 12. Although the pore waters contain the lowest isotopic compositions for the lowest precipitation in layers 3 and 13 (Table 2.2; Fig. 2.7) the rate of change of the deuterium and precipitation values are linearly related in the years 2001 and 1991 (layers 3 and 13) (Figure 2.10). Hence, it is safe to assume that the factors that modify the isotopic compositions in layers coinciding with lowest precipitation do not affect the change in the isotopic compositions and the fresh water input in each inclined unit.

A strong inverse relation also exists between the second derivatives (rate of change of the derivatives) of the curves of salt ions (Na and Cl) and amount of fresh water that is brought in to mix with the pore waters by the Shepody River (Table 2.3; Fig.

2.11). The second derivatives are derived by taking the difference of the first derivatives of the salt concentrations or annual precipitation from one layer to the previous layer. Although derivatives indicate the extent to which the variables are increasing or decreasing, the second derivatives control whether the rate of variables will increase, decrease or remain the same. The increase of the rate of change of the derivatives of precipitation in the second layer (est. year 2002) is very sharp (Fig. 2.11). It abruptly decreases in layer 3, gradually increases to layer 4 and falls to layer 5 (inferred as year 1999). The second derivatives of the inferred precipitation accelerate to layer 6, suddenly fall to layer 7 (est. year 1997) and gradually increase to layer 10 (Fig. 2.11). However, the rate of change of the concentration gradients of Na and Cl ions decrease abruptly in layer 2 and steadily increases to layer 4 (inferred as year 2002). It steadily decreases to layer 6, slightly increases to layer 7 and gradually falls to layer 10 (Fig. 2.11).

Unfortunately, the relation is weak at layer 4 (depth of 49 cm). This may be coincidental or probably due to diffusion of the salt ions from a higher concentration to a lower concentration (Palmer, 1996). Nevertheless, the depositional history of salt and fresh water mixing can be better understood by comparing the salinity records to the annual fresh water input.

A linear relationship also exists between the rate of change of the derivatives of δD and associated annual precipitation (Fig. 2.11). An increase in the second derivatives of δD and corresponding annual precipitation is noticed in layer 2 with a decrease in layer 3 (inferred as year 2001). A gradual increase is seen in layer 4 followed by a fall in layer 5 (Fig. 2.11). A steep rise in δD and concurrent annual precipitation is noticeable in layer 6 followed by a sudden fall in layer 7 (inferred as year 1998) and a gradual increase from layer 8 to layer 10. The negative deuterium values that correspond to the small amount of precipitation do not affect the rate of change of the derivatives of isotopic compositions and annual freshwater input seen in the sedimentary layers through the years.

2.5. DISCUSSION

Deducing the years in which recent beds of the IHS were deposited can help establish sedimentation rates; useful data for stratal correlation can be derived as well. In this case, IHS are reported to be formed by annual deposition of mud and silt deposited in

the form of point bars instead of deposition of grain particles during neap tide cycles. This information can easily help to determine the accumulation rates and can contribute to the correlation of sedimentary beds of similar ages. Moreover, the suggested method can deduce the ages of most recent stratigraphic horizons for which not many dating methods can be used. By determining the ages of sedimentary horizons, useful data regarding local sedimentation rates, changes in depositional configuration and stratal correlation can be derived. Comparisons of isotopic signals and salinity records with the annual precipitation data of the local area can identify intervals of equivalent ages (Isochrons), which can be used to establish a stratigraphic framework and thereby represent tools to discern sediment distribution patterns through time. The established framework can be compared to sedimentary deposits (in this case IHS) of a similar age. This can be seen in Appendix 3 in which the age of deposition is inferred to the sedimentary layers of the IHS at locations 1 and 3 in the Shepody River Estuary. In this way, it is possible to consider the context of a sedimentary accumulation with regards to the sedimentary history of an entire coastline.

As discussed earlier, the fresh water influx fluctuates annually in the Shepody River Estuary (Fig. 2.7) with presumably maximum amount of precipitation during winter to late spring due to heavier rainfall and runoff of oversaturated water. Both salinity and isotope values show large annual fluctuations in response to changes in fresh water input into the estuary (Fig. 2.7; Fig. 2.9; Fig. 2.10; Fig. 2.11).

The fine-grained particles (silt and clay) that are brought into the upper estuary stick together to form flocs and their settling speeds increase (Milligan et al., 2001). The rapid sedimentation by the settling of flocs during slack tide periods has the ability to trap pore water in the large spaces between the settling flocs (Pearson and Gingras, 2006). Thus, settled muds accumulate with “ambient” water that will likely accumulate with the deposited mud due to the low permeability of the aggregates (Lettley, 2004). Thus, the isotopic signal varies with the fluvial/ Bay mixing that resulted by the oversaturation of water from the rainfalls delivered by the Shepody River.

Figure 2.12 summarizes the deposition of the salt and fresh-water mixing in the IHS. The Na ion concentrations and corresponding precipitation trends show an inverse relation in the stratified layers of the IHS in location 2. The deuterium isotopes and the

associated precipitation data show a linear relation. This is because the pore waters are diluted by the local runoff as a result of the fresh water brought in by the fluvial system. The variations of the Na salt ion concentrations in the pore waters of the IHS units and the corresponding fresh water (rainwater and snow) delivered annually into the estuary clearly indicate annual deposition of the IHS beds. Hence, the year of deposition of each recent stratified beds can be inferred

The weak relation between the Na ion concentrations and amount of fresh water stored in the pore waters between 49 and 87.2 cm (layer 4 to layer 6) in Figure 2.9, Figure 2.10, Figure 2.11 and Figure 2.12 may be due to slight modification of Na ions by diffusion as concentrations of salt ions tend to diffuse from regions of high concentrations to regions of low concentrations (Palmer, 1996; Hoefs, 1997; Fetter, 1999). Diffusion can become important in heterogeneous deposits such as IHS as fluids flow from permeable to less permeable strata (Palmer, 1996) although it can occur as long as a concentration gradient exists, even if the fluid is not moving (Fetter, 1999).

Diffusion can also cause significant isotope fractionations; light isotopes being more mobile are more affected by diffusion than heavy isotopes (Hoefs, 1997). Fick's law can be used to estimate how rapidly salt ions or isotopes diffuse annually through the layers by estimating the mass flux of the salt ion concentrations or isotopic compositions. Mass flux or diffusion flux (F) is the total mass of salt ion particles which move across a surface layer per unit time and is given by:

$$F = - D_{\text{efficient}} \times \frac{\Delta \text{Salt ion concentrations or isotope compositions}}{\Delta (\text{depth of each bed})}$$

The concentration gradient (rate of change of salt ion concentrations or isotope compositions with depth- cm^2/s) governs the mass flux of the system as the concentrations of salt ions diffuse through the layers (Palmer, 1996; Hoefs, 1997). The efficient diffusion coefficient or efficient diffusivity ($D_{\text{efficient}}$) for a porous media is derived from the below equation:

$$D_{\text{efficient}} = D \times \frac{\text{Porosity } (\phi)}{(\text{Tortuosity})^2 (\theta)^2}$$

The diffusion coefficients (D) for Na (1.0×10^{-7} cm²/s) and Cl (2.0×10^{-7} cm²/s) in pore waters (or pure waters) were acquired from Friedman et al. (2004) and Fetter (1999). Self-diffusion coefficient of water in pure water at 25°C was obtained from Tanaka (1978). Porosity (ϕ) is the percentage of sediments that is void of material (Charbeneau, 2000) and it varies with the textures of materials. In this study the porosity of silt (35-50 %) acquired from Fetter (2001) and Sen (1995) is used to estimate the diffusion flux of the salt ion concentrations. This is because silt is dominant in the sediments of the IHS of the Shepody River Estuary. Tortuosity (θ) is the measure of the mean additional distance when solutes travel between two arbitrary points in the pore water of the porous medium (Boudreau and Meysman, 2006). It depends on the porosity of the material in which the fluid moves. The tortuosity is estimated to be 1.647 by subtracting the natural log of the square of porosity from 1. The following equation is acquired from (Boudreau and Meysman, 2006) is mainly applied for aqueous and soft mud.

$$\theta^2 = 1 - \ln \phi^2$$

However, the above equation has also been applied to predict the tortuosity of a variety of sediments and soils that are rich in mud.

The estimated fluxes of Na and Cl salt ions from the above equations are approximately 5 ug/cm²/year and 21 ug/cm²/year for a sediment depth of 20 cm. These fluxes are considered to be relatively small and have a negligible effect on the overall variations of the Na and Cl ion concentrations. The estimated diffusion flux of δD and $\delta^{18}O$ are 0.5 ‰/ cm²/year and 0.01 ‰/ cm²/year respectively for a sediment depth of approximately 20 cm. Thus, although the effect of diffusion on salt ions is negligible, diffusion plays a significant role in the modification of the isotopic signals and may account for the depletion of isotopic compositions in layers that coincide with low precipitation values.

It is because fluvial influx plays a dominant role in the modification of the salt ion concentrations (Fig. 2.5) by the dilution of pore waters trapped in the sedimentary units, it is useful to evaluate the degree to which the fresh-water mixing can reduce the concentrations of salt ions in the pore waters. As mentioned previously, the concentrations of Na and Cl ions of marine waters are known (~10,750 ug/mL for Na and ~19,350 ug/mL for Cl) Table 2.4. The ratios of the concentrations of salt ions in the pore

water to those in the seawater are used to estimate the percentage of salt ion concentrations present in the pore waters of the IHS in location 2 (Table 2.4). Figure 2.12 shows that the pore waters comprise of approximately 20 % of rainwater that was mixed with the sea water (80 %) in the sediments during sedimentation. Figure 2.12 also shows a significantly lower isotope values for the freshwater endmember than the primary pore waters in the recharge area. It is possible that the high salt percentage could be due to the holding ions on to the sediment particles as the fresh water is flushed out of the pores during compaction. This may be a reason for the disagreement with the seawater components with the isotope compositions in the fresh water. Another possibility of the disagreement with the end-member salts and isotopes end-members in fresh water would be due to the diffusion of the mobile isotopes in various sedimentary layers.

Previous studies have suggested that the IHS rhythmic beds can record deposition of the IHS from tidal cycles (Thomas et al., 1987; Choi et al, 2004). The alternations of thick and thin laminae units in the Han River Delta is interpreted to represent a diurnal cycle with thick laminae being deposited by a larger tide and thin laminae being deposited by a smaller tide (Choi et al, 2004). Although the rhythmic Shepody units represent seasonal processes, the variations in laminae thickness found in the IHS of the Shepody River are documented to be a result of a neap-spring tidal cyclicity (a synodic cycle), which has a length of 28 cycles (Pearson and Gingras, 2006). In the case of neap-spring tidal cyclicity, the thinner and muddier laminae represent neap tides and the thicker or siltier laminae indicate spring tides. The thicker or coarser neap-spring cycles can alternate with the diurnal cycles in some IHS and they represent the anomalistic tidal cycle. In short, some of the work in the literature (for e.g. Choi et al., 2004) considers IHS to be a tidal indicator. Although the laminations of the IHS units may record tidal signals, the IHS beds represent annual deposition

2.6. CONCLUSION

In this study, the salinities and the isotope compositions of the pore waters of the IHS vary in response to changes in annual precipitation (fresh water stored in the stratified layers) in the Shepody River Estuary. The systematic variations of isotopic compositions and salt ion concentrations in pore water as well as the annual precipitation

record studied reflect annual deposition of the sedimentary beds in the IHS. The corresponding precipitation data which represent the fresh water portion of the pore waters can be inferred to the sedimentary units. Thus, the ages of these annual beds in the IHS can be discerned.

The pore waters in Shepody units comprise of approximately 80 % of marine water that is mixed with 20 % of freshwater (rainwater and snow) delivered by the Shepody River when the IHS are exposed during ebb tides. The mixing of the dominant marine signal with the runoff results in a negative shifting of isotopic compositions below the meteoric water line. The heavy rainfalls mixed in the pore waters of these estuarine sediments tend to be more negative in isotopic compositions. Thus, intense rains tend to deliver more runoff that has more negative isotope values when the sediments are oversaturated by the waters from precipitation in the recharge area. Thus, the isotopic signal varies with the local runoff that resulted by the oversaturation of water from the rainfalls delivered by the Shepody River.

Fine-grained particles (silt and clay) that are brought into the estuary by the Shepody River are trapped by the estuarine circulation (Kranck, 1981). They stick and cluster together to form flocs and settle to the bottom (Milligan et al., 2001). The rapid sedimentation by the settling of flocs during slack tide periods has the ability to trap pore water in the large spaces between the settling flocs (Pearson and Gingras, 2006). Thus, the settled muds accumulate with “ambient” water due to the low permeability of the aggregates (Lettley, 2004). The “ambient” waters are trapped in the pores of the flocculated sediments during compaction as sediments are stacked during deposition to form sedimentary sequences.

Comparing the salinity record and isotope signatures amount of fresh water that mixes with the marine water can contribute to the depositional history of the IHS. The study also demonstrates the potential use of δD and $\delta^{18}O$ variations for reconstructing the variability in seasonal salinity over short time periods. The established annual salinity in recent years can contribute to the depositional history of sea water and fresh water mixing in the Shepody River estuarine system.

2.7. REFERENCES

- Arnason, B. and Sigurgeirsson, T. H. (1966). Hydrogen isotopes in hydrological studies in Iceland. In: *Symposium on isotopes in hydrology*. (Ed. International Atomic Energy Agency). IAEA, Austria, p 35-47.
- Benway, H.M. and Mix, A.C. (2004). Oxygen isotopes, upper-ocean salinity, and precipitation sources in the eastern tropical Pacific. *Earth and Planetary Science Letters*, 24, 493-507.
- Boggs, S. (2001). Continental environments. In: *Principles of sedimentology and stratigraphy*. (Ed. Boggs, S). Prentice Hall, New Jersey, p 267- 320.
- Boudreau, B. P. and Meysman, F.J.R. (2006). Predicted totuosity of muds. *Geological Society of America*, 34 (8), 693-696.
- Burton, J. D. (1976). Basic properties and processes in estuarine chemistry. In: *Estuarine Chemistry*. (Ed. Burton, J.D. and Liss, P.S.).Academis Press Inc, U.S.A, p 1-36.
- Charbeneau, R.J. (2000). Introduction to groundwater hydrology. In: *Ground water hydraulics and pollutant transport*. (Ed. Charbeneau, R.J.). Prentice Hall Inc., New Jersey, p 1-17.
- Choi, K.S., Dalrymple, R.W., Chun, S.S. and Kim, S. (2004). Sedimentology of modern, inclined heterolithic stratification (IHS) in the macrotidal Han River delta, Korea. *Journal of Sedimentary Research*, 74, 677-689.
- Clark, I. and Fritz, P. (1997). Precipitation. In: *Environmental isotopes in Hydrology*. (Ed. Clark, I., and Fritz, P.). Lewis Publishers, Boca Raton, Florida, p 63-77.
- Coleman, M.L., Shepherd, T.J., Durham, J.J., Rouse, J.E. and Moore,G.R. (1982). Reduction of Water with Zinc for Hydrogen isotope Analysis, *Analytical Chemistry*, 54, 993-995.
- Craig, H. (1961). Isotopic variations in meteoric waters. *Science*, 133 (3465), 1702-1703.
- Dansgaard, W. (1975). Stable isotopes in precipitation. In: *Geochemistry of water*. (Ed. Kitano, Y.). Halsted press, U.S.A, p 160-192.
- Delaygue, G., Bard, E. and Rollion, C. (2001). Oxygen isotope/salinity relationship in the northern Indian Ocean. *Journal of Geophysical Research*, 106, 4565-4574.
- Drever, J. I. (1997). Evaporation of saline water. In: *Geochemistry of natural waters*. (Ed. Drever, J.I.). Prentice Hall, U.S.A., p 327-351.
- Environment Canada (2004). Alma Station.
www.climate.weatheroffice.ec.gc.ca

- Fetter, C.W. (1999). Mass Transport in Saturated Media. In: *Contaminant hydrogeology* (Ed. Fetter, C.W.), MacMillan Publishing, U.S.A, p 45-119.
- Fetter, C.W. (2001). Properties of aquifers. In: *Applied Hydrogeology*. (Fetter, C.W.). Prentice Hall, New Jersey, p 66- 112.
- Friedman, G., M., Sanders, J.E. and Kopaska-Merkel, D.C. (1992). Nonmarine environments: deserts, rivers, lakes, and glaciers. In: *Principles of stratigraphy and sedimentary deposits: Stratigraphy and sedimentology*. (Ed. Friedman, G., M., Sanders, J.E., and Kopaska-Merkel, D.C.), Macmillan Publishing Company, U.S.A, p 515- 526.
- Gingras, M.K., Rasanen, M. and Ranzi, A. (2002). The significance of bioturbated inclined heterolithic stratification in the Southern part of the Miocene Solimes Formation, Rio Acre, Amazonia Brazil. *Palaios*, 17, 591-601.
- Hoeffs, J. (1997). Theoretical and experimental principles. In: *Stable Isotope Geochemistry*. (Ed. Hoeffs, J.). Springer-Verlag, Germany, p 1-26.
- Horita, J. and Kendall, C. (2004). Stable Isotope analysis of Water and Aqueous Solutions by Conventional dual-inlet Mass Spectrometry. In: *Handbook of Stable Isotope Analytical Techniques. Volume 1*. (Ed. De Groot, P.A), Elsevier, South Africa and Belgium, p 1-37.
- IAEA (2004). GNIP maps and animations, international Atomic energy Agency, Vienna.
<http://isohis.iaea.org/userupdate/waterloo>
- Ingram, B.L., Conrad, M.E. and Ingle, J.C. (1996). Stable isotopes and salinity systematics in estuarine waters and carbonates: San Francisco Bay. *Geochimica et Cosmochimica*, 60 (3), 455-467.
- Kendal, C. and Doctor, D.H. (2005). Stable isotope applications in hydrological studies. In: *Surface and ground water, weathering and soils*. (Ed. Drever, J.I.), vol. 5 *Treatise on Geochemistry*. (Eds. Holland, H.D. and Turekian, K.K.), Elsevier-Pergamon, Oxford, p 319- 364.
- Knighton, D. (1984). Sediment deposition. In: *Fluvial forms and processes*. (Ed. Knighton, D), The Chaucer Press, Great Britian, p 44-84.
- Krank, K. (1981). Particulate matter grain-size characteristics and flocculation in a partially mixed estuary. *Sedimentology*, 28:107-114.
- Leeder, M. (1999). Rivers. In: *Sedimentology and sedimentary basins: From turbulence to tectonics* (Ed. M. Leeder), The Blackwell Science, U.K., p 307-329.
- Lettey, C.D. (2004). Elements of a genetic framework for inclined heterolithic strata of the McMurray Formation , NorthEast Alberta, dissertation, University of Alberta.

- Lettley, C. D., Pemberton, S. G., Gingras, M. K., Ranger, M. J. and Blakney, B.J. (2006). Integrating sedimentology and ichnology to shed light on the system dynamics and paleogeography of an ancient riverine estuary. In: *Applied Ichnology, Society of Economic Paleontologists and Mineralogists short course notes*. (Ed. MacEachern, J.A., Bann, K.L., Gingras, M.K. and Pemberton, S.G.), p 142-160.
- McSween, H.Y., Richardson, S.M., Uhle, M.E. (2003a). The oceans and atmosphere as a geochemical system. In: *Geochemistry : Pathways and processes*.(Ed. McSween, H.Y., Richardson, S.M., Uhle, M.E.). Prentice Hall Inc., p 137-168.
- McSween, H.Y., Richardson, S.M., Uhle, M.E. (2003b). Diagenesis: A study in kinetics. In: *Geochemistry : Pathways and processes*.(Ed. McSween, H.Y., Richardson, S.M., Uhle, M.E.). Prentice Hall Inc., p 79- 93.
- Merlivat, L. and Jouzel, J. (1979). Global climatic interpretation of the deuterium-oxygen 18 relationship for precipitation. *Journal of Geophysical Research*, 84, 5029-5033.
- Milligan, T.G., Kineke, G.C., Alexander, C.R. and Hill, P.S. (2001). Flocculation and sedimentation in the ACE Basin, South Carolina. *Estuaries*. 24 (5), 734-744.
- Palmer, C.M. (1996). Contaminant pathways- Subsurface investigation and monitoring approach. In: *Principles of contaminant hydrogeology*. (Ed. Palmer, C.M). R.C. Press, U.S.A, p 25-56.
- Pearson, N.J. and Gingras, M.K. (2006). An ichnological and sedimentological facies model for muddy point-bar deposits. *Journal of Sedimentary Research*, 76, 1-12.
- Schone, B.R., Tanabe, K., Dettman, D.L. and Sato, S. (2003). Environmental controls on shell growth rates and $\delta^{18}\text{O}$ of the shallow bivalve mollusk *Phacosoma japonicum* in Japan. *Marine biology*, 142, 473-485.
- Sen, Z. (1995). Aquifer properties. In: *Applied Hydrogeology for scientists and engineers*. (Ed. Sen, Z). C.R.C. Press, U.S.A, p 69-89.
- Tanaka, K. (1978). Self-diffusion coefficients of water in pure water and in aqueous solutions of several electrolytes with ^{18}O and ^2H as tracers. *J.Chem. Soc.*, 74, 1879-1881.
- Thomas, R.G., Smith, D.G., Wood, J.M., Visser, J., Calverley-Range, E.A. and Koster, E.H. (1987). Inclined Heterolithic Stratification- terminology, description, interpretation and significance. *Sedimentary Geology*, 53, 123-179.
- Ullman, W.J. and Aller, R.C. Diffusion coefficients in nearshore marine sediments, *Limnol Oceanogr.*, 27 (3), 552-556.

Table 2.1. Isotopic compositions at locations 1, 2 and 3 in the Shepody River Estuary. $\delta D_{(MWL)}$ represents the theoretical deuterium values that lie on the meteoric water line which represent the relationship $\delta D = 8 \delta^{18}O + 10$ (Craig, 1961).

Location 1					Location 2					Location 3				
Depth (cm)	Layer number	δD (‰)	$\delta^{18}O$ (‰)	$\delta D_{(MWL)}$ (‰)	Depth (cm)	Layer number	δD (‰)	$\delta^{18}O$ (‰)	$\delta D_{(MWL)}$ (‰)	Depth (cm)	Layer number	δD (‰)	$\delta^{18}O$ (‰)	$\delta D_{(MWL)}$ (‰)
0	1	-34.7								0	1	-41.7		
23.2	2									50.7	2	-45.0	-2.9	-13.5
30.9	3	-28.7			0.0	1	-25.5			77.8	3	-18.2	-1.6	-2.5
46.4	4	-13.3			14.2	2	-24.0			152.2	4	-28.8	-1.4	-0.9
64.9	5	-27.5	-2.9	-13.4	36.0	3	-29.7			253.7	5	-41.9	-15.6	-114.6
80.3	6	-24.5	-3.1	-16.9	49.0	4	-18.0			297.7	6	-48.8	-2.3	-8.3
95.8	7	-22.0	-2.8	-14.2	65.4	5	-14.6	-2.5	-12.1	348.4	7	-37.3	-1.8	-4.1
					87.2	6	-5.5	-2.3	-10.2	405.9	8	-30.6	-1.6	-2.5
					103.6	7	-28.6	-2.3	-10.8	456.6	9	-31.5	-1.6	-2.8
					123.2	8	-4.9	-2.4	-11.4	490.4	10	-35.4		
					136.3	9				541.2	11	-35.8	-6.7	-43.3
					145.0	10	-18.7							
					158.0	11								
					169.0	12	-24.6							
					193.0	13	-9.5	-2.4	-11.4					

Table 2.2. Annual precipitation obtained from the Alma station from 1991 to 2005 and isotopic compositions in the IHS layers at locations 1, 2 and 3.

Year	Total Precipitation (mm)	Location 1				Location 2				Location 3			
		Depth (cm)	Layer number	δD (‰)	$\delta^{18}O$ (‰)	Depth (cm)	Layer number	δD (‰)	$\delta^{18}O$ (‰)	Depth (cm)	Layer number	δD (‰)	$\delta^{18}O$ (‰)
2005	1605.5	0	1	-34.7					0	1	-41.7		
2004	1225.0	23.2	2						50.7	2	-45.0	-2.9	
2003	1535.3	30.9	3	-28.7		0.0	1	-25.5	77.8	3	-18.2	-1.6	
2002	1631.6	46.4	4	-13.3		14.2	2	-24.0	152.2	4	-28.8	-1.4	
2001	977.2	64.9	5	-27.5	-2.9	36.0	3	-29.7	253.7	5	-41.9	-15.6	
2000	1356.2	80.3	6	-24.5	-3.1	49.0	4	-18.0	297.7	6	-48.8	-2.3	
1999	1454.5	95.8	7	-22.0	-2.8	65.4	5	-14.6	-2.5	348.4	7	-37.3	-1.8
1998	1600.6					87.2	6	-5.5	-2.3	405.9	8	-30.6	-1.6
1997	1146.8					103.6	7	-28.6	-2.3	456.6	9	-31.5	-1.6
1996	1513.0					123.2	8	-4.9	-2.4	490.4	10	-35.4	
1995	1315.9									541.2	11	-35.8	-6.7
1994	1557.5					145.0	10	-18.7					
1993	1486.9												
1992	1247.6					169.0	12	-24.6					
1991	1564.3					193.0	13	-9.5	-2.4				

Table 2.3. The derivatives and second derivatives of precipitation, salt ion concentrations (Na and Cl) and isotopic compositions (δD) in the IHS at location 2.

Layer number	Inferred Year	Total Precipitation (mm)	Total Precipitation		Na ($\mu\text{g/mL}$)	Na ($\mu\text{g/mL}$)		Cl ($\mu\text{g/mL}$)	Cl ($\mu\text{g/mL}$)		δD (\square)	δD (\square)	
			First derivatives	2nd derivatives		First derivatives	2nd derivatives		First derivatives	2nd derivatives		First derivatives	2nd derivatives
1	2003	1535.3	96.3	-750.7	9740	-1580.0	2560.0	17840	-3290.0	4750.0	-25.5	1.5	-7.2
2	2002	1631.6	-654.4	1033.4	8160	980.0	-900.0	14550	1460.0	-1000.0	-24.0	-5.7	17.4
3	2001	977.2	379.0	-280.7	9140	80.0	-470.0	16010	460.0	-930.0	-29.7	11.7	-8.3
4	2000	1356.2	98.3	47.8	9220	-390.0	410.0	16470	-470.0	770.0	-18.0	3.4	5.7
5	1999	1454.5	146.1	-599.9	8830	20.0	-40.0	16000	300.0	-290.0	-14.6	9.1	-32.2
6	1998	1600.6	-453.8	820.0	8850	-20.0	-170.0	16300	10.0	-270.0	-5.5	-23.1	46.8
7	1997	1146.8	366.2	-344.0	8830	-190.0	295.0	16310	-260.0	385.0	-28.6	23.7	-30.6
8	1996	1513.0	22.3	-88.6	8640	105.0	75.0	16050	125.0	0.0	-4.9	-8.9	1.975
10	1994	1557.5	-155.0	235.8	8850	255.0	-292.5	16300	125.0	-162.5	-18.7	-2.95	9.025
12	1992	1247.6	316.7		9360	-330.0		16550	-200.0		-24.6	15.1	
13	1991	1564.3			9030			16350			-9.5		

Table 2.4. Estimated seawater and freshwater percentages in the pore waters in the sedimentary layers of the IHS at location 2.

Layer number	Depth (cm)	Na (ug/mL)	Seawater (Na) (%)	Cl (ug/mL)	Seawater (Cl) (%)	Seawater (%)	Freshwater (%)
1	0.0	9740	90.45	17840	92.20	91.32	8.68
2	14.2	8160	75.78	14550	75.19	75.49	24.51
3	36.0	9140	84.88	16010	82.74	83.81	16.19
4	49.0	9220	85.62	16470	85.12	85.37	14.63
5	65.4	8830	82.00	16000	82.69	82.34	17.66
6	87.2	8850	82.19	16300	84.24	83.21	16.79
7	103.6	8830	82.00	16310	84.29	83.15	16.85
8	123.2	8640	80.24	16050	82.95	81.59	18.41
9	145.0	8850	82.19	16300	84.24	83.21	16.79
10	169.0	9360	86.92	16550	85.53	86.23	13.77
11	193.0	9030	83.86	16350	84.50	84.18	15.82

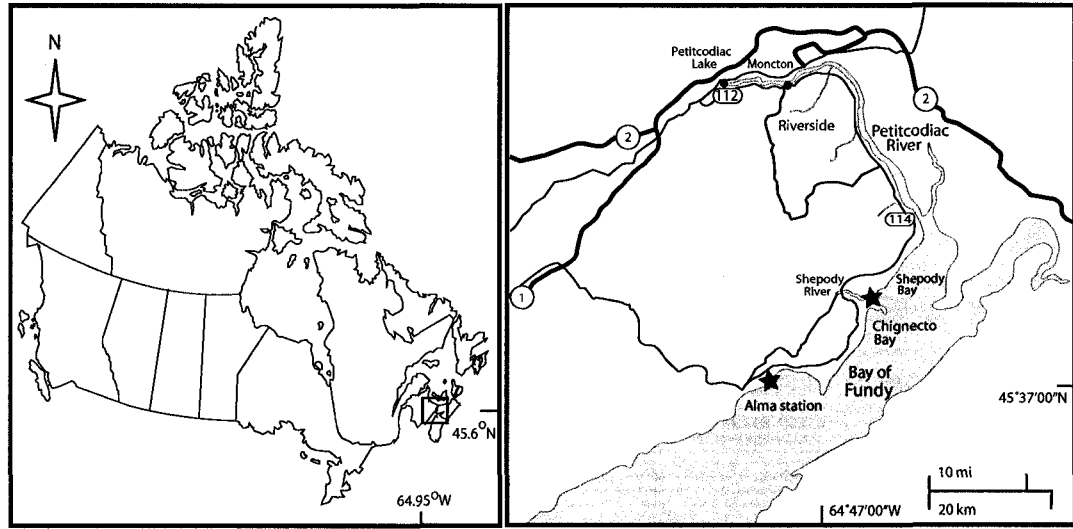


Figure 2.1. Location map of the Shepody River located in the northeast of Chignecto Bay.



Figure 2.2. Photograph of IHS deposit in location 1 showing the sampled layers correlated to their depths.

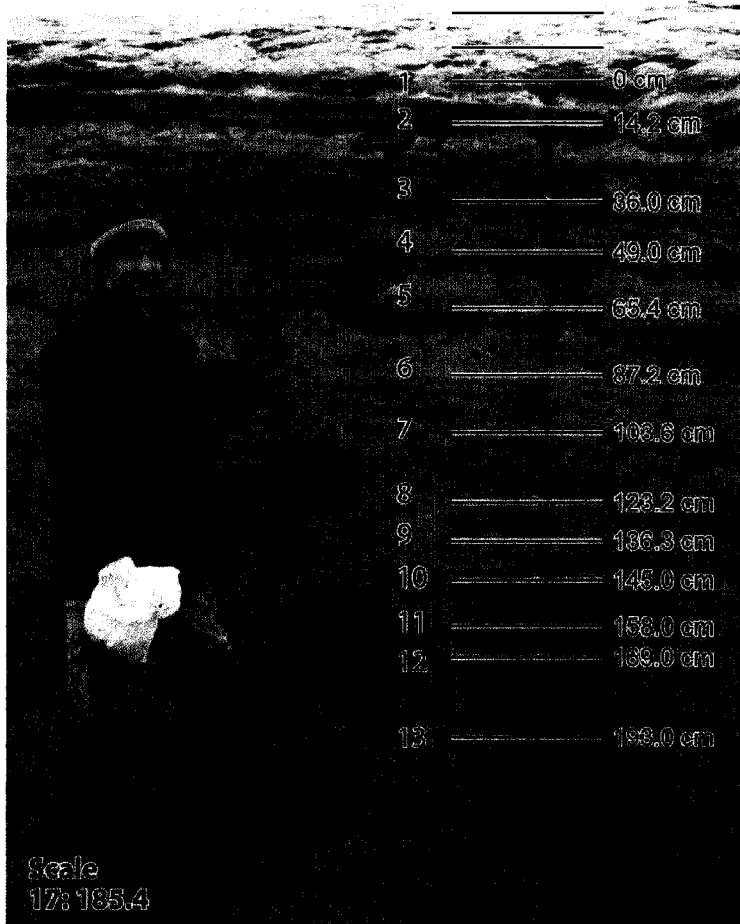


Figure 2.3. Photograph of IHS deposit in location 2 showing the sampled layers correlated to their depths.

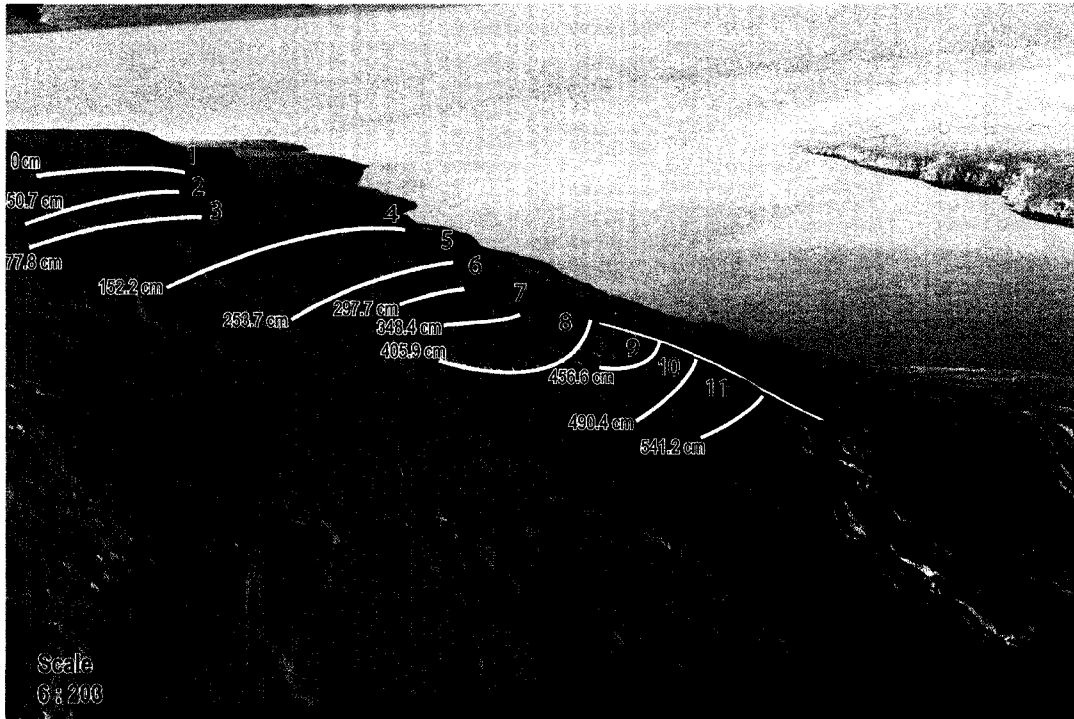


Figure 2.4. Photograph of IHS deposit at location 3 showing the inclined sampled layers correlated to their depths.

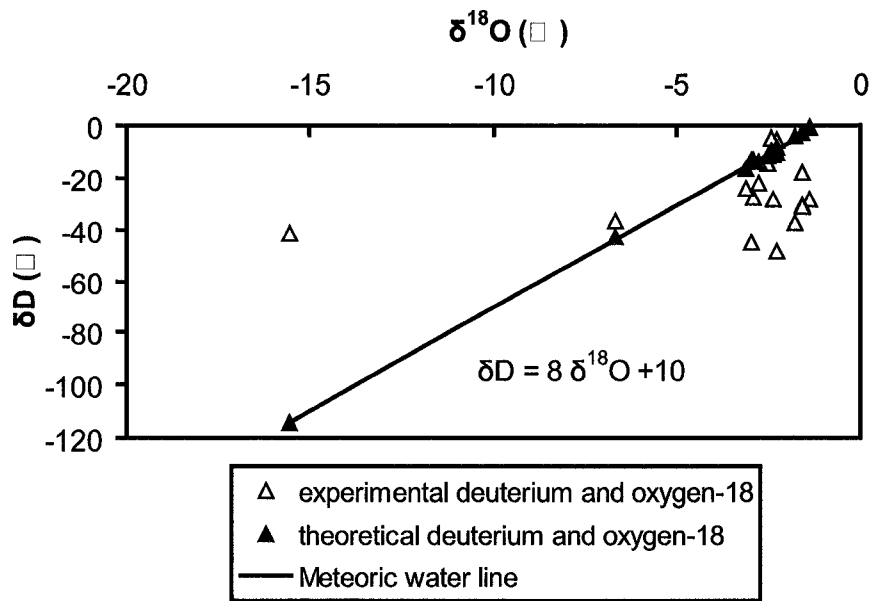


Figure 2.5. Correlation of δD and $\delta^{18}\text{O}$ in the pore waters of the IHS from locations 1, 2 and 3. The shaded triangles represent the theoretical deuterium and oxygen-18 values that lie on the meteoric water line.

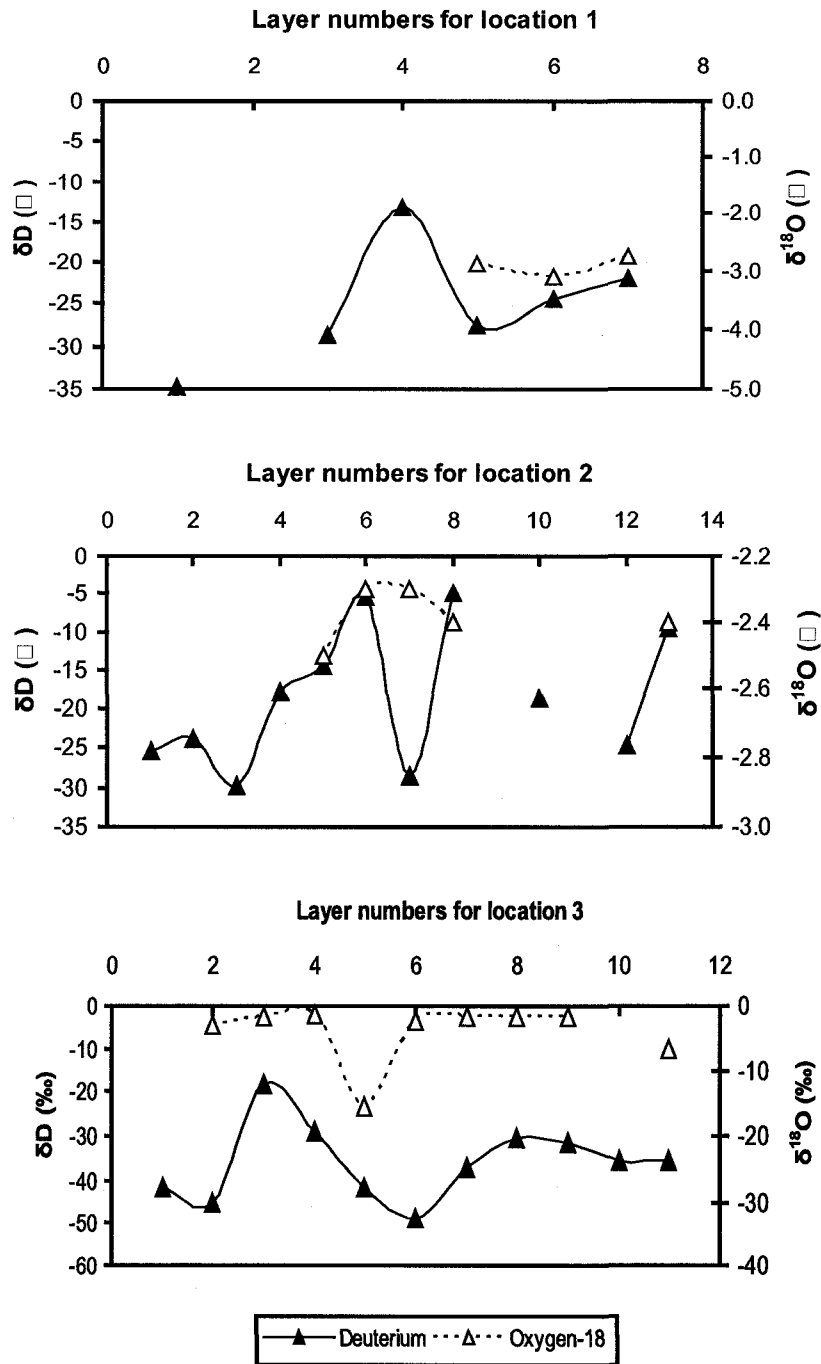


Figure 2.6. Variations of δD and $\delta^{18}O$ with depth in the IHS deposits from locations 1, 2 and 3.

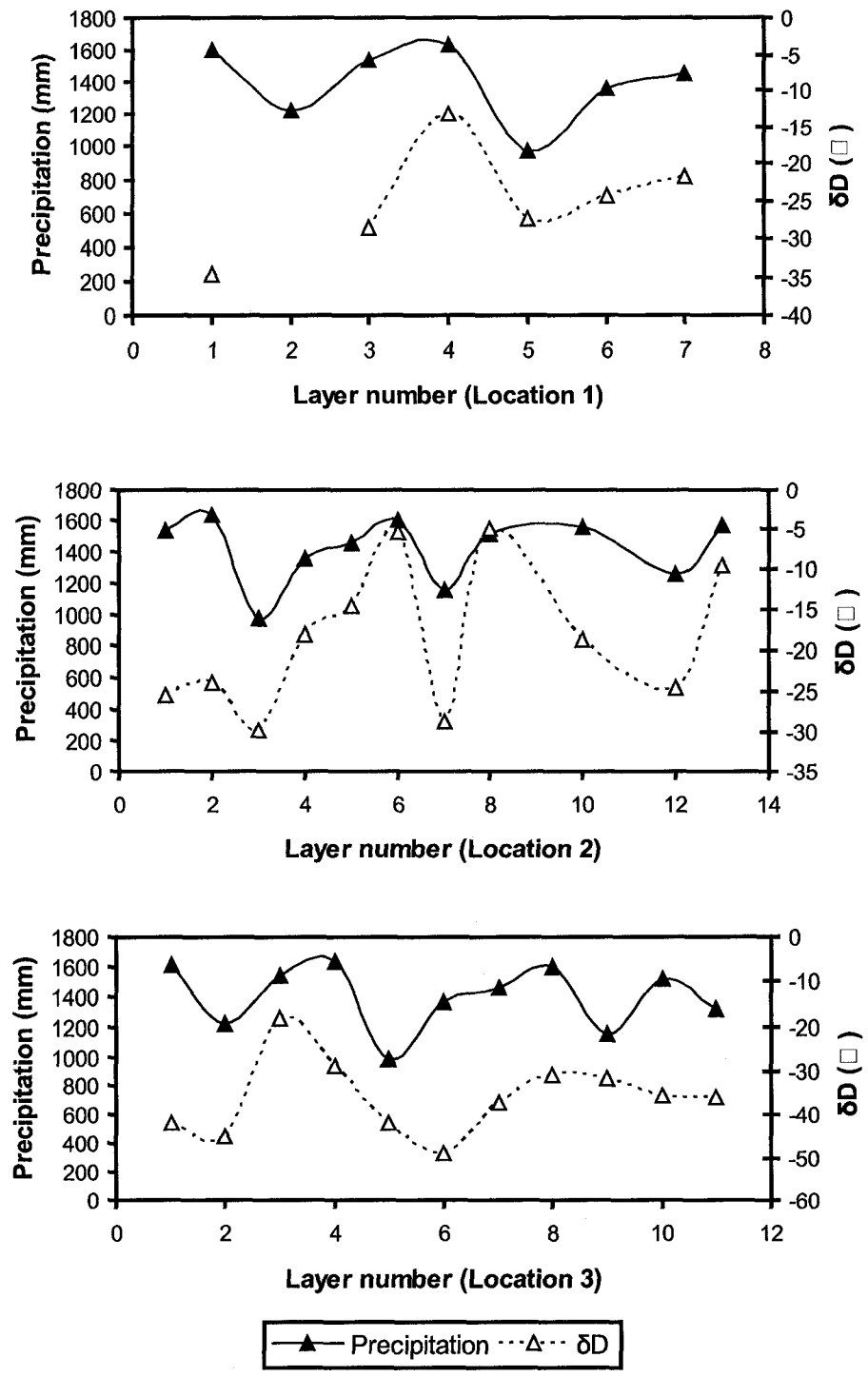


Figure 2.7. The variations of isotopic signatures and corresponding annual precipitation record in the IHS deposits from locations 1, 2 and 3. The annual precipitation is obtained from the Alma weather station.

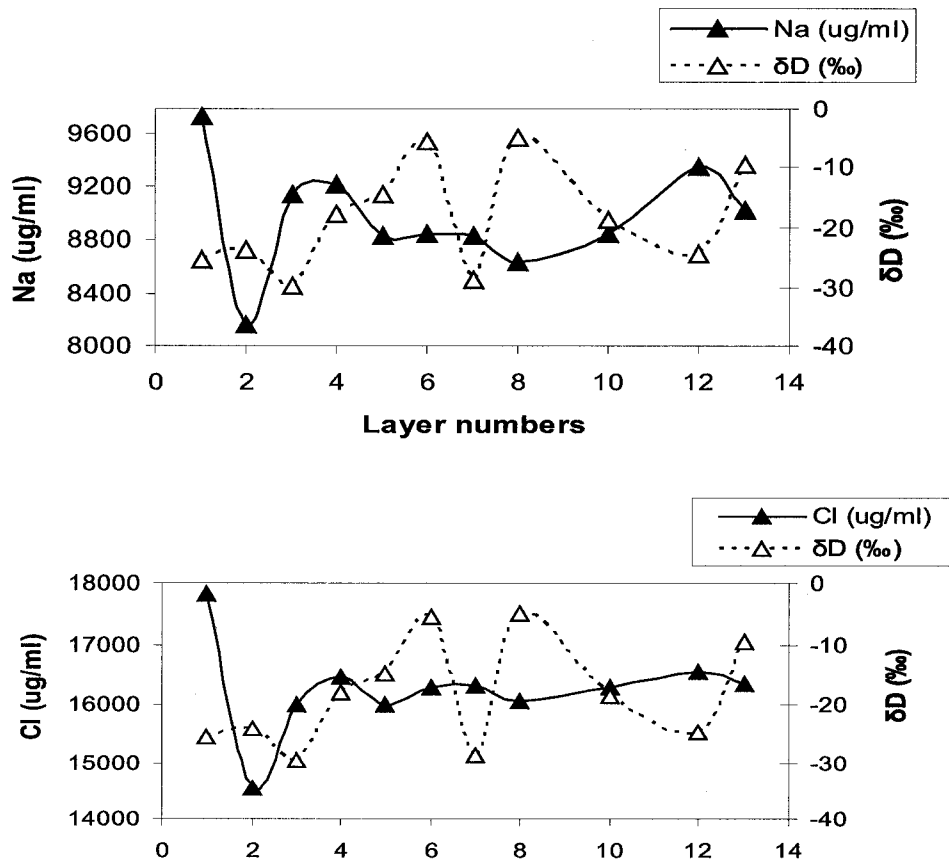
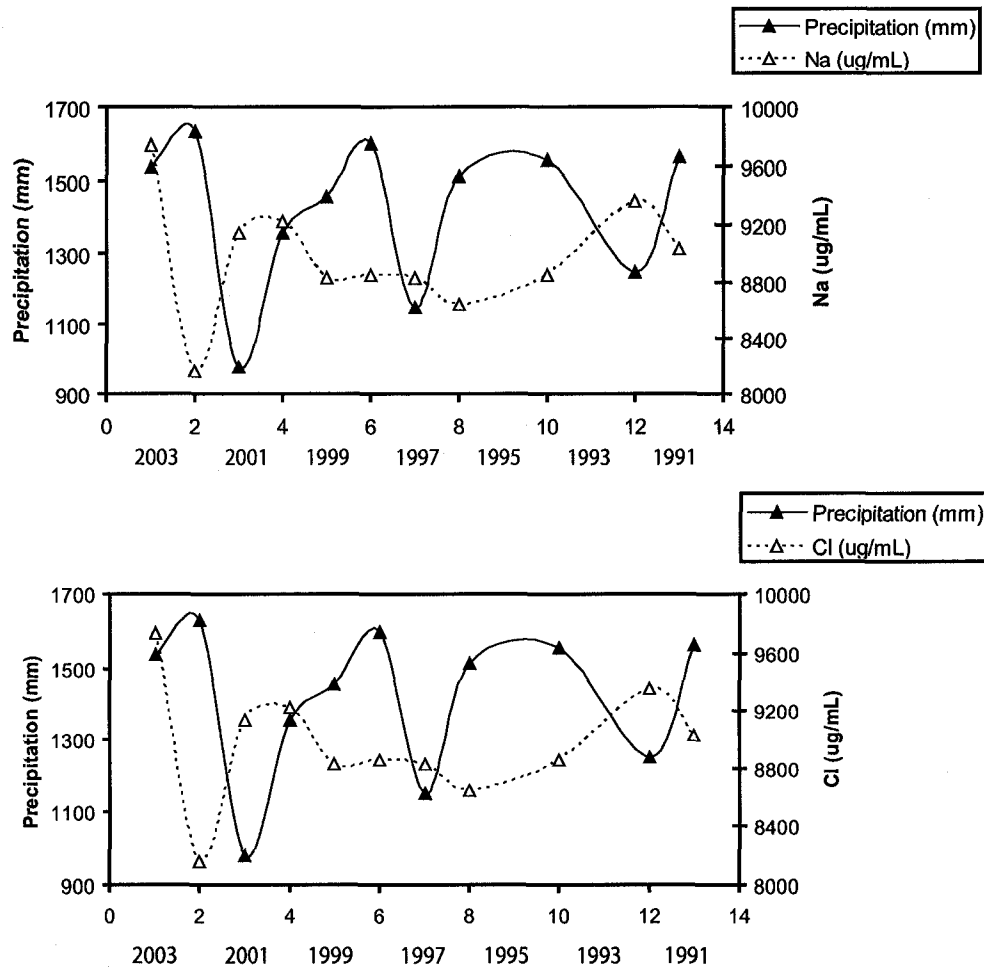
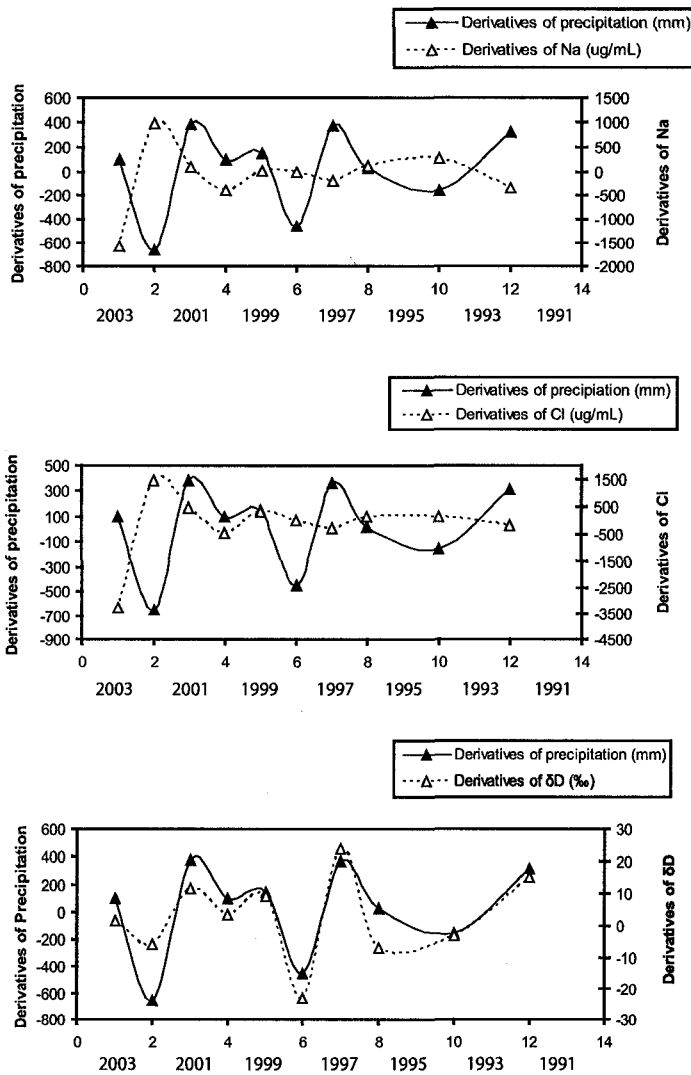


Figure 2.8. The variations of δD and salt ion concentrations in the IHS at location 2.



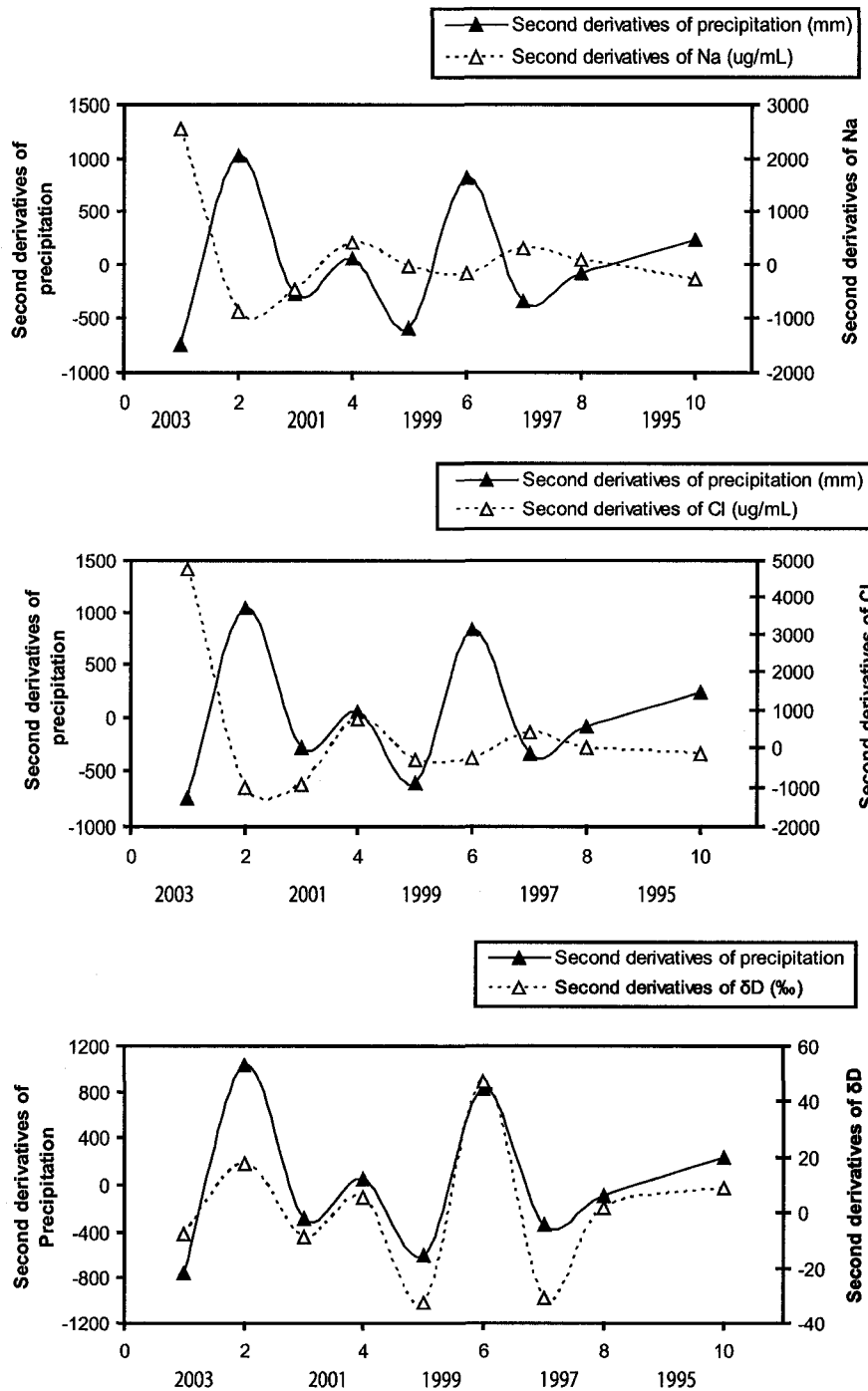
Inferred year and layer numbers in location 2

Figure 2.9. Time series of the annual precipitation record (rainwater brought into the estuary by the fluvial system) and the salt ion concentrations (representing seawater compositions) at location 2.



Inferred year and layer numbers in location 2

Figure 2.10. The rate of change of freshwater (precipitation), salt ion concentrations and isotopic compositions (δD) through the layers of the IHS at location 2.



Inferred year and layer numbers in location 2

Figure 2.11. The rate of change of the derivatives of freshwater (precipitation), salt ion concentrations (Na and Cl) and isotopic compositions (δD) through the stratified layers of the IHS at location 2.

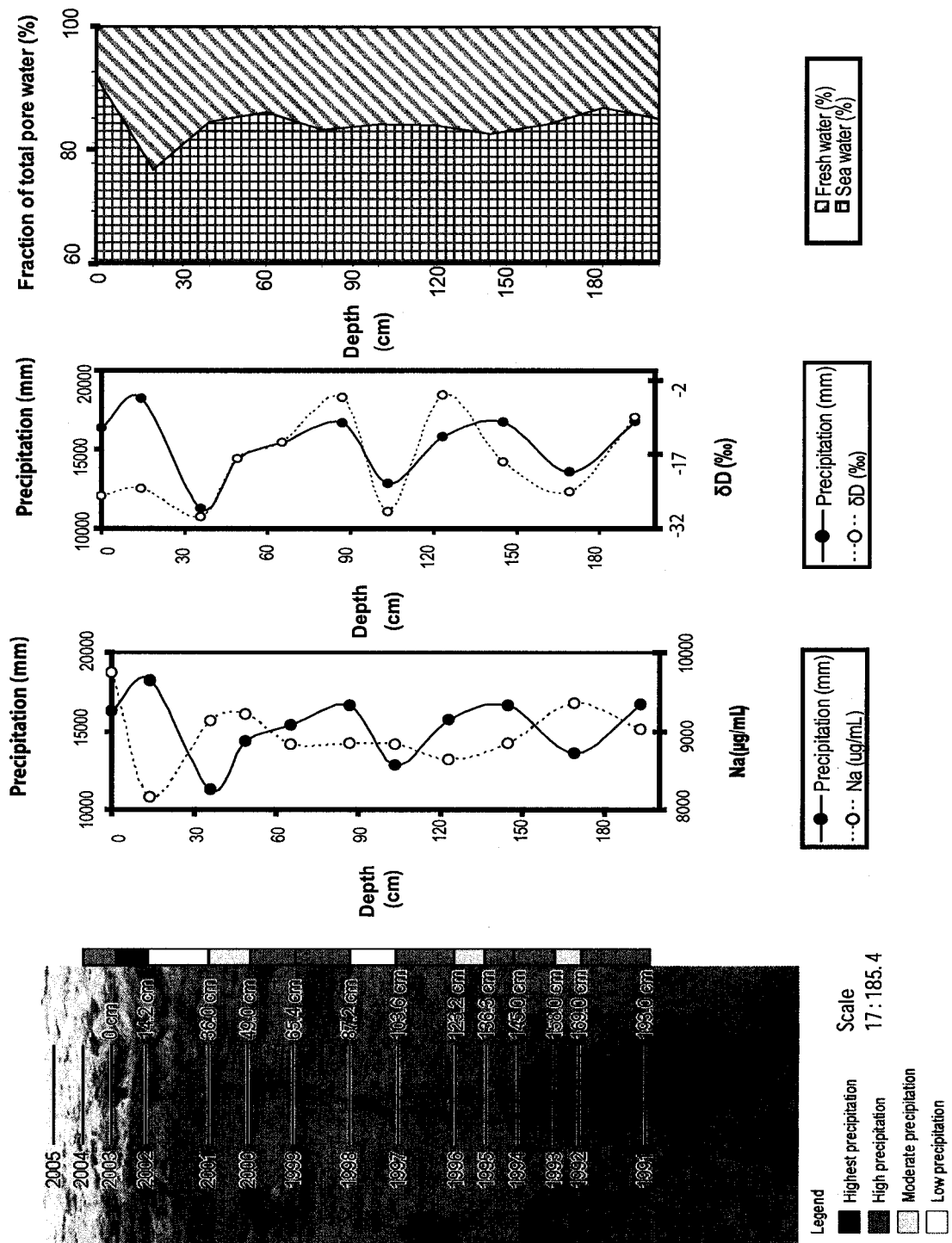


Figure 2.12. The annual deposition of fresh and marine-water mixing in the IHS of the Shepody River Estuary during recent years.

CHAPTER 3. IMPORTANCE OF MICRO-ORGANISMS IN PROMOTING FLOCCULATION AND THEIR RELATION TO SEDIMENT DYNAMICS.

3.1 INTRODUCTION

Flocculation is the process by which smaller particles collide and stick together by the absorption of ions of opposite charge to form an aggregate. Typically, suspended particles in fresh water are negatively charged and they repel each other. Where fresh water mixes with seawater, such as in an estuary or delta, the sodium chloride (NaCl) ions affect the charges on the small particles such that they possess an electrostatic attraction. As a consequence of the modified surface charge, particles are attracted to each other, and they clump together forming a floc (Gibbs et al., 1989; Yariv and Cross, 1979).

The collision of particles is promoted by 3 mechanisms: differential particle settling velocity, Brownian motion, and hydraulic turbulence (Eisma, 1986; Dyer and Manning, 1999). Of the three mechanisms differential settling is considered to be the most dominant. Denser particles have a higher settling speed and they aggregate during their descent thereby coalescing into flocs (Lick et al., 1993). During conditions characterized by high concentration of suspended particles, smaller particles move rapidly in a random motion (Gibbs et al., 1989; Dyer and Manning, 1999). Similarly, as a consequence of Brownian motion, particles collide and promote floc formation. Turbulence can also enhance flocculation by bringing particles together; this process is constructive at low turbulence levels. Under high turbulence, flocs are destroyed because aggregates that are greater than 125 μm (macroflocs) are loosely bound and fragile (Hill, 1998; Eisma, 1986; Milligan and Hill, 1998; Fennessy et al., 1994b; Fettweis et al., 2006).

Flocculation is also affected by various factors such as particle concentration, salinity, turbulence intensity, and micro-organisms (Burban et al., 1989). Higher concentration of particles yields larger aggregates by increasing the frequency of collision and promoting the adhesion of particles (Milligan and Hill, 1998). As the concentration of suspended sediment increases, the floc settling velocity accelerates resulting in the rapid aggregation of particles (Hill, 1998; Milligan et al., 2001; Dyer and

Manning, 1999). However, very high concentrations of suspended particles can have a negative effect on the maximum floc size (Milligan and Hill, 1998; Burban et al., 1989). When particles collide, only a fraction of the collisions result in the adhesion of particles and formation of flocs (Tsai et al., 1987). Collisions between particles occur mostly due to fluid shear and when they have sufficient translational energy they result in the disaggregation of flocs (Milligan and Hill, 1998). Electrolytes serve as excellent coagulation agents by joining particles together and bridging (i.e. absorption of different parts of the same molecule on the surfaces of more than one particle) large dissimilar ions (Miall, 1961; Yariv and Cross, 1979). Thereby, the rate of collision especially adhesion increases with salinity resulting in flocculation (Milligan et al., 2001). Because the stability of an aggregate is partly dependant to its surface charge, any effect that destabilizes a colloidal particle such as addition of electrolytes can induce flocculation (Miall, 1961; Yariv and Cross, 1979). Thus, particles typically coagulate faster in brackish- and marine- waters than in fresh water (Burban et al., 1989; Milligan et al., 2001). Finally, biological materials can provide fibrous structures that bind particles together (Fennessy et al., 1994a). These bacterially derived compounds stabilize the aggregates (Tisdall and Oades, 1982). They also produce robust flocs under high dissolved organic-matter concentrations (Muschenheim et al., 1989; Kirchman, 1983). Notably, the surface chemistry of inorganic particles is favourable for heterotrophic bacterial activities where fresh water and salt water meets (Bell and Albright, 1981).

Previous studies show that high abundances of heterotrophic bacteria and flocs are present in turbid environments (Muschenheim et al., 1989; Bell and Albright, 1981). When particles in suspension begin to flocculate, the turbidity levels decrease. The number of free-floating bacteria is also reduced. Therefore, physicochemical aggregation and micro-organisms can influence turbidity. Their relative importance is, however, difficult to estimate as their influence on sedimentation is commonly linked to seasonal sedimentation patterns (Chang, 2005).

The size, density and settling velocity of flocs are linked and are influenced by the aforementioned factors (particle concentration, salinity, turbulence and micro-organisms). In marginal marine-marine settings, each is likely to change throughout the tidal cycle, so, the balance between the forces of aggregation and disruption are variable (Fennessy et

al., 1994a). Rapid sedimentation is promoted by large rapidly settling flocs in the mouth of the river. The large flocs are deposited during low energy conditions or under the duress of very high suspended particle concentrations: the flocs are resuspended due to higher energy conditions (i.e. rapid currents or energetic waves) (Chen, 2005; Chang, 2005). Conceptual models for floc formation and deposition are further complicated, as high-energy conditions can also promote flocculation (Milligan et al., 2001).

Previous studies of flocculation have focused on the physical, chemical and biological processes associated with floc formation. However, the influence and effect of these processes have yet to be quantified (Fennessy et al, 1994b). Assessing the significance of all of the parameters in the inducement of floc formation would be useful for the prediction of flocculation and assessing its significance in the rock-record. Thereby, the objectives of this study are to: 1) determine the importance of bacteria in controlling the floc size and turbidity under various physicochemical parameters with time; and 2) develop a procedure for the artificial production of aggregates similar to the natural flocs under various hydrodynamics regimes.

3.2. STUDY AREA

Samples of flocculated river mud were collected from Riverside and Moncton near the head of the Petitcodiac River estuary in September, 2005 (Fig. 3.1). The Petitcodiac River is located on the southeast coast of New Brunswick and drains into the Bay of Fundy (Fig. 3.1). In 1968, a causeway was constructed at Moncton, 22 km from the head of the tide. The construction of the causeway affected tidal exchange and sediment transport. It also reduced the tidal prism by 2.89 million meters cubed (Mm^3) of water from the tidal system (AMEC Earth and Environmental, 2005).

The Petitcodiac River Estuary is macrotidal (in this case tides locally exceed 9 m). The concentration of total suspended sediment in the estuarine water is extremely high (about 30,000 mg/L). The sediments near Moncton/Riverside are composed of about 60 % silt, 10 % clay, and 30 % sand (Appendix 1). The majority of the particles are silt and thus small, with a high surface area. Flocculation processes are present in the upstreams of the Petitcodiac River in Riverside and Moncton. Flocs up to centimeter-scale are locally observed (Fig. 3.2).

3.3. METHODS

Three experiments were conducted to show a range of flocculation and turbidity responses to physicochemical and biological parameters. The experiments included: (1) assessing the effects of physicochemical aggregation on turbidity; (2) considering the bacterial effects on turbidity; and (3) establishing the effects hydrodynamic turbulence might have on aggregation, bacteria and turbidity.

3.3.1. Experiment 1: Effects of physicochemical aggregation on turbidity

In order to establish a relationship between turbidity and floc size, experiments were performed for a range of suspended-sediment concentrations, salinities and turbulence. All beakers used in the following experiments were first placed in an ultrasonic bath for approximately ten minutes to disaggregate the clumped sediment particles present in them. One litre of distilled water was added to the sediments in each beaker before sediments were allowed to settle for several (about fifteen) minutes for measuring the turbidity and floc sizes.

In order to study the influence of sediment concentration on the growth of sediment particles, an experiment was performed with sediment amounts of 20, 40, 80 and 145 g/L. The salinity of the water in each beaker was 20 ppt (50 % NaCl and 50 % KCl) and the temperature was held at 21°C. The second set of experiments was done at 0, 5, 10, 15 and 20 ppt salinity to assess the effects of salinity on *Petitcodiac* mud. The sediments in each beaker were 145 g/L and the temperature was held at 21°C. A turbulent experiment was conducted to establish the effect of turbulence on flocculation. In this experiment two beakers were employed and a mechanical stirrer was introduced to one of these beakers. Both beakers consisted of 145 g/L of sediments and salinity of 20 ppt held at 21°C. The induced turbulent energy by the mechanical stirrer was at 25 Hz (low energy).

The turbidity and floc size for the above experiments were measured at the starting point of the experiment and then two, four and 24 hours after the starting point. The measurements were then carried out every 24 hours of running time. The turbidity was measured using an Oakton T-100 waterproof turbidity meter. To reduce floc breakage a 3mm pipette was used for collecting the aggregates from the surface of the settled sediments. These flocs were sucked by the pipette and transferred into Petri-

dishes. The number and size of flocs were determined by using a microscope capable of 16 to 40 X magnification. After 2 weeks of experimental run time, the flocs were collected, and carefully examined for microscopic constituents using the scanning electron microscope (SEM) (JEOL JSM.6301FXV).

The sample preparation involved placing each floc on a specimen chamber. These flocs were sputter coated with a sputter coated with a Nanotech SEMPRFP2 sputter coater before examining the floc specimens by the SEM. The gold sputter coat on the surface of the flocs acts as a conductive material and prevents the accumulation of static electric fields at the surface of the flocs due to the electron irradiation during imaging. Gold has a high atomic number and produces high topographic contrast and resolution but the information thus produced can obscure the underlying fine detail of the specimen under examination. The resolution of the SEM can fall somewhere between less than 1 nm and 20 nm. The scanning process involves emission of electrons from a tungsten (which has the highest melting point and lowest vapour pressure among the metals) cathode which travel towards an anode. An electron beam is emitted over a rectangular area of the sample surface. When the primary electron beam interacts with the sample, the electrons lose energy because they are scattered and absorbed by the floc specimen. The energy exchange between the electron beam and the floc sample results in the emission of electrons and electromagnetic radiation, which can be detected to produce an image on the screen of the SEM.

Parameters:

Sediment concentration- The sediment amounts of 20, 40, 80 and 145 g/L were decided because to compare the changes of floc size with the increase of sediment concentrations. Very high particle concentrations and very low particle concentrations can have a negative effect on the size of grains (Lick et al., 1993).

Salinity - The salinity parameters 0, 5, 10, 15 and 20 ppt varied from fresh water (0 ppt) to very saline water (20 ppt) to study the change in floc size with the increase in salinity. Although the sizes of flocs increase with salinity, the extreme parameters (20 ppt) can negatively effect the size of flocs (Lick et al., 1993). A turbulent energy of 25 Hz is enough to break particles without A mixed solution of 50 % NaCl and 50 % KCl was used to replicate a natural seawater setting. However, high valence cations (Ca^{2+} and

Mg²⁺) are more effective as flocculants than monovalent cations such as Na⁺ and K⁺ (Tsai et al., 1987; Droppo and Ongley, 1994). The concentrations of Na⁺, Ca²⁺ and Al³⁺ required for the flocculation of negatively charged particles are approximately in the ratio of 1:10⁻²: 10⁻³ (Tsai et al., 1987). Hence no high-valence cations were added into the mixed salt solution. Although Na and Cl ions dominant in marine waters (Drever, 1997; Burton, 1976; McSween et al., 2003), Na and K ions have very similar effects as flocculants on the negatively charged particles. Hence, the ratio of the mixing of NaCl and KCl would not affect the flocculation process. In this experiment, an equal mixture of NaCl and KCl of 20 ppt was chosen as the salinity control.

Turbulence- 25 Hz is the optimal turbulent energy that can break sediment particles without changing the overall sediment properties in the beaker (i.e. any turbulent energy above 25 Hz can convert the muddy sediments into a solution). A beaker with no stirrer (0 Hz) was used as a control.

3.3.2. Experiment 2: Bacterial effects on turbidity

In an effort to improve the understanding of the effect of bacteria as an agent in controlling the changes in turbidity and the changes in the size of the Petricodiac cohesive sediments, a series of experiments were conducted on several aspects of the bacterial population associated with sediment particles. Autoclaving was used to sterilize beakers. *Staphylococcus aureus* (gram-positive bacteria) and pseudomonas (gram-negative bacteria) were cultivated in flasks. The bacteria were then inoculated in Tryptic Soy Broth (TBS) medium following transfer with a sterilized platinum loop. The TBS medium provided nutrition for the bacteria. The bacterial culture were incubated at 37°C and shaken for 24 hours at 200 Rpm using an Innova 4300 Incubator shaker to ensure homogeneous distribution of nutrients for the bacteria in the flasks.

Approximately 89 g of sediments were added to each of the six beakers; this was done in close vicinity of a burning flame, to prevent airborne microorganisms from entering the beakers. Each beaker was subsequently filled with 1000 ml of distilled water. The stock cultures maintained in the TBS medium were added into two pairs of beakers. One pair of beakers (each beaker containing 89 g of sediments and 1000 ml of distilled water) was deployed for gram-positive bacterial cultures and another pair was employed for gram-negative stock cultures. The final pair of beakers, which also consisted of 89 g

of sediments and 1000 ml of distilled water in each beaker, was left to replicate the micro-organisms in the natural setting of the Petitcodiac River system. Each pair of beakers had a control beaker in which a sterile environment was generated in them. This was done by the addition of 0.7 g/L (.02-.1 %) of sodium azide (NaN_3) into one beaker from each pair to kill the bacteria (and leave bodies within). The three control beakers containing the NaN_3 were covered with autoclaved aluminum foil to ensure a comparatively closed system.

The sediments were stirred thoroughly for several minutes at the initiation of the experiment and left to settle so that the turbidity levels in each beaker would have similar values at the start of the experiment. The turbidity was measured every 24 hours using an Oakton T-100 waterproof turbidity meter. Ethyl alcohol was sprayed around the beakers before 10 ml of water samples were taken for turbidity measurements and 2 ml were taken for bacterial counting. The purpose of the ethyl alcohol was to force the airborne microorganisms to settle so that they could not enter into the closed environments.

The beakers covered with autoclaved aluminium foil were subjected to bacterial counting at the beginning and the end of the experiment. This was done to ensure that the bacteria were killed during the experiments. Twenty ml of Mudler-Hinton agar were poured into petri-plates for the preparation of Mudler-Hinton agar plates. The water culture samples from each of six beakers were diluted with phosphate buffer solution (0.61 g of dibasic, 0.96 g of potassium phosphate (KH_2PO_4), and 8.5 g of NaCl in one liter of distilled water). In a test tube, 1 ml of culture was mixed with 9 ml of phosphate buffer. A series of 6 dilutions were carried out (down to 10^{-6} of the original concentration). Using a pipette, three drops of 20 μl were taken from each dilution and poured in the agar plate. The agar plates were then incubated for 16 hours after colonies developed in them. Then, the procedure was repeated at the end of the experiments.

Parameters:

Gram-positive and gram-negative bacteria- The experiment procedures required the cultivation of gram-negative (thin cell wall of peptidoglycan) and gram-positive bacteria (thick wall of peptidoglycan) to compare their effects with the bacteria *in situ* with the sediments (Ehrlich, 2001). Gram-positive bacteria have stronger cell walls that provide

them with better resistance than the gram-negative bacteria. Also, some bacteria were killed to investigate the variation of mud floc sizes with metabolic activities of bacteria. Sterile and non-sterile beakers- These beakers were used to replicated the alive and dead bacteria in natural settings to compare their effects on floc size with those of the cultivated bacteria.

Distilled water- To limit the study to the affects of bacteria without any intervention of salt ions, distilled water was used in this experiment.

Sodium azide- This chemical is a very toxic chemical that bacteria have no tolerance. To assure that a good number of bacteria was killed, sodium azide was used.

3.3.3. Experiment 3: Hydrodynamic effects on turbidity, aggregation and bacteria

Although the turbidity and flocculated mud properties vary with the physicochemical and bacterial parameters, the floc and bacterial populations are affected by the hydrodynamic turbulence levels. A series of experiments were carried out to determine the effects of turbulent energies in promoting turbidity, flocculation and floating micro-organisms. This was done by producing artificial turbulence of various energies in every set of beakers at the initiation of the experiments.

Approximately 70 g of sediments was added to each three autoclaved beakers. Each beaker was then filled with 1000 ml of Reverse Osmosis Water. Reverse Osmosis is a separation process where water is demineralized using pressure to force a solvent from a region of high solute concentration through a semipermeable membrane (thin film composite membrane) to a region of low solute concentration. The solute is retained on one side and the pure solvent passes to the other side of the membrane at high pressure. Water was poured from the tap to generate low turbulent energy for the first beaker. For the second beaker, 1000 ml of water was poured laterally from another flask to produce medium turbulent energy. The sediments in the last beaker were stirred manually using a spatula to promote a high turbulent energy in them. All the beakers were kept in the ultrasonic bath for approximately 10-15 minutes.

The above series of experiments were duplicated with a second set and both series of experiments were run at the same time (second set parallel to the first set). This was done to study whether the changes in turbidity and floc sizes with increased levels of turbulent energies could be accurately reproduced.

The turbidity and floc size were measured at 3, 6, and 9 hours after the starting point on the first day from all the six beakers. They were subsequently measured every 24 hours for a period of ten days. The turbidity was measured using an Oakton T-100 waterproof turbidity meter. The flocs were collected from the surface of sediments using a 3 mm pipette for the first set of beakers; a 4 mm pipette was utilized for the second set. Both pipettes extracted about 10 ml of water each time flocs were collected from the beakers. The flocs were then placed in Petri dishes. They were measured using a ruler and counted with the aid of a hand lens.

Bacterial counts were determined at the starting point and every 24 hours for a period of 9 days. The bacterial counting method was similar to the procedure outlined in for experiment 2.

Parameters:

70 g of sediment concentration- Because very small amounts of sediments remained for the final experiment 70 g of sediments were added to each beakers.

Turbulent energies- Low turbulent energy, medium turbulent energy and high turbulent energy were generated at the initial of the experiment to compare the turbidity , bacterial numbers and floc sizes of various hydrodynamic settings.

Reverse Osmosis Water- To study to effects of bacteria on the size of flocs and changes in turbidity without the intervention of salt ion concentrations, Reverse Osmosis Water, which contains no solutes, was used in this experiment.

3.4. RESULTS

3.4.1. Effects of physicochemical aggregation on turbidity

The turbidity and floc-size trends (*versus* time) for a range of sediment concentrations under non-turbulent conditions are shown in Table 3.1 and Figure 3.3. With increasing sediment concentration, a general increase in average floc size (horizontal diameter) was observed, but no significant effect of turbidity was seen in this experiment. The turbidity was observed to be fairly constant with the exception of increased turbidity observed as small peak on the fifth day and a large peak on the seventh day. These peaks in turbidity were observed for all sediment concentrations (Fig. 3). The general trend of floc size shows a progressive increase in particle size with time

(Table 3.1). When examined in detail, similar trends are evident with smaller sediment concentrations (i.e. 20g/L and 40 g/L). An increase in trend was observed in the first six days and subsequently remained constant. At sediment concentration of 80 g, the mean floc size increased for the first five days of testing to 2 mm and decreased dramatically on Day 6 to 0.5 mm (Fig. 3.3), then remained constant for the remainder of the experiment. With increased sediment concentrations (145 g/L), the average floc size rose to approximately 4 mm on the first and seventh days of the experiment (Table 1; Fig. 3). The average floc size remained constant (about 2 mm) between days 4 and 5.

Table 3.2 and Figure 3.4 display the time series of variations in floc size and also turbidity (at various salinities). The beaker with distilled water shows two large peaks in turbidity (479 and 595 NTU) at the initiation of the experiment. The turbidity was lowest on Day 3 (25 NTU); it then climbed on Day 4 to 209 NTU and remained constant for the remainder of the experiment. At 5 ppt, the turbidity decreased from 383 NTU, observed at the start of the experiment, down to 152 NTU (Fig. 3.4). Two peaks of about 200 NTU are seen on Days 2 and 6, and a small peak of about 100 NTU occurred on the fourth day. The turbidity trends are generally similar at 10, 15 and 20 ppt (i.e. the other fixed-salinity experiments). On the second day, there was a small drop in turbidity from 150 NTU to 60 NTU, but the most significant reduction occurred on Day 6 when the turbidity fell to approximately 10 NTU. The turbidity also produced two small peaks of 40 NTU on the fourth and sixth days (Table 3.2; Fig. 3.4). An exceptionally high peak for turbidity (155 NTU) is observed at 10 ppt.

The experimental investigations above show that the floc sizes and turbidity levels increase with increased particle concentrations (Fig. 3.3) and increased salt concentrations (Fig. 3.4). Previous theoretical investigations (Hill, 1998; Eisma, 1986; Milligan and Hill, 1998; Fennessy et al., 1994b; Fettweis et al., 2006) show that under high turbulence, flocs are broken down. In this study, although no overall effect was seen in turbidity under the influence of a mechanical stirrer, the average floc size results (Table 3.3; Fig. 3.5) show that sediment particles break in turbulent conditions.

The macroflocs collected from the aforementioned experiments were measured using a ruler, described in Table 3.2 and Table 3.3, and examined in great detail under the Scanning Electron Microscope (SEM). Diatoms were the most common organisms

present in these flocs (Table 3.1; Table 3.2; Fig. 3.6). The diatoms were not identified in this study. Other particles (organic and inorganic), including clay, organic detritus, planktons, phytoliths, bacteria and minerals, were also present (Fig. 3.6; Fig. 3.7). Scanning electron microscopy also shows that *Sphaerotilus* (Fe-bacteria) were only seen in the flocs that were cultivated in beakers with waters of low salinity ranges (Table 3.2; Fig. 3.7). These bacteria occur in fresh water streams and they excrete ferric iron sheaths (Fenchel et al., 1998). They oxidize iron by the expolymers that constitute their sheaths (Ehrlich, 2002). On the other hand, phytoliths present in Figure 3.4 were removed from beakers containing waters of high salinity ranges. Diatoms were the most common microorganisms and their dissolution was more noticeable in flocs that have a high amount of salt in them.

3.4.2. Bacterial effects on turbidity

Although NaN_3 was added to the control beakers to see the affect of the dead cells on sediment aggregates, many bacteria survived. The bacterial counts for gram negative and gram positive bacteria were determined to be $5.8 \times 10^8 \text{ ml}^{-1}$ and $1.28 \times 10^9 \text{ ml}^{-1}$ at the beginning of the experiment. By the end of the experiment the number of bacteria was $5.2 \times 10^7 \text{ ml}^{-1}$ for gram-negative bacteria and $7.2 \times 10^7 \text{ ml}^{-1}$ for gram-positive bacteria. The survival of the bacteria is due to their unexpected high resistance to NaN_3 . The sterilized beaker had the least number of bacteria ($2.3 \times 10^4 \text{ ml}^{-1}$) at the end of the experiment.

The turbidity levels measure in each of the six beakers were slightly higher than 1000 NTU at the initiation of the experiment due to the stirring of the sediments. Because of the negligible difference in turbidity achieved in all beakers, the turbidity measurements were considered to be 1000 NTU in this experiment (Table 3.4). The turbidity decreased through time for all beakers. Although, the turbidity levels fell from 1000 NTU to approximately 700 NTU in the sterile beakers on Day 1, the turbidity levels ranged between 500 NTU to 650 NTU for the non-sterile environments (Table 3.4, Fig. 3.8). Although the turbidity levels remained approximately 100 NTU in the sterile environments for the last four days, they ranged between 20 and 60 NTU for the final days in the rest of the other beakers. The turbidity representing the sterile environment decreased at a slower rate than both the non-sterile environments and those that contained cultivated bacteria — both alive and dead (Fig. 3.8).

3.4.3. Hydrodynamic effects on turbidity, aggregation and bacteria

In the following experiment, it was observed that water poured from the tap generated the lowest turbulent energy and manual mixing/stirring of sediment with water induced the highest turbulent energy (Table 3.5; Fig. 3.9).

Figure 3.10 and 3.11 compare bacterial counts to average floc size under various turbulent conditions through time. From these figures it can be seen that floc size increased concurrently with the rise in the number of the bacteria. The number of bacteria was high (up to 10,000 /ml) between Days 2 and 7 (Table 3.5; Fig. 3.10). The growth of flocs was delayed for a day in the first two beakers of the second set of experiments for the beakers with low and medium turbulent energies (Fig. 3.10). The floc size subsequently decreased as the bacteria died and remained constant for the remainder of the experiment (Table 3.5, Fig. 3.10; Fig. 3.11). In the presence of high turbulent energies, the sizes of particles were very small (0 - 1 mm) for the most part of the experiment; the size of flocs grew to 4 mm towards the end of the experiment. Bacterial counts were very high between Days 2 and 6 (approx. 18, 000 /ml) and decreased abruptly on the seventh day. The bacterial counts also increased slightly on Day 9 and decreased on the last day (Fig. 3.10; Fig. 3.11).

3.5. INTERPRETATION

3.5.1. Effects of physicochemical aggregation on turbidity

Physicochemical parameters such as sediment concentrations and salt concentrations contribute to the formation and settling of flocs by promoting particle adhesion. The mass of flocs can increase or decrease due to their growth enhancement, accelerating the settling speed of the flocs (Lick et al., 1993; Krank and Milligan, 1980; Fennessy et al., 1994a). The turbidity levels decrease as the aggregates settle to the bottom sediments and the turbidity increases when the flocs are resuspended due to physical disturbances in the beakers. Hence, an inverse linear relationship exists between the turbidity levels and average floc size: this is as a result of floc settling (Fig. 3; Fig. 4; Fig. 5).

The results from the turbulence experiment (Table 3.3; Fig. 3.5) demonstrate that the shearing action of turbulence can limit floc size and break flocs into smaller particles

(Milligan and Hill, 1998; Hill, 1998). The beaker with the high turbulent energy had a higher turbidity level at the starting point because of the resuspension and flotation of flocs as a result of turbulence produced by the mechanical stirrer (Fig. 3.5). The turbidity peaks in Days 2 and 3 in both beakers are explained below.

3.5.2. Bacterial effects on turbidity

The clumps and aggregates are broken and resuspended when the sediments are mixed with water for several minutes; this also increases the turbidity levels to approximately 1000 NTU at the starting point (Table 3.4). Free-floating bacteria also promote the turbidity levels. When the number of the free-floating bacteria increases the water also becomes more turbid (Lind and Davalos-Lind, 1999). Through time, the free-floating bacteria attach themselves to the suspended particles to obtain substrates and eventually settle with the aggregates (Bell and Albright, 1981). Thus, the turbidity decreases with time due to both electrostatic clumping and biological binding. Under sterilized conditions, the dead bacteria do not attach themselves to the suspended particles. Thus, the turbidity of the sterilized environment decreases at a slower rate than the non-sterile examples (including those with cultivated bacteria (both alive and dead) (Table 3.4, Fig. 3.8). Had most of the gram-positive and gram-negative bacteria would have been dead in this experiment, they would have probably behaved very similar to the dead bacteria in the natural setting.

3.5.3. Hydrodynamic effects on turbidity, aggregation and bacteria

The various turbidity levels generated by various water discharges in Figure 3.9 are indicative that a stirring action is generally required to increase the turbidity levels in water bodies. Normally, high turbulent energies generate high turbidity levels. Figure 3.3, Figure 3.7 and Figure 3.9 support the hypothesis that a physical disturbance in the sediments caused by the production of microbial by-products resulted in floc suspension (Eisma, 1986). The microbial by-products are speculated to be either carbon dioxide (CO₂), oxygen (O₂), or biogas, which is composed of: 55-60 % methane (CH₄), 30-35 % carbon dioxide and 5-10 % hydrogen (H₂) (Subba Rao, 1999). These gases present in a biogas are produced by the biological breakdown of organic matter in the absence of oxygen. Low density aggregates and suspended single grains are also noticed in Tables 3.1 and 3.2. These suspended flocs of approximately 0.25 mm resulted in a sudden

increase in turbidity. Hence, bacteria and the physicochemical parameters facilitate floc settling by increasing the size of aggregates once they are clustered. However, the metabolic processes generate gases that can facilitate fluctuations in turbidity by resuspending the aggregates.

Except for the beakers with high turbulent energies, a linear relation exists between the number of bacteria and size of flocs (Fig. 3.10; Fig. 3.11). This is probably due to the large surfaces provided by the aggregates for microbial growth (Muschenheim et al., 1989). Bacteria, in turn, modify the particle surface chemistry such that they clump together to form aggregates (Fennessy et al., 1994a).

The bacterial counts for mixed sediments were very high between the second and the sixth days (Fig. 3.10). This is potentially because mixing of sediments increased the dissolution rate of soluble nutrients available for the bacteria in the beakers. If the mixing of sediments continued for more days, it would have delayed the formation of flocs and the number of bacteria would have remained high for longer periods of time. Moreover, mixing of sediments delays the formation of flocs as the initial shear is very high during the first few days.

To summarize, the reason for the suggested occurrence of peaks by turbidity on Day 7 in Figure 3.3 and Days 2, 4, 5 and 6 in Figure 3.4 is a result of floc flotation generated by the by-products of micro-organisms. The flotation of flocs is also reported in Table 3.1 and Table 3.2 when suspended particles are floating.

3.6. DISCUSSION

Although salinity and particle concentration are known to influence flocculation (Fennessy et al., 1994b; Meade, 1972; Miall, 1961; Yariv and Cross, 1979; Milligan et al., 2001), a few studies have shown the importance of micro-organisms on particle surfaces (Burban et al., 1989; Fennessy et al., 1994a). The experiments in this paper outline the potential significance of bacteria in facilitating flocculation and turbidity under various physico-chemical conditions.

The break up and re-clustering of flocs in response to changes due to current and wave energy can elucidate our understanding of the dynamics of sediments in marginal-marine settings (Chen, 2005; Chang, 2005; Droppo and Ongley, 1994; Pearson and

Gingras, 2005). The most significant factors in the transport and deposition of sediments in estuaries are the hydrodynamic processes influenced by river discharge, tide and turbulence that circulate and mix water.

When the turbulent energies are low, physicochemical and microbial parameters facilitate flocculation. A decrease in shear velocities due to the low turbulent energies results in a large supply of sediments and rapid accumulation rates (Milligan et al., 2001). The turbidity levels decrease as a result of settling of aggregates. As heterotrophic bacteria tend to stick to the aggregates to feed on nutrients, they settle along with the sediment clumps and contribute some what to the decrease in turbidity levels (Lind and Davalos-Lind, 1999; Bell and Albright, 1981). However, microbial by-products such as carbon dioxide and hydrogen can generate suspension of sediment particles resulting in sudden increases in turbidity.

The above findings in a laboratory can be applied to the natural system such as an estuary. Within turbulent mixing zones, flocs disintegrate and result in high concentration of small particles which get transported through a system of suspension (Gibbs et al., 1989). Nutrients are distributed throughout the system leading to the increase in free-floating bacteria. Hence, the turbidity levels are increased due to the increase in suspended particles, floating bacteria and dissolved nutrients. Suspended particles settle during slack tide and are re-suspended during early ebb or early flood (Eisma and Li, 1993). However, the microbial interactions with the aggregates can influence the sedimentation processes as is demonstrated in the recycling of waste water in various industries such as effluents. Biogenic coagulant treatment, for example, is one of the most profound physicochemical steps in industrial water waste treatment and it reduces the suspended particles responsible for high turbidity levels in waste water. When coagulants such as bacteria (both alive and dead) or organic materials are added into the waste water, they destabilize the suspended particles (Sarkar et al., 2006; Smith and Miettinen, 2006). These suspended particles collide and cluster together as a consequence of Brownian motion to form aggregates (Eisma, 1986).

The by-products of micro-organisms are also used in commercial operations (Smith and Miettinen, 2006). For example, turbulent micro-flotation of suspended or flocculated particles is another major stage for water purification from fine contaminants

(Rulyov, 1999). In this process, micro-bubbles are produced from the by-products of micro-organism and loaded with floating contaminants. They are then removed from the water through sedimentation. This process can be significant when bubbles are separated and aggregated in large foam bubbles containing of many initial micro-bubbles (Rulyov, 1999). Thus, micro-organisms and their by-products have potential significance on flocculation in commercial as well as natural settings.

3.7. CONCLUSION

The study of the relation of biological parameters to aggregation and turbidity under various physico-chemical parameters and hydrodynamics is useful for understanding mud accumulation in the rock-record. The summary of the flocculation process in Figure 3.12 demonstrates that physicochemical parameters, sediment biota and turbidity are interlinked and support that bacteria play a vital role during the process such as facilitating floc settling. The metabolic processes of bacteria generate gases such as carbon dioxide to promote fluctuations in turbidity. The relation of bacteria and flocculation process is better understood under the influence of various turbulent energies of the river or estuarine system. Under high energy conditions, flocs disintegrate and result in high concentration of suspended particles and nutrients (Fig. 3.12). Nutrients also dissolve in water and hence become readily available to the bacteria. Thus, the number of bacteria is high in turbid conditions. During low energy conditions, large flocs are formed due to physicochemical and biological parameters (Fig. 12). While physicochemical parameters modify the surface charge of sediment particles, bacteria also produces a fibrous structure, mucopolysaccharides to glue the particles together. These flocs settle with the micro-organisms rapidly promoting sedimentation resulting in reduction in turbidity levels (Fig. 3.12). Thus, the interactions between aggregates and sediment biota can have significant effects on sedimentary dynamics, nutrient cycling and aquatic ecology.

3.8. REFERENCES

- AMEC Earth and Environmental. (2005). *Environmental Assessment report for Modifications to the Petitcodiac River Causeway*. (Technical Report Series, YB299A, TE23520.4). A division of Amec Americas Limited. Submitted to New Brunswick Department of Supply and Services.
- Bell, C.R and Albright, L.J. (1981). Attached and free-floating bacteria in the Fraser River Estuary, British Columbia, Canada. *Mar. Ecol. Prog. Ser.*, 6, 317-327.
- Burban, P., Lick, W. and Lick, J. (1989). The flocculation of fine-grained sediments in estuarine waters. *Journal of Geophysical Research*, 94, 8323-8330.
- Burton, J. D. (1976). Basic properties and processes in estuarine chemistry. In: *Estuarine Chemistry*. (Ed. Burton, J.D. and Liss, P.S.). Academic Press Inc, U.S.A, p 1-36.
- Chang, T.S. (2005). Dynamics of fine-grained sediments and stratigraphic evolution of a back-barrier tidal basin of the German Wadden Sea (Southern North Sea), dissertation, Bremen University, Bremen.
- Chen, S., Wartel, S. and Temmerman, S. (2005). Seasonal variation of floc characteristics on tidal flats, the Scheldt estuary. *Hydrobiologia*, 540, 181-195.
- Drever, J. I. (1997). Evaporation of saline water. In: *Geochemistry of natural waters*. (Ed. Drever, J.I.). Prentice Hall, U.S.A., p 327-351.
- Droppo, I.G. and Ongley, E.D. (1994). Flocculation of suspended sediment in rivers of Southeastern Canada. *Wat. Res.*, 28 (8), 1799-1809.
- Dyer, K.R. and Manning, A.J. (1999). Observation of the size, settling velocity and the effective density of flocs, and their fractal dimensions. *Journal of Sea Research*, 41, 87-95.
- Ehrlich, H.L. (2002). Geomicrobiology of Iron. In: *Geomicrobiology* (Ed. Ehrlich, H.L.). MarcelDekker Inc, p 345- 428.
- Eisma, D. (1986). Flocculation and de-flocculation of suspended matter in estuaries. *Netherlands Journal of Sea Research*, 10 (2/3), 183-199.
- Eisma, D. and Li, A. (1993). Changes in suspended-matter floc size during the tidal cycle in the Dollard estuary. *Netherlands Journal of Sea Research*, 31(2), 107-117.
- Fencel, T., King, G.M. and Blackburn, T.H. (1998). Microbial mats and stratified water columns. In: *Bacterial Biogeochemistry: The ecophysiology of mineral cycling*. (Ed. Fencel, T., King, G.M. and Blackburn, T.H.). Academic Press, U.S.A, p 142- 165.

- Fennessy, M.J., Dyer, K.R. and Huntley, D.A. (1994a). INNSSEV: An instrument to measure the size and settling velocity. *Marine Geology*, 117, 107-117.
- Fennessy, M.J., Dyer, K.R. and Huntley, D.A. (1994b). Size and settling velocity distributions of flocs in the Tamar estuary during a tidal cycle. *Netherlands journal of aquatic ecology*, 28 (3-4), 275-282.
- Fettweis, M., Franken, F., Pison, V. and Van den Eynde, D. (2006). Suspended particulate matter dynamics and aggregate sizes in a high turbidity area. *Marine Geology*, 235, 63-74.
- Gibbs, R.J., Tshudy, D.M., Konwar, L. and Martin, J.M. (1989). Coagulation and transfer of sediments in the Gironde estuary. *Sedimentology*, 36, 986-999.
- Hill, P.S. (1998). Controls of floc size in sea. *Oceanography*, 11 (2), 13-18.
- Kirchamn, D. (1983). The production of bacteria attached to particles suspended in a freshwater pond. *Limnology and Oceanography*, 28 (5), 858-872.
- Krank, K. and Milligan, T. (1980). Macroflocs: Production of Marine snow in the Laboratory. *Marine Ecology- Progress series*, 3, 19-24.
- Lick, W., Huang, H. and Jepsen, R. (1993). Flocculation of fine-grained sediments due to differential settling. *J. Geophys. Res.*, 97, 10279-10288.
- Lind, O.T. and Davalos-Lind, L. (1991). Association of turbidity and organic carbon with bacterial abundance and cell size in a large turbid, tropical lake. *Limnology and Oceanography*, 36(6), 1200-1208.
- McSween, H.Y., Richardson, S.M., Uhle, M.E. (2003b). Diagenesis: A study in kinetics. In: *Geochemistry : Pathways and processes*. (Ed. McSween, H.Y., Richardson, S.M., Uhle, M.E.). Prentice Hall Inc., p 79- 93.
- Meade, R.H. (1972). Transport and deposition of sediments in estuaries. In: *Environmental Framework of coastal plain estuaries*. (Ed. B.W. Nelson). *Geol. Soc. Amer. Mem.*, 133, 91-120.
- Miall, L.M. (1961). Coagulation. In: *A new dictionary of chemistry*. (Ed. Miall, L.M.). Interscience Publishers Inc, New York. p139-140.
- Milligan, T.G. and Hill, P.S. (1998). A laboratory assessment of the relative importance of turbulence, particle composition, and concentration in limiting maximal floc size and settling behaviour, *Journal of Sea Research*, 39, 227-241.
- Milligan, T.G., Kineke, G.C., Alexander, C.R. and Hill, P.S. (2001). Flocculation and sedimentation in the ACE Basin, South Carolina. *Estuaries*, 24 (5), 734-744.

- Muschenheim, D. K., Kepkay, D.K. and Kranck, K. (1989). Microbial growth in turbulent suspension and its relation to marine aggregate formation. *Netherlands Journal of Sea Research*. 23 (3), 283- 292.
- Pearson, N.J. and Gingras, M.K. (2006). An ichnological and sedimentological facies model for muddy point-bar deposits. *Journal of Sedimentary Research*. 76, 1-12.
- Rulyov, N. (1999). Application of ultra-foculation and turbulent micro-flotation to the removal of fine contaminants from water. *Colloids and surfaces A: Physicochemical and engineering aspects*, 151, 282-291.
- Sarkar, B., Chakrabarti, P.P., Vijaykumar, A. and Kale, V. (2006). Wastewater treatment in diary industries- possibility of reuse. *Desalination*, 195, 141-152.
- Smith, R.W and Miettinen, M. (2006). Microorganisms in flotation and flocculation: Future technology or laboratory curiosity? *Minerals Engineering*, 19, 548-553.
- Subba Rao, N.S. (1999). Organic matter decomposition. In: *Soil microbiology*. (Ed. Subba Rao, N.S.), Science Publishers Inc., U.S.A. p 252- 270
- Tisdall, J.M. and Oades, J.M. (1982). Organic matter and water-stable aggregates in soil. *Journal of Soil Science*, 62, 141-163.
- Tsai, C.H., Iocobellis, S., and Lick, W. (1987). Flocculation of the fine-grained lake sediments due to uniform shear stress. *Journal of Great Lakes Research*, 13, 135-146.
- Yariv, S. and Cross, H. (1979). Interaction between solid particles dispersed in colloid systems. In: *Geochemistry of colloid systems for earth scientists*. (Ed. Yariv, S. and Cross, H.). Springer-Verlag, Germany. p 335- 373.

Table 3.1. Turbidity and average floc size for different particle concentrations.

Time (days)	Turbidity (NTU)	Average Floc size (mm)	Notes on floc size and internal structure 20 g/L
0	23.60	0	Largest size is 0.5 mm but most grains can't be measured.
1	18.76	1	Beaker was disturbed a little. Mostly flocs are 1mm and a few are of 3 mm.
2	16.57	0.5	Most flocs are 0.5 -1mm and very few are between 3 and 4 mm.
3	8.80	1.5	Most flocs are 1-2 mm and very few are about 5-7mm.
4	44.50	1	Few flocs of 2-3 mm are present.
5	71.90	1.25	Flocs ranged from 0.5 to 2 mm and were distributed equally.
6	12.20	2	Mostly 1-3 mm in size. Few flocs are 0.25-0.5 mm. Few flocs of 4 mm also seen.
7	557.00	2	Mostly 1-3 mm. Few flocs of 0.25-0.5 and 4mm also seen. Suspended particles also seen.
8	68.50	2	Mostly 1-3 mm. Few flocs of 0.25-0.5 and 4mm also seen. Suspended particles also seen.
9			SEM observation- clays, debris, phytolith, diatoms and minerals.
Time (days)	Turbidity (NTU)	Average Floc size (mm)	Notes on floc size and internal structure 40 g/L
0	34.70	0.5	Most flocs are 0.5 mm.
1	7.30	1	Most flocs are 1mm. Few are 3 mm.
2	6.37	1	Most flocs are 1mm. Few are 5 mm.
3	4.34	1.5	Mostly 1-2 mm of flocs with a few ranging between 3-5 mm.
4	10.39	1.5	Most flocs are about 1-2 mm.
5	67.70	1.25	Flocs range from 0.5 to 2mm.
6	14.02	1.125	Most flocs range from 0.25 to 2mm. Few flocs of 4mm also noticed.
7	285.00	1.5	Mostly 1-2mm. Few range from 0.25 to 0.5 mm as well as 4 to 5mm. Suspended particles seen.
8	25.10	1.5	Mostly 1-2mm. Few range from 0.25 to 0.5 mm as well as 4 to 5mm. Suspended particles seen.
9			SEM observation-planktons, phytoliths, diatoms and erected salts.
Time (days)	Turbidity (NTU)	Average Floc size (mm)	Notes on floc size and internal structure 80 g/L
0	63.90	0.5	A 4 mm sized lump is present with many flocs of 0.5 mm
1	7.78	1	Most flocs are 1 mm. One lump of 4mm noticed.
2	14.26	0.75	Most flocs are about 0.5-1mm and a few are about 3-5 mm.
3	20.50	1.75	Some flocs are 0.5 mm. Others are 1-2 mm with a few ranging between 5 and 7 mm.
4	6.52	1.5	All flocs are between 1 and 2 mm.
5	26.60	2	Flocs range from 1-3 mm. Few are 0.5mm.
6	10.92	0.75	Most flocs range from 0.5 to 1mm. Few range from 2 to 5 mm.
7	158.00	0.75	Mostly 0.5-1mm of flocs. Few are 2 mm. Suspended particles noticed floating in the beaker.
8	14.03	1	Most flocs are 0.5-1mm, some are 1-2 mm and a few are 7 mm. Suspended particles seen.
9			SEM observation- diatoms.
Time (days)	Turbidity (NTU)	Average Floc size (mm)	Notes on floc size and internal structure 145 g/L
0	81.80	0.375	Flocs range from 0.25 to 0.5 mm.
1	8.50	3.5	Mostly 3-4 mm of flocs present. Some are about 1-2 mm.
2	14.47	2	Mostly 2 mm of flocs seen with a few ranging from 5 to 7 mm.
3	6.86	1.75	Some flocs are 0.5 mm. Others are 3 mm. A few lumps of 10 mm also present.
4	16.07	2	Most flocs are about 2-4 mm.
5	27.50	1.5	Lots of flocs are present. Some are 0.5 mm but most of them are 1-2 mm. Few were 4-5 mm.
6	7.77	3.5	Mostly 3-4 mm, some were 1-2mm and a few are 0.5 mm.
7	78.00	4	Mostly 3-5 mm, some 1-2mm and a few of 0.5 mm flocs seen. Suspended particles also present.
8	8.51	3	Mostly 3 mm of flocs. Some are 0.25-1mm and a few are 5 mm. Suspended particles present.
9			SEM observation- phytoliths, diatoms, Sphaerotilus (Fe-bacteria) and erected salt.

Table 3.2. Turbidity and average floc size under various saline conditions.

Time (days)	Turbidity (NTU)	Avg floc size (mm)	Notes on floc size and internal structure
Distilled water			
0	47.90	0.375	Most flocs are 0.25-0.5 mm. Some are 1mm. Very few lumps (5-10 mm) also present.
0.08	171.00	0.625	Most flocs are 0.5- 1 mm. A lot of 0.25 mm as well with very few 5 mm in size.
0.2	445.00	0.25	All are 0.25 mm except for one lump of 3 mm.
1	307.00	0.625	Most flocs are 0.5- 1 mm. Some are 1 mm in size.
2	595.00	0.375	Mostly .25-0.5 mm sized flocs. Some are 1 mm.
3	25.00	1	Most flocs are 1 mm. Few are 5-6 mm.
4	209.00	1	Most flocs are 1 mm. Few are 0.25 and 2-3 mm.
5	162.00	1	Mostly 1 mm with some 0.5 mm and a few of 6 mm. Suspended flocs seen (0.25-0.5 mm).
6	191.00	1	Most flocs are 1 mm and a few are 0.5 mm. Very few large lumps of 6mm also see.
7	282.00	1	Most flocs are 1 mm. A lump of 10 mm also present.
8			SEM observations- minerals, diatoms, debri and Sphaerotilus (Fe-bacteria).
Notes on floc size and internal structure			
5 ppt			
0	383.00	0.25	Mostly flocs are 0.25 mm and a few are 1 mm.
0.08	244.00	0.25	Mostly flocs are 0.25 mm. Few flocs of 1mm and 4 mm also present.
0.2	318.00	0.5	Most flocs are 0.5 mm. A few are 2 mm. One lump of 6 mm also seen.
1	152.00	0.375	Most flocs range from 0.25 to 0.5mm. A few are 2 mm.
2	205.00	0.5	Most flocs are 0.5mm . One lump of 4 mm also present.
3	16.38	1	Most flocs are 1mm. A few range between 3 and 5 mm.
4	99.50	0.375	Most flocs range from 0.25 to 0.5 mm. Some are 1-3 mm in size.
5	76.30	1	Mostly 1mm with a few of 4 mm. Suspended flocs are 0.25-0.5 mm (mostly organic materials).
6	254.00	1	Most flocs are 1mm with a few ranging from 4 to 5 mm.
7	67.00	1	Few flocs present. Most of them are 1mm. Some suspended flocs seen (approx.0.25 mm).
8			SEM observations- diatoms, debri and Sphaerotilus (Fe-bacteria).
Notes on floc size and internal structure			
10 ppt			
0	133.00	0.5	Most flocs are 0.5 mm. A few range between 1 and 3 mm.
0.08	99.70	0.5	Most flocs are 0.5 mm. Some are 1 mm and few range from 2 to 4 mm.
0.2	317.00	0.5	Most flocs are 0.5 mm with a few of 2 mm.
1	55.50	0.375	Most flocs range from 0.25 to 0.5 mm. Few are 1 mm.
2	74.40	0.25	All flocs are 0.25 mm except for one lump of 4 mm.
3	11.14	1	Most flocs are 1mm. Some are 0.25 and 4-5 mm. Floc number increased as well.
4	155.00	0.375	Most flocs are about 0.25-0.5 mm. Some are 1-2 mm and a few are of 3-4 mm.
5	16.74	0.75	Many flocs are 0.5-1 mm. Some are 0.25 mm. Few are 4-5 mm with suspended flocs of 0.25 mm.
6	67.70	2	Floc number increased with mostly 2 mm. Few are 0.5 mm and 5 mm. Suspended flocs are 0.25- 0.5 mm.
7	50.80	2	Most flocs are 2 mm with a few of about 2-4 mm. Suspended flocs are 0.25 mm.
8			SEM observations- diatoms and clays.
Notes on floc size and internal structure			
15 ppt			
0	145.00	0.75	Most flocs range from 0.5 to 1 mm. Few are 4-5 mm.
0.08	97.00	0.375	Most flocs range from 0.25 to 0.5 mm. Some are 1 mm. Few flocs of 4 mm also exist.
0.2	160.00	0.75	Some flocs are 0.5 mm. Others are 1 mm and few are about 4 mm.
1	69.40	0.25	Most flocs are 0.25 mm and some are 1 mm.
2	109.00	1	Most flocs are 1 mm. Few flocs of 5 mm also present.
3	8.56	1.5	Many flocs are 1-2 mm. Few are 4 mm.
4	49.70	1.5	Flocs increased in number. Most flocs are 1-2 mm. Some are 0.25-0.5 mm.
5	29.60	2	Mostly flocs are 1-3 mm with few flocs of 5-7 mm. Some are 0.25-0.5 mm. Few, tiny suspended particles seen.
6	39.90	2	Lots of flocs. Most are 2 mm. Few are 0.5-1 mm and 5mm. Few suspended flocs (0.25-0.5 m) also observed.
7	28.60	2	Mostly flocs are 2mm with few 0.25 and 5 mm. Suspended flocs range from 0.25mm to 0.5 mm.
8			SEM observations- diatoms, minerals and phytoliths.
Notes on floc size and internal structure			
20 ppt			
0	120.00	0.25	All flocs are 0.25 mm except for a few 0.5 mm.
0.08	55.30	0.25	Most flocs are 0.25 mm. Some are 1mm a few of 5 mm also exist.
0.2	136.00	0.375	Most flocs are 0.25-0.5 mm. Some are 1-2 mm. One lump of 6 mm aslo exists.
1	59.10	0.25	All flocs are 0.25 mm.
2	110.00	1	Most flocs are 1mm with a few flocs of 5mm.
3	6.15	1	Floc number decreased. Mostly flocs are 0.25 mm with some 2 mm. A few of them are about 4mm.
4	27.30	1.5	Lots of flocs present. Most of them are 1-2 mm. Some are 0.25-.5 mm.
5	17.63	2	Lots of flocs present. Most are 2-4 mm with some 0.5-1 mm. Suspended flocs are mostly clays and few organics.
6	44.70	2	Floc number increased. Most are 2-4 mm and a few are 0.5mm and 5mm. Few suspended (0.25-0.5 mm) seen.
7	12.78	2	Most flocs are 2-4 mm with a few of 5 mm. Suspended flocs increased in number (0.25-0.5 mm).
8			SEM observation- diatoms, planktons and phytoliths.

Table 3.3. Turbidity and average floc size from a turbulent experiment.

Time (days)	Turbidity (NTU)	Avg floc size (mm)	Notes on floc size (Mechanical stirrer rotating at 25 Hz)
0	120.00	0.25	All flocs are 0.25 mm except for a few of 0.5 mm.
1	59.10	0.25	All flocs are 0.25 mm.
2	110.00	1	Most flocs are 1mm with a few of 5mm.
3	6.15	1	Floc number decreased. Most flocs are 0.25 with some 2mm and a few of 4mm.
4	27.30	1.5	Lots of flocs present. Most are 1-2 mm. Some are 0.25-.5 mm.
5	17.63	2	Lots of flocs present. Most are 2-4 mm and some are 0.5-1 mm.
6	44.70	2	Floc number increased. Most are 2-4 mm with a few of 0.5mm and 5mm.
Time (days)	Turbidity (NTU)	Average Floc size (mm)	Notes on floc size (No mechanical stirrer)
0	653.00	0.75	Most flocs are 0.5-1mm with a few of 4mm in size.
1	358.00	1	Most flocs are 1mm with a few of 4mm.
2	260.00	0.25	Most flocs are 0.25 mm with some 0.5-1mm. Others are 3-4 mm.
3	452.00	0.25	Most flocs are 0.25 mm with some ranging from 1 to 3 mm.
4	244.00	0.25	Most flocs are 0.25 mm and lesser. Very few are 1-3 mm.
5	90.80	0.125	Most particles or flocs are lesser than 0.25. A few are 1-2 mm.
6	102.00	0.125	Most flocs are lesser than 0.25. A few are 3 mm.

Table 3.4. Representation of turbidity under different bacterial condtions.

Time (days)	Non- sterile	Sterile	Gram positive (dead)	Gram positive (alive)	Gram negative (dead)	Gram negative (alive)
0	1000.0	1000.0	1000.0	1000.0	1000.0	1000.0
1	536.0	744.0	634.0	521.0	654.0	605.0
2	210.0	606.0	194.0	52.7	274.0	287.0
3	135.0	392.0	67.5	53.5	142.0	50.4
4	72.1	294.0	67.9	47.9	77.2	46.4
5	55.9	238.0	77.7	46.0	90.5	47.4
6	47.3	103.0	66.5	40.1	94.9	39.2
7	41.7	97.9	56.5	34.5	83.3	33.9
8	36.5	98.9	50.1	29.0	72.3	29.1
9	40.5	102.0	44.8	25.4	63.9	19.2

Table 3.5. Representation of turbidity, average floc size and bacterial counts under various turbulent energies.

Time (Days)	Low turbulent energy 1					Low turbulent energy 2				
	Turbidity (NTU)	Avg floc size (mm)	Avg floc size (log mm)	Bacterial count (ml ⁻¹)	Bacterial count log (ml ⁻¹)	Turbidity (NTU)	Avg floc size (mm)	Avg floc size (log mm)	Bacterial count (ml ⁻¹)	Bacterial count log (ml ⁻¹)
0	474	0		16	1.204	534	0		0	
0.125	380	0				484	0			
0.25	360	0				447	0			
0.375	326	0				413	0			
1	248	0		16	1.204	331	0		0	
2	176	0		0		233	0		0	
3	136	0.25	-0.602	63333	4.802	226	0.125	-0.903	16667	4.222
4	100	0.25	-0.602	14833	4.171	170	1	0.000	65000	4.813
5	80	0.75	-0.125	51667	4.713	127	1	0.000	56667	4.750
6	66	2	0.301	98333	4.993	99.7	3.75	0.574	1333	3.125
7	57	1	0.000	4166	3.620	112	1	0.000	6333	3.802
8	54	2	0.301	9167	3.962	89.1	1	0.000	5500	3.740
9	44	3	0.477	3333	3.523	82	1	0.000	4833	3.684
10	38	1.5	0.176	1833	3.263	71.4	1	0.000	333	2.520
Time (Days)	Medium turbulent energy 1					Medium turbulent energy 2				
	Turbidity (NTU)	Avg floc size (mm)	Avg floc size (log mm)	Bacterial count (ml ⁻¹)	Bacterial count log (ml ⁻¹)	Turbidity (NTU)	Avg floc size (mm)	Avg floc size (log mm)	Bacterial count (ml ⁻¹)	Bacterial count log (ml ⁻¹)
0	770	0		25	1.398	787	0		16	1.204
0.125	720	0				760	0			
0.25	689	0				716	0			
0.375	648	0				661	0.125			
1	526	0		16	1.204	540	0		33	1.519
2	376	0		33	1.519		0		17	1.230
3	257	0.125	-0.903	40000	4.602	269	0.25	-0.602	60000	4.778
4	172	0.125	-0.903	15000	4.176	205	0.6	-0.222	5167	3.713
5	145	0.125	-0.903	96667	4.985	155	7	0.845	11833	4.073
6	110	0.75	-0.125	68333	4.835	168	0.125	-0.903	68333	4.835
7	94	0.6	-0.222	4333	3.637	109	1	0.000	9500	3.978
8	100	0.5	-0.301	50000	4.699	145	0.75	-0.125	6333	3.802
9	80	2	0.301	4500	3.653	124	2	0.301	3833	3.584
10	67	2	0.301	833	2.921	92	1	0.000	1833	3.263
Time (Days)	High turbulent energy 1					High turbulent energy 2				
	Turbidity (NTU)	Avg floc size (mm)	Avg floc size (log mm)	Bacterial count (ml ⁻¹)	Bacterial count log (ml ⁻¹)	Turbidity (NTU)	Avg floc size (mm)	Avg floc size (log mm)	Bacterial count (ml ⁻¹)	Bacterial count log (ml ⁻¹)
0	1030	0		158	2.199	1128	0		108	2.033
0.125	1592	0				1626	0			
0.25	1604	0				1434	0			
0.375	1526	0				1254	0			
1	704	0.125	-0.903	72	1.857	634	0.125	-0.903	41	1.613
2	526	0		33	1.519	486	0.125		0	
3	435	0.125	-0.903	170000	5.230	440	1.5	-0.903	190000	5.279
4	386	0		175000	5.243	369	0.125		130000	5.114
5	368	0		73333	4.865	348	1		33333	4.523
6	331	0		12333	4.091	291	1		2333	3.368
7	299	0		5333	3.727	300	0.75		8833	3.946
8	302	0		6166	3.790	234	0.75		9000	3.954
9	249	0		30000	4.477	208	4		12000	4.079
10	208	4	0.602	15000	4.176	180	1.5	0.602	3833	3.584

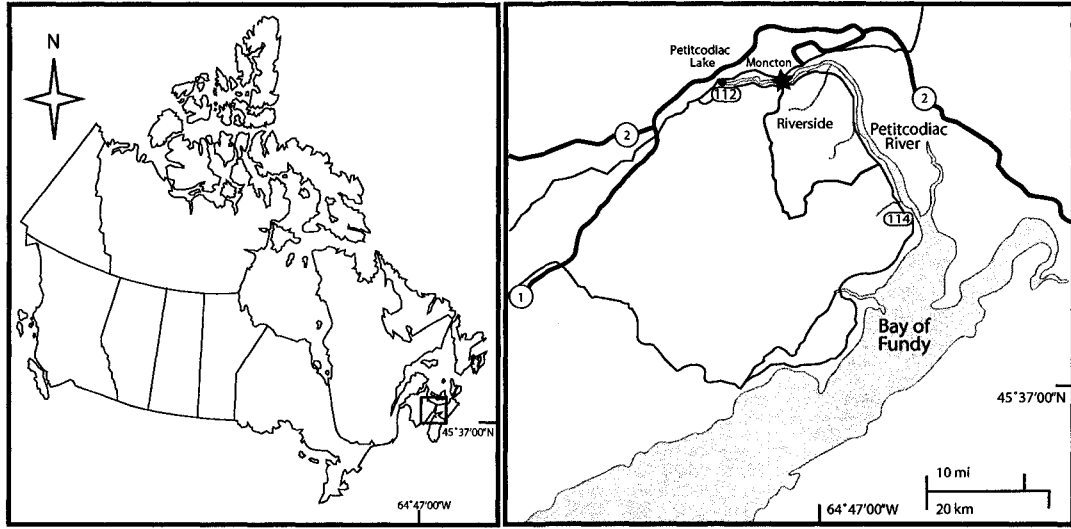


Figure 3.1. Map of Moncton and Riverside situated in the upstream of the Petitcodiac River, New Brunswick.

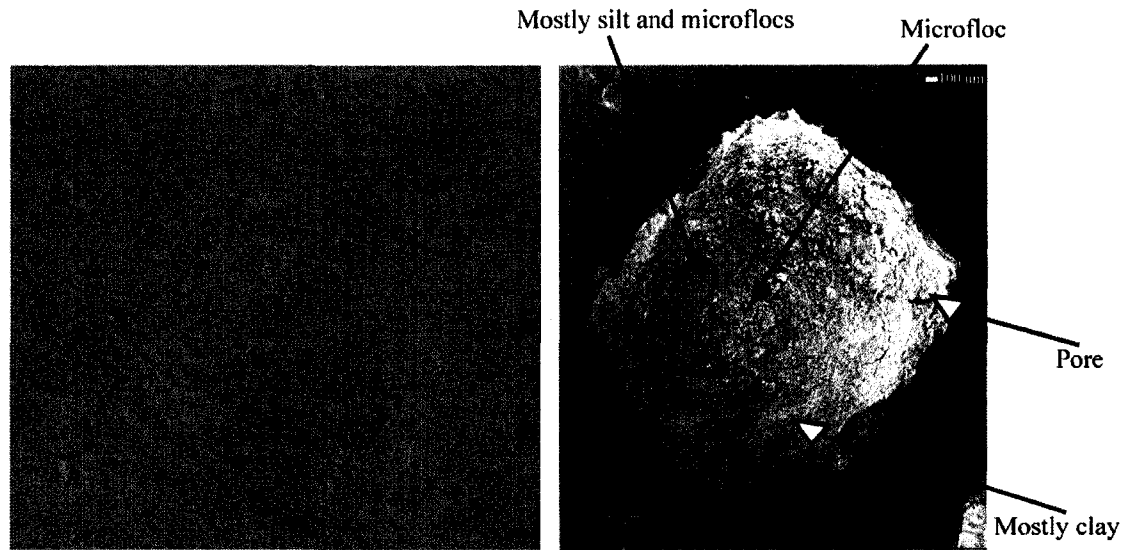


Figure 3.2. Macroflocs of approximately 5 cm in scale are observed floating in muddy water (to the left). A loosely bound macrofloc mainly composed of clay and silt particles observed by the Scanning Electron Microscope (SEM) (to the right).

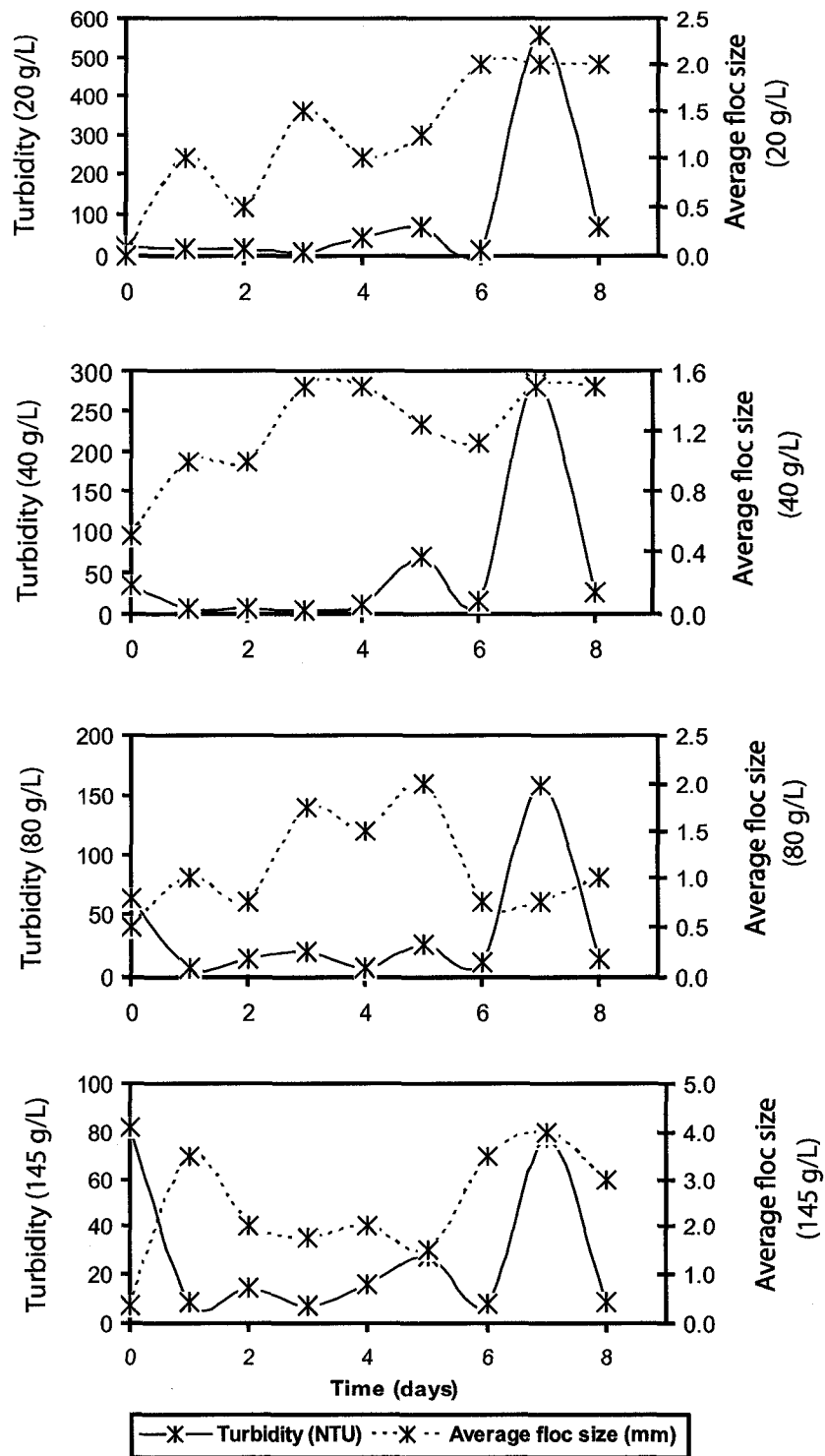


Figure 3.3. Time series of turbidity and average floc size with a range of particle concentrations.

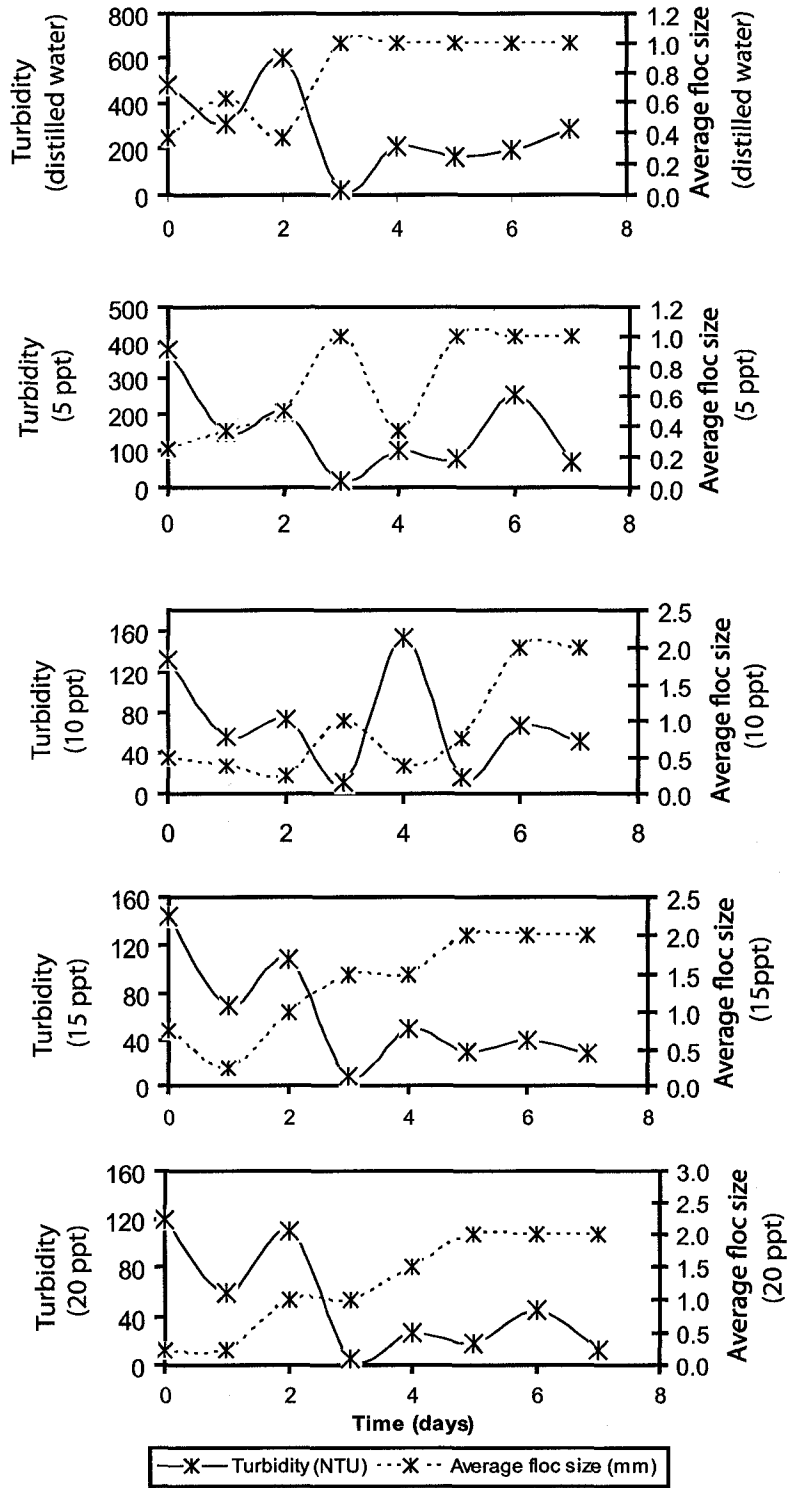


Figure 3.4. Time series of turbidity and average floc size in different saline conditions.

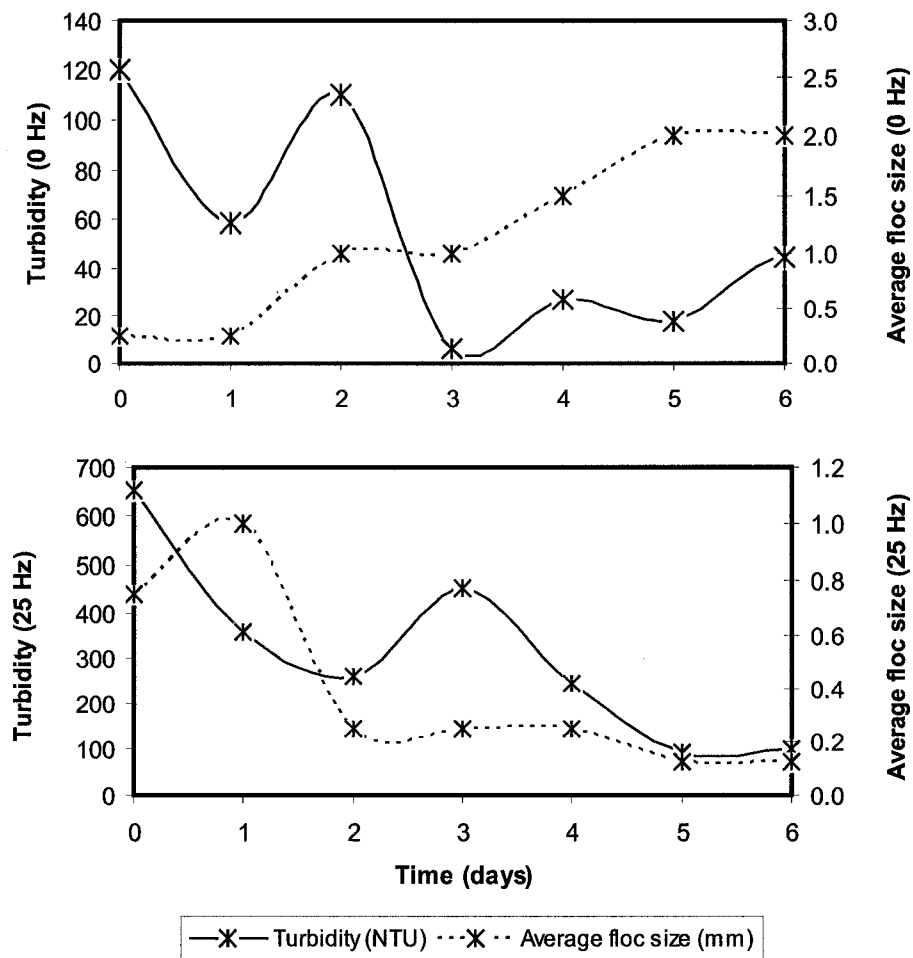


Figure 3.5. Variations of turbidity and floc size with time from a turbulent experiment.

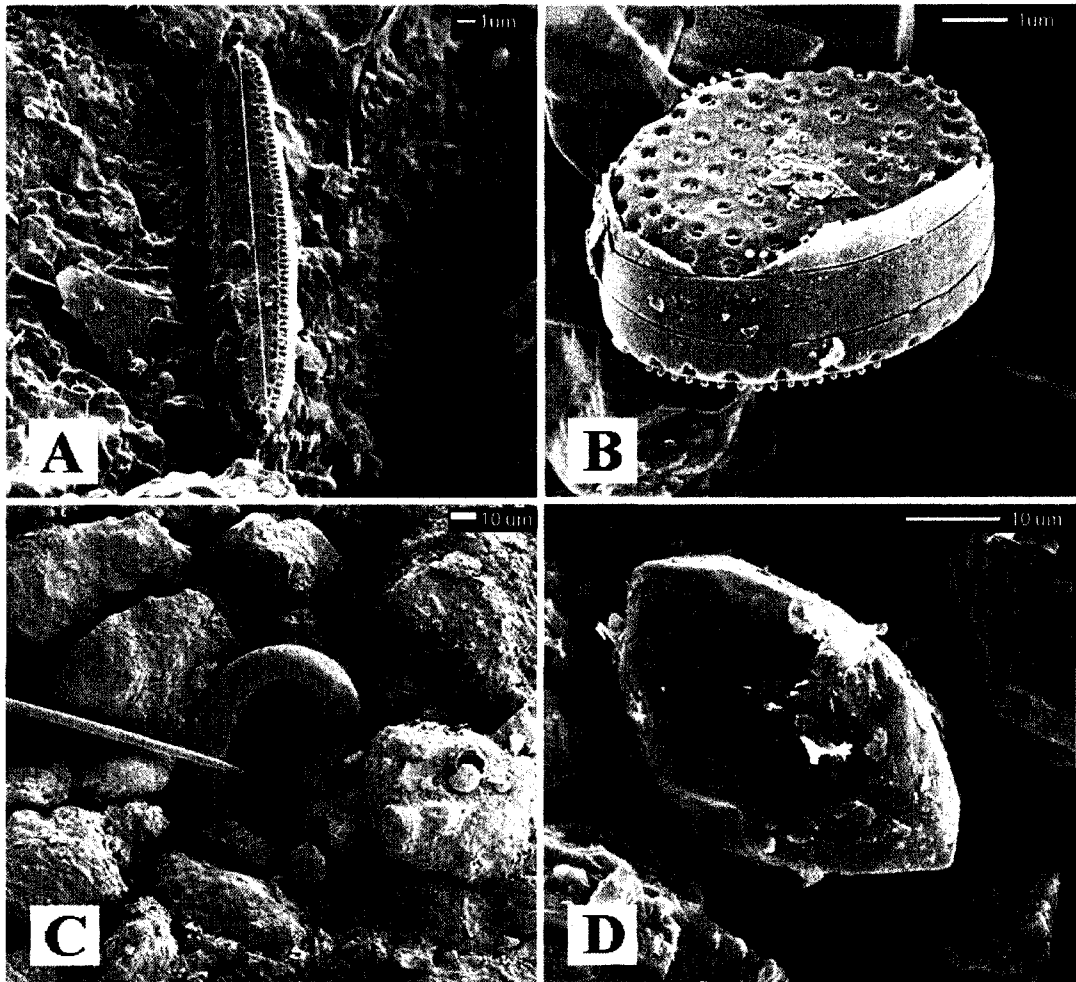


Figure 3.6. The internal structure of flocs; A) a rod-shaped diatom; B) a diatom, C) a phylolith in the left is close to a U-shaped nematode in the right; D) a zircon grain.

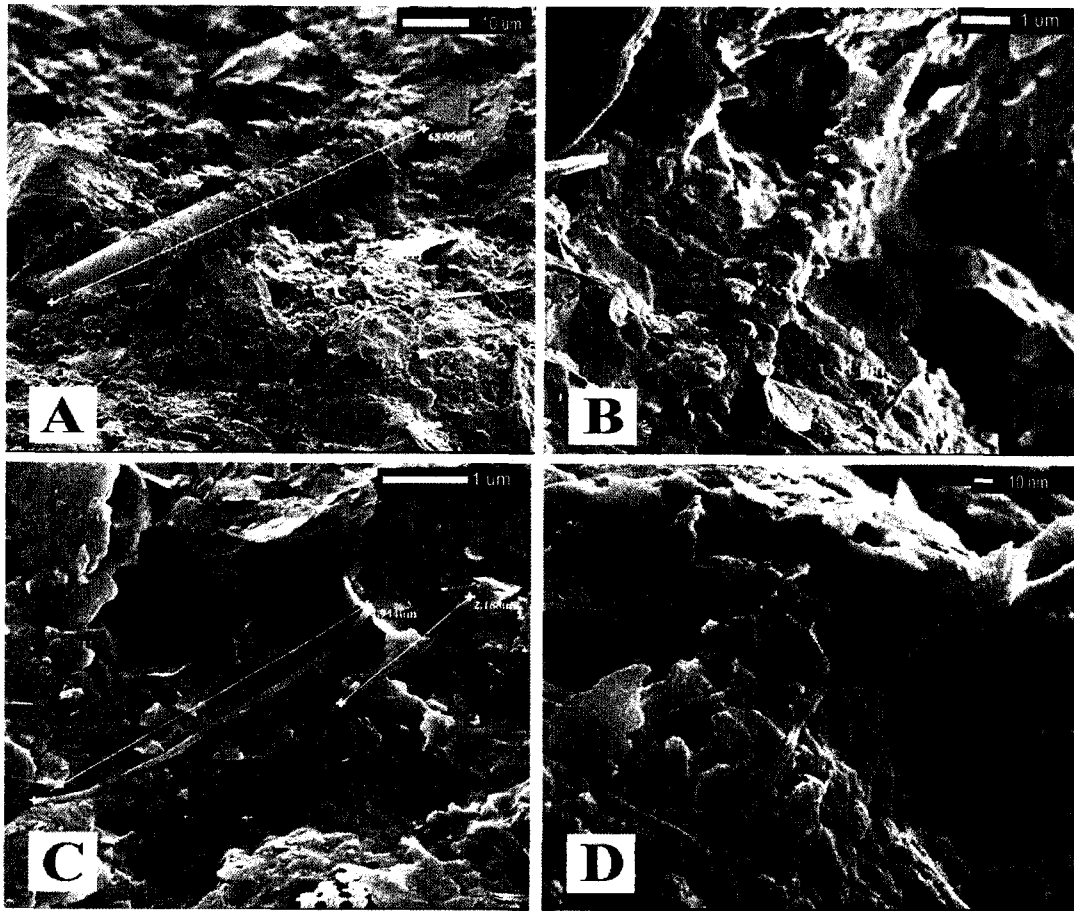


Figure 3.7. Internal constituents of flocs; A) a rod shaped plankton; B) a phytolith observed in the flocs taken from very saline water; C) *Sphaerotilus* (a type of a long iron-bacteria) observed in flocs taken from dilute waters; D) Some scattered organic debris.

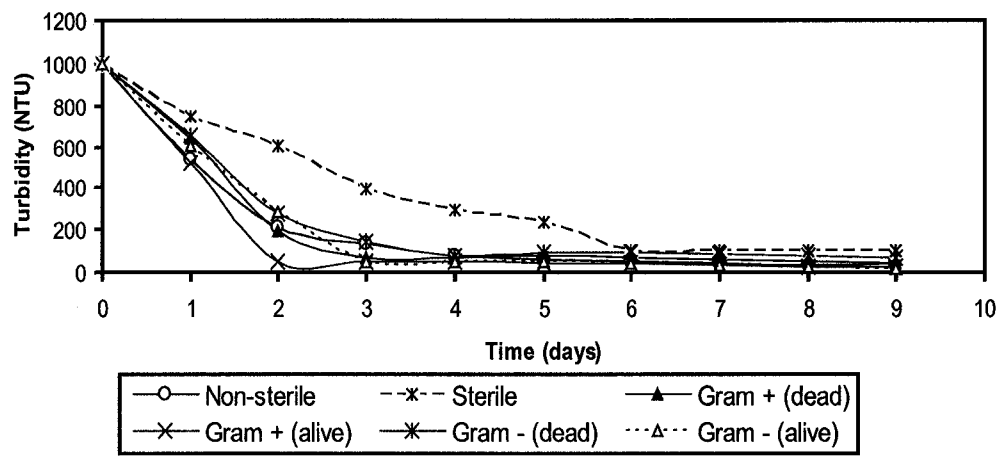


Figure 3.8. Time series of turbidity under different bacterial conditions.

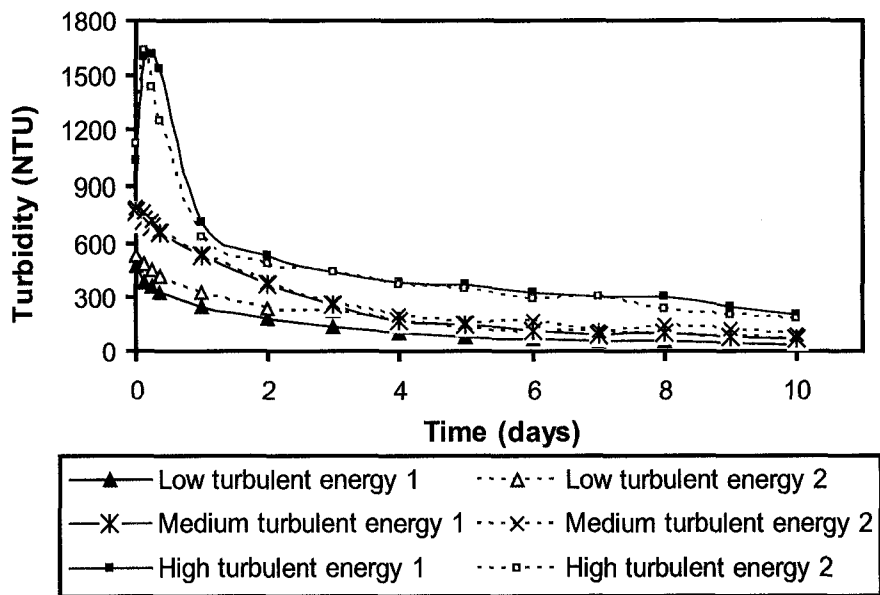


Figure 3.9. Variations of turbidity levels by various turbulent energies.

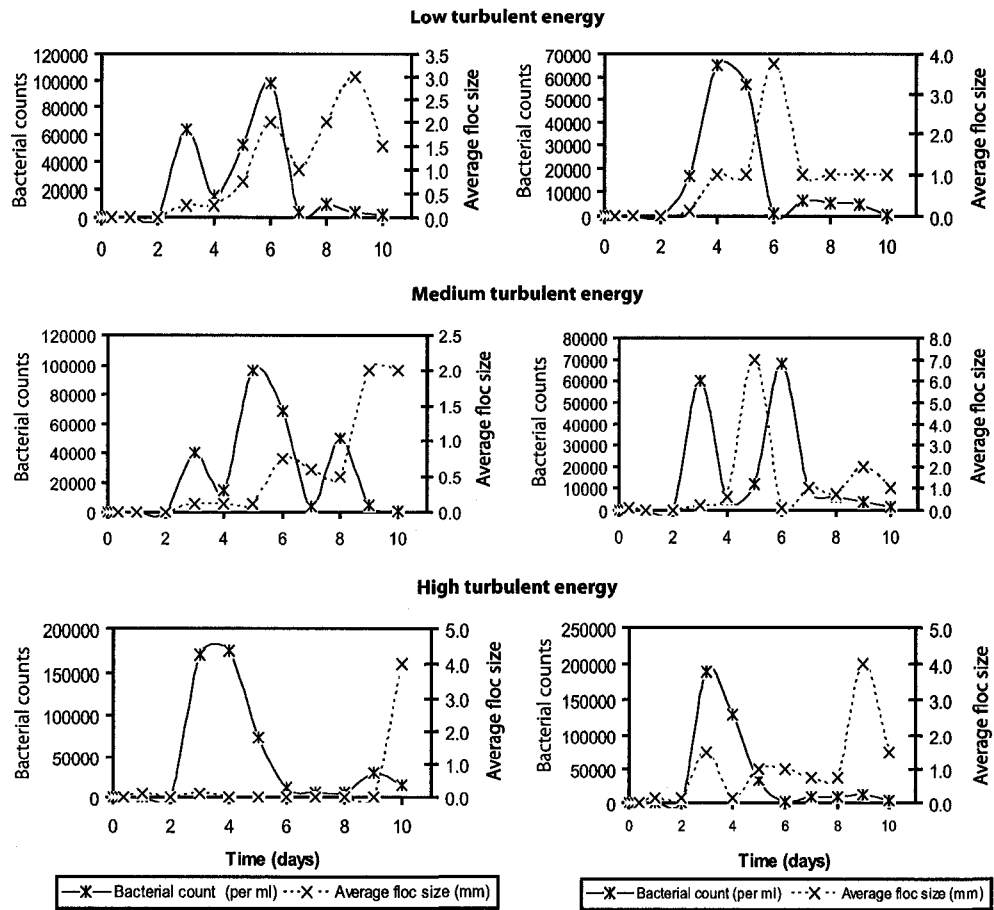


Figure 3.10. Variations of bacterial number and floc size with time under the influence of various turbulent energies.

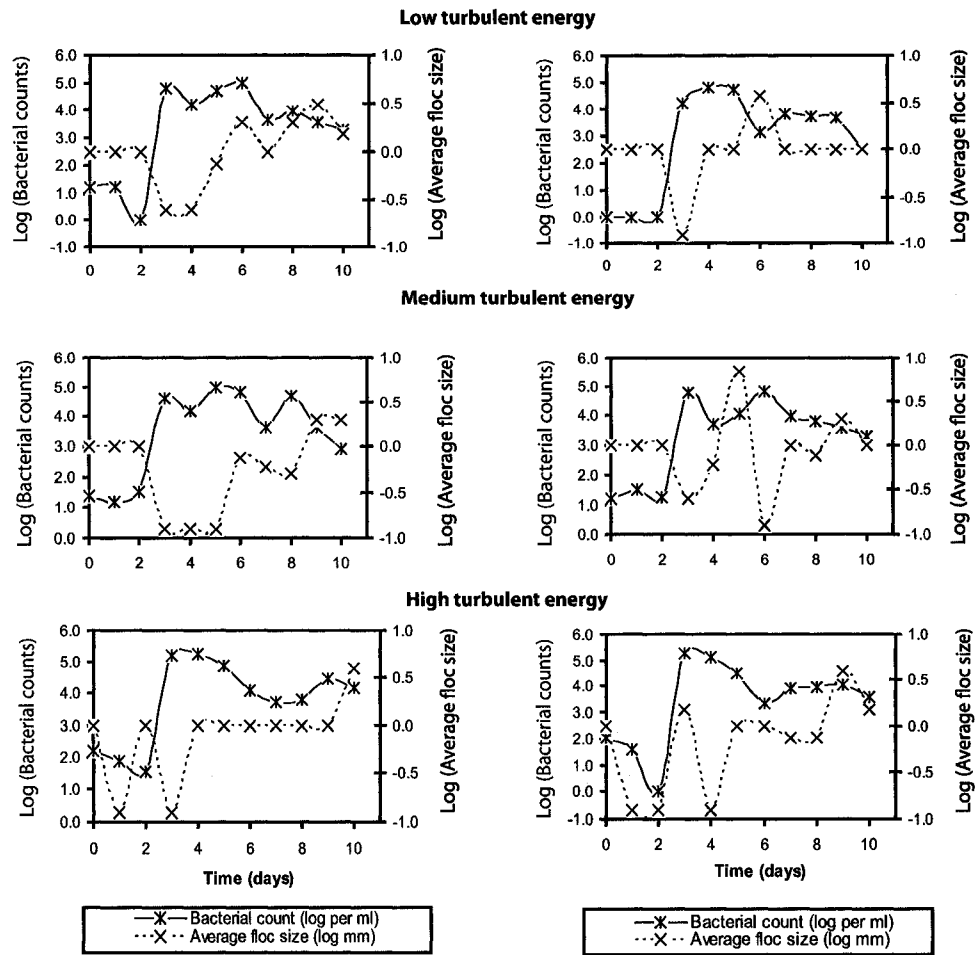


Figure 3.11. Variations of the log of bacterial number and log of floc size with time under the influence of various turbulent energies.

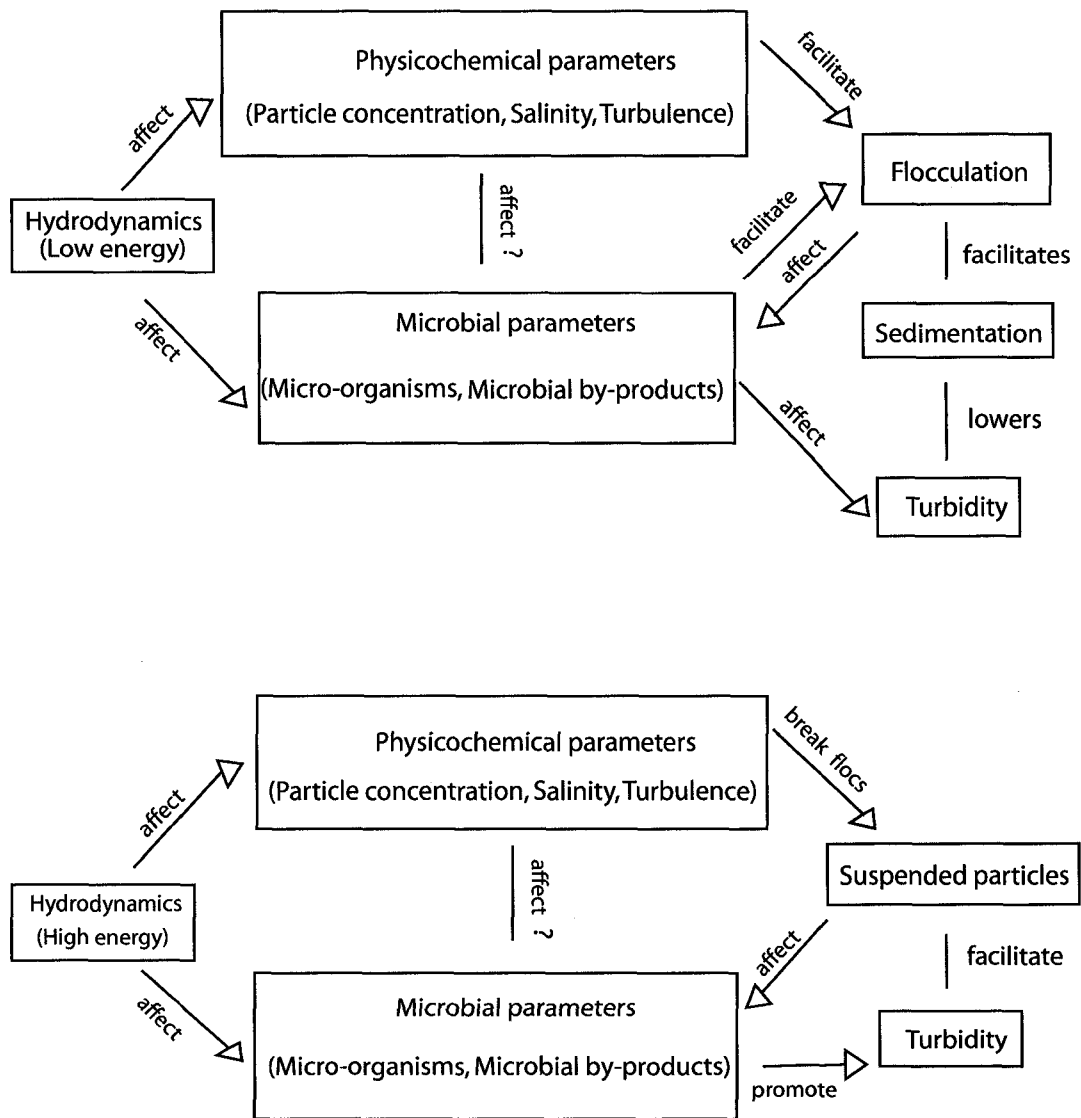


Figure 3.12. Predicting the roles played by aggregation, sediment biota and their multiple interactions as well as their significant effects on sediment dynamics.

CHAPTER 4: CONCLUSION

4.1 INTRODUCTION

This chapter summarizes the main findings of this thesis and draws out their implications for estuarine sedimentology, stratal correlation, microbial ecology and industrial solutions. After highlighting the geochemical techniques such as stable isotope analyses and salinity measurements, chapter 2 outlines a method for determining the ages of recently deposited IHS beds. Besides underlining the significance of micro-organisms, chapter 3 aims to provide an understanding of the sediment dynamics in marginal marine environments.

4.2 RESEARCH FINDINGS IN CHAPTER 2

The sedimentary beds of the IHS in the Shepody system are shown to store annual precipitation and salinity. Comparing the isotopic signature and annual precipitation with time can be used to infer the age or relative age of these rhythmic beds. The study has also shown a mixing relationship contributed by the rainfalls and river waters into the estuarine system. Nevertheless, recent salinity records in river and estuarine deposits can be established from systematic variations of stable isotopes (δD and $\delta^{18}O$) with changing precipitation.

The study also demonstrates the potential use of δD and $\delta^{18}O$ variations for reconstructing the variability in seasonal salinity over short time periods. Using this technique, precipitation can be used to speculate the ages of sedimentary horizons to obtain local sedimentation rates, changes in depositional configuration and stratal correlation. Moreover, this technique can be used to speculate the ages of the most recent stratigraphic horizons for which not many dating methods can be used. The salinity record established from seasonal rhythmites and stable isotopes can contribute to the depositional history of the Shepody River Estuary.

4.3 RESEARCH FINDINGS IN CHAPTER 3

The experiments in chapter 3 outline the significance of bacteria in facilitating flocculation and turbidity under various influences of hydrodynamics. The effects of physicochemical and biological parameters in promoting aggregation and turbidity would be useful for the prediction of flocculation and deposition in estuaries.

As discussed in chapter 3, bacteria and the physicochemical parameters facilitate floc settling by increasing the size of aggregates once they are clustered. However, metabolic processes of bacteria such as biogas induce fluctuations in turbidity. The bacteria and floc size time series profiles show that the interaction between aggregates and sediment biota are influenced by the hydrodynamics in estuaries. When the water energy level is high, flocs disintegrate and result in high concentration of suspended particles and nutrients. During low energetic conditions, large flocs are formed due to physicochemical and biological parameters. The flocs and micro-organisms settle rapidly forming mud blankets and promoting sedimentation. The accumulation of sediments results in reduction of turbidity levels.

Although biological parameters enhance flocculation, large aggregates can limit oxygen diffusion and nutrient absorption. Hence, micro-organisms in the microbial community are reduced due to the deficiency of nutrients. The interactions between aggregates and sediment biota can have significant effects on sedimentary dynamics, nutrient cycling, aquatic ecology and industrial waste water treatment.

4.4 LIMITATIONS

The isotopic and salinity signals become weaker with increasing depth of sedimentary layers of the IHS of the Shepody River Estuary and their correlation with the precipitation data becomes more difficult and inaccurate. Hence, the isotopic compositions and salinity records can not be used to determine the age or relative age of older inclined beds.

Although the sediment amount was adequate for the experiments in chapter 3, the natural estuarine system would have been better replicated if the sediments were of larger quantities of sediments were present and larger vessels with larger areas were used. Also, although the pipetting method is one of the best in the extraction of flocs, macroflocs are very loosely bound and they tend to break very easily. Pipettes with large tip openings (>

2000 um) are very efficient in minimizing floc breakage. However, the pressure due to suction can break some of the loose flocs during the extraction process.

4.5 FUTURE RESEARCH

Previous papers have shown that the IHS of the Shepody River are seasonal; bioturbated beds are formed in the summer and the spring deposits are characterized by parallel laminations with little or no bioturbation. Chapter 2 introduced an interesting method of comparing the time series of the stable isotopes to those of the local precipitation to determine the mode of preservation. These time series can also be extended to the ichnological facies model by comparing them to the ichnological characteristics (such as number of burrows or tracts) of these seasonal deposits.

Deducing the age of the recent beds in the IHS deposits can help establish sedimentation rate and can help correlate deposits (in this case IHS) with similar ages. The research can be extended to studying the accumulation rates and the correlation of similar strata to better understand the sedimentary history (particularly of salt and fresh-water mixing) of the entire coastline. Comparisons of the three data: isotopic compositions, salt ion concentration and annual precipitation can be used to establish a stratigraphic framework and thereby represent tools to discern sediment distribution patterns through time. Thus, the future research can involve the study of sediment dynamics near the shoreline.

Research findings of previous papers and this thesis confirm that physicochemical parameters (particle concentration, salinity and turbulence) and bacteria facilitate flocculation. However, these parameters have not been quantified. In order to quantify parameters, the research can be extended to study the effect of metals such as Fe, Mg and Ca as well as the effects other common micro-organisms such as diatoms on the number and size of flocs through time. As an alternative to measuring turbidity, a flocculator can be used to measure the settling velocity with time. The settling velocity can also help in estimating the sedimentation rates since sedimentation is induced by coagulation. Another direction for future research is to study the flocculation of sand. Although the size of sand is larger than 62.5 um, previous studies have shown them to flocculate. The cause of the sand aggregates may be due to the presence of electrolytes in the water and

diatoms in quartz. The effects of physicochemical factors and micro-organisms on sand flocs could be an extension of the research on flocculation and contribute to the estuarine sedimentology.

Appendix 1. Grain size distribution in the Petitcodiac River system. The grain sizes of the sampled sediments were determined using a sedigraph.

ID	Study area	Clay % ($< 3.9 \mu\text{m}$)	Silt % ($3.9- 62.5 \mu\text{m}$)	Mud % ($< 62.5 \mu\text{m}$)	Sand % ($62.5- 2 \text{ mm}$)	Gravel % ($> 2\text{mm}$)
1	Petitcodiac Lake/ Causeway	10.03	18.18	28.21	69.44	1.44
2	Riverside	10.9	62.4	73.3	27.5	0
3	Riverside (wet)	24.4	72.2	96.6	6.7	0
4	Riverside (dry)	63.9	23.9	87.8	13.4	0
5	Hilsborough	73.1	25.4	98.5	1.4	0
6	Chocolate River	78.5	21.3	86.83	12.95	0
7	Shepody River	27.2	61.8	89	12.29	0
8	Shepody Reservoir					
9	Cape enrage	36.75	57.2	93.95	4.42	0
10	Long marsh Creek	44.1	54.9	99	1	0

Appendix 2. The annual precipitation data obtained from the Alma weather station. The amount of rain obtained from snow involved the following conversion: 1.5 cm of snow = 1mm of water.

Year-month	Total Rain (mm)	Total Snow (cm)	Total snow (mm)	Snow conversion to water	Total Precipitation (mm)
1991-01	30.0	105.2	1052.0	70.1	100.1
1991-02	13.6	51.6	516.0	34.4	48.0
1991-03	115.8	76.0	760.0	50.7	166.5
1991-04	108.2	15.8	158.0	10.5	118.7
1991-05	144.9	0.0	0.0	0.0	144.9
1991-06	42.9	0.0	0.0	0.0	42.9
1991-07	71.9	0.0	0.0	0.0	71.9
1991-08	186.3	0.0	0.0	0.0	186.3
1991-09	236.5	0.0	0.0	0.0	236.5
1991-10	197.0	0.0	0.0	0.0	197.0
1991-11	148.2	0.0	0.0	0.0	148.2
1991-12	41.0	93.4	934.0	62.3	103.3
1992-01	91.7	44.6	446.0	29.7	121.4
1992-02	20.8	130.7	1307.0	87.1	107.9
1992-03	105.8	6.2	62.0	4.1	109.9
1992-04	21.0	33.3	333.0	22.2	43.2
1992-05	36.2	10.5	105.0	7.0	43.2
1992-06	149.3	0.0	0.0	0.0	149.3
1992-07	128.9	0.0	0.0	0.0	128.9
1992-08	127.3	0.0	0.0	0.0	127.3
1992-09	51.1	0.0	0.0	0.0	51.1
1992-10	133.4	0.0	0.0	0.0	133.4
1992-11	105.2	9.4	94.0	6.3	111.5
1992-12	64.0	84.7	847.0	56.5	120.5
1993-01	100.0	36.4	364.0	24.3	124.3
1993-02	19.1	50.7	507.0	33.8	52.9
1993-03	59.6	91.9	919.0	61.3	120.9
1993-04	79.0	28.3	283.0	18.9	97.9
1993-05	121.7	0.0	0.0	0.0	121.7
1993-06	164.2	0.0	0.0	0.0	164.2
1993-07	108.4	0.0	0.0	0.0	108.4
1993-08	5.8	0.0	0.0	0.0	5.8
1993-09	142.5	0.0	0.0	0.0	142.5
1993-10	234.9	0.0	0.0	0.0	234.9
1993-11	155.3	0.0	0.0	0.0	155.3
1993-12	126.9	47.0	470.0	31.3	158.2

Appendix 2 contd.

Year-month	Total Rain (mm)	Total Snow (cm)	Total Snow (mm)	Snow conversion to water	Total Precipitation (mm)
1994-01	83.6	73.5	735.0	49.0	132.6
1994-02	0.0	40.8	408.0	27.2	27.2
1994-03	258.6	95.2	952.0	63.5	322.1
1994-04	164.7	0.0	0.0	0.0	164.7
1994-05	213.8	0.0	0.0	0.0	213.8
1994-06	141.6	0.0	0.0	0.0	141.6
1994-07	68.5	0.0	0.0	0.0	68.5
1994-08	62.3	0.0	0.0	0.0	62.3
1994-09	82.8	0.0	0.0	0.0	82.8
1994-10	32.6	0.0	0.0	0.0	32.6
1994-11	173.7	13.2	132.0	8.8	182.5
1994-12	99.8	40.6	406.0	27.1	126.9
1995-01	140.8	58.6	586.0	39.1	179.9
1995-02	5.4	132.3	1323.0	88.2	93.6
1995-03	74.3	17.0	170.0	11.3	85.6
1995-04	62.1	22.0	220.0	14.7	76.8
1995-05	72.9	29.2	292.0	19.5	92.4
1995-06	132.2	0.0	0.0	0.0	132.2
1995-07	122.9	0.0	0.0	0.0	122.9
1995-08	59.2	0.0	0.0	0.0	59.2
1995-09	88.8	0.0	0.0	0.0	88.8
1995-10	116.7	0.0	0.0	0.0	116.7
1995-11	198.4	4.8	48.0	3.2	201.6
1995-12	22.3	66.0	660.0	44.0	66.3
1996-01	117.6	30.0	300.0	20.0	137.6
1996-02	134.4	33.5	335.0	22.3	156.7
1996-03	60.4	73.4	734.0	48.9	109.3
1996-04	111.1	35.5	355.0	23.7	134.8
1996-05	109.6	0.0	0.0	0.0	109.6
1996-06	64.7	0.0	0.0	0.0	64.7
1996-07	225.6	0.0	0.0	0.0	225.6
1996-08	9.1	0.0	0.0	0.0	9.1
1996-09	181.1	0.0	0.0	0.0	181.1
1996-10	135.0	0.0	0.0	0.0	135.0
1996-11	61.1	11.2	112.0	7.5	68.6
1996-12	168.4	18.7	187.0	12.5	180.9

Appendix 2 contd.

Year-month	Total Rain (mm)	Total Snow (cm)	Total Snow (mm)	Snow conversion to water	Total Precipitation (mm)
1997-01	103.4	82.5	825.0	55.0	158.4
1997-02	65.4	66.6	666.0	44.4	109.8
1997-03	96.8	95.2	952.0	63.5	160.3
1997-04	35.6	30.3	303.0	20.2	55.8
1997-05	153.5	0.0	0.0	0.0	153.5
1997-06	89.5	0.0	0.0	0.0	89.5
1997-07	71.4	0.0	0.0	0.0	71.4
1997-08	57.1	0.0	0.0	0.0	57.1
1997-09	95.6	0.0	0.0	0.0	95.6
1997-10	30.0	0.0	0.0	0.0	30.0
1997-11	55.0	52.5	525.0	35.0	90.0
1997-12	24.8	76.0	760.0	50.7	75.5
1998-01	181.2	110.9	1109.0	73.9	255.1
1998-02	74.7	1.2	12.0	0.8	75.5
1998-03	85.9	52.1	521.0	34.7	120.6
1998-04	162.1	3.2	32.0	2.1	164.2
1998-05	102.0	0.0	0.0	0.0	102.0
1998-06	150.8	0.0	0.0	0.0	150.8
1998-07	48.2	0.0	0.0	0.0	48.2
1998-08	105.2	0.0	0.0	0.0	105.2
1998-09	141.4	0.0	0.0	0.0	141.4
1998-10	212.7	0.0	0.0	0.0	212.7
1998-11	119.7	2.0	20.0	1.3	121.0
1998-12	82.4	32.0	320.0	21.3	103.7
1999-01	154.9	60.3	603.0	40.2	195.1
1999-02	97.9	12.0	120.0	8.0	105.9
1999-03	100.6	107.1	1071.0	71.4	172.0
1999-04	37.0	30.2	302.0	20.1	57.1
1999-05	86.6	0.0	0.0	0.0	86.6
1999-06	32.3	0.0	0.0	0.0	32.3
1999-07	78.3	0.0	0.0	0.0	78.3
1999-08	138.4	0.0	0.0	0.0	138.4
1999-09	312.9	0.0	0.0	0.0	312.9
1999-10	78.1	0.0	0.0	0.0	78.1
1999-11	92.3	1.2	12.0	0.8	93.1
1999-12	87.5	25.7	257.0	17.1	104.6

Appendix 2 contd.

Year-month	Total Rain (mm)	Total Snow (cm)	Total Snow (mm)	Snow conversion to water	Total Precipitation (mm)
2000-01	116.8	77.0	770.0	51.3	168.1
2000-02	76.6	22.8	228.0	15.2	91.8
2000-03	95.4	78.2	782.0	52.1	147.5
2000-04	131.2	1.6	16.0	1.1	132.3
2000-05	145.1	0.0	0.0	0.0	145.1
2000-06	49.9	0.0	0.0	0.0	49.9
2000-07	64.2	0.0	0.0	0.0	64.2
2000-08	76.0	0.0	0.0	0.0	76.0
2000-09	104.1	0.0	0.0	0.0	104.1
2000-10	142.4	0.0	0.0	0.0	142.4
2000-11	92.0	13.0	130.0	8.7	100.7
2000-12	102.2	47.8	478.0	31.9	134.1
2001-01	0.0	113.6	1136.0	75.7	75.7
2001-02	14.2	80.6	806.0	53.7	67.9
2001-03	36.2	60.2	602.0	40.1	76.3
2001-04	66.1	12.9	129.0	8.6	74.7
2001-05	149.0	0.0	0.0	0.0	149.0
2001-06	117.2	0.0	0.0	0.0	117.2
2001-07	32.2	0.0	0.0	0.0	32.2
2001-08	31.6	0.0	0.0	0.0	31.6
2001-09	84.9	0.0	0.0	0.0	84.9
2001-10	93.2	0.0	0.0	0.0	93.2
2001-11	119.0	12.8	128.0	8.5	127.5
2001-12	28.2	28.0	280.0	18.7	46.9
2002-01	30.4	80.3	803.0	53.5	83.9
2002-02	77.8	25.5	255.0	17.0	94.8
2002-03	187.1	32.7	327.0	21.8	208.9
2002-04	164.4	47.2	472.0	31.5	195.9
2002-05	101.4	0.0	0.0	0.0	101.4
2002-06	83.1	0.0	0.0	0.0	83.1
2002-07	97.2	0.0	0.0	0.0	97.2
2002-08	47.8	0.0	0.0	0.0	47.8
2002-09	212.4	0.0	0.0	0.0	212.4
2002-10	125.4	0.0	0.0	0.0	125.4
2002-11	269.1	47.0	470.0	31.3	300.4
2002-12	59.2	31.8	318.0	21.2	80.4

Appendix 2 contd.

Year-month	Total Rain (mm)	Total Snow (cm)	Total Snow (mm)	Snow conversion to water	Total Precipitation (mm)
2003-01	8.2	76.9	769.0	51.3	59.5
2003-02	91.8	33.2	332.0	22.1	113.9
2003-03	230.0	27.2	272.0	18.1	248.1
2003-04	90.5	15.5	155.0	10.3	100.8
2003-05	102.1	0.0	0.0	0.0	102.1
2003-06	90.4	0.0	0.0	0.0	90.4
2003-07	165.3	0.0	0.0	0.0	165.3
2003-08	91.2	0.0	0.0	0.0	91.2
2003-09	70.6	0.0	0.0	0.0	70.6
2003-10	227.2	0.0	0.0	0.0	227.2
2003-11	123.3	0.3	3.0	0.2	123.5
2003-12	82.0	91.0	910.0	60.7	142.7
2004-01	3.0	60.0	600.0	40.0	43.0
2004-02	1.8	55.6	556.0	37.1	38.9
2004-03	28.4	41.4	414.0	27.6	56.0
2004-04	131.9	9.6	96.0	6.4	138.3
2004-05	86.2	0.0	0.0	0.0	86.2
2004-06	101.1	0.0	0.0	0.0	101.1
2004-07	64.7	0.0	0.0	0.0	64.7
2004-08	157.4	0.0	0.0	0.0	157.4
2004-09	93.7	0.0	0.0	0.0	93.7
2004-10	93.0	0.0	0.0	0.0	93.0
2004-11	198.5	12.0	120.0	8.0	206.5
2004-12	108.8	56.2	562.0	37.5	146.3
2005-01	16.8	75.5	755.0	50.3	67.1
2005-02	44.7	25.1	251.0	16.7	61.4
2005-03	98.2	45.8	458.0	30.5	128.7
2005-04	136.5	12.1	121.0	8.1	144.6
2005-05	188.6	0.0	0.0	0.0	188.6
2005-06	64.9	0.0	0.0	0.0	64.9
2005-07	65.1	0.0	0.0	0.0	65.1
2005-08	70.3	0.0	0.0	0.0	70.3
2005-09	167.8	0.0	0.0	0.0	167.8
2005-10	308.1	0.0	0.0	0.0	308.1
2005-11	226.9	0.0	0.0	0.0	226.9
2005-12	87.7	36.3	363.0	24.2	111.9

Appendix 3. Age of deposition determined for the sedimentary layers of the IHS at location 1 (top) and IHS at location 3 (bottom) by comparing the isotopic signature to the associated annual precipitation.

